The Meso-Cenozoic deformation history of Thailand and Myanmar; insights from calcite U-Pb and apatite fission track thermochronology

Thesis submitted in accordance with the requirements of the University of Adelaide for an Honours Degree in Geology

Alexander David Wighton Simpson

October 2018

THE UNIVERSITY of ADELAIDE

CALCITE AND APATITE GEOCHRONOLOGY OF THAILAND AND MYANMAR

ABSTRACT

Given the absence of suitable dating methods, the timing of low-temperature crustal deformation is usually established by indirect methods (such as apatite fission track (AFT) thermochronology). Only few studies have previously ventured into directly constraining the absolute timing of brittle deformation (such as authigenic illite dating). U-Pb dating of calcite in tectonic veins represents a new method to potentially directly date brittle deformation events (Roberts and Walker, 2016). By utilising this method in combination with apatite U-Pb and fission track thermochronology, this study sheds new light on the upper crustal deformation history of Thailand and Myanmar. U-Pb calcite ages demonstrate tectonic activity at ~216-209Ma in the Khao Kwang Fold and Thrust Belt associated with the Indosinian stage 2 collision between the Sibumasu Block and the Indochina Block. Brittle deformation along the Three Pagodas Fault Zone (TPFZ) was dated at ~45Ma and ~24Ma (and possibly as recently as ~1.3Ma). AFT thermochronology suggests exhumation in the Tin province of southern Myanmar at ~26Ma-18Ma. These dates are in agreement with previous regional AFT studies in Thailand and with calcite U-Pb dates for the TPFZ, suggesting fault reactivation in response to the India-Eurasia collision and rifting in the Andaman Sea. Calcite U-Pb ages were obtained with uncertainties as low as ~1%, which is an unprecedented precision for the timing of brittle deformation. This work further demonstrates that calcite elemental mapping, in combination with U-Pb dating, can be used to distinguish different calcite growth events. Particularly enrichments in Mn or depletions in LREE concentrations in calcite seem useful to distinguish different fluids and associated calcite (re)crystallisation events. Although further work is required to enhance our understanding of both Pb diffusion in calcite as well as geochemical tracers for calcite recrystallization, the combination of calcite U-Pb with apatite fission track thermochronology is a promising novel tool to enhance our understanding of the timing of brittle deformation.

KEY WORDS

Calcite, Apatite, Geochronology, Thailand, Myanmar, U-Pb dating, Khao Kwang Fold and Thrust Belt, Three Pagodas Fault Zone, Tin Province

CONTENTS

LIST OF FIGURES AND TABLES

[1] INTRODUCTION

A variety of techniques have been used to constrain the geological history of Thailand, from U-Pb and Ar-Ar dating of igneous and metamorphic minerals to biostratigraphy (Lacassin et al, 1997; Ridd, Barber, Crow., 2011). However, the exact timing of major tectonic events that affected Thailand, such as the onset and extent of the Indosinian Orogeny, remain controversial (e.g. Morley et al., 2013). Similarly, the timing of Cenozoic deformation, in relation to the India-Eurasia collision (Rhodes et al., 2005) and/or rifting in the Andaman Ocean (Morley & Searle, 2017) are poorly constrained and mostly inferred from indirect techniques such as regional apatite fission track (AFT) studies (Upton et al., 1999). Although this technique provides important constraints on Cenozoic cooling, the relation between cooling and (brittle) deformation is not well established for Thailand. For Myanmar, the Cenozoic deformation history is largely constrained by only few ^{40}Ar-^{39}Ar dates (Bertrand et al., 1999). Particularly in the so-called Tin Province in southern Myanmar (figs. 1 and 4) (Gardiner et al., 2018), time constraints on the deformation history are lacking. This work focusses on three key-regions in central Thailand and neighbouring southern Myanmar that record structural evidence for Meso-Cenozoic deformation (fig. 1).

The Saraburi region, in Central Thailand, is characterised by the Khao Kwang Fold and Thrust belt (KKFTB, fig. 2), which formed during the Indosinian Orogeny (Morley et al., 2013). Zircon U-Pb dates on granitoid intrusions (Morley et al., 2013), K-Ar dates on Authigenic illites (Hansberry et al., 2017), and U-Pb dating on detrital zircons (Arboit et al., 2016) have provided high to medium temperature insights into the tectonic history of the area. Low-temperature constraints are largely lacking (constrained by a single AFT date of 39Ma; Upton, 1999).

The Three Pagodas Fault Zone (TPFZ), in western Thailand (figs. 1 and 3), represents a Cenozoic structure that developed in response to the India-Eurasia collision (e.g. Rhodes et al., 2005). ^{40}Ar-^{39}Ar dates, obtained from micas in gneisses within the TPFZ, suggest that ductile (left-lateral) slip occurred during the late Eocene – early Oligocene (Lacassin et al. 1997), which is broadly agrees with the timing of cooling and exhumation in the hinterland, defined by apatite fission track thermochronology (Upton et al., 1999). Direct constraints on the timing of brittle faulting in the TPFZ are, however, currently lacking.

Both locations contain extensive calcite veining that can be linked to major structures that deformed the study areas. Previous studies (Roberts and Walker 2016; Nuriel et al. 2017) have demonstrated that in situ laser ablation inductively coupled mass spectrometry (LA-ICP-MS) U-Pb dating of calcite veins can produce accurate constraints on the timing of calcite growth. Given the field-relations between calcite growth and brittle deformation, this method has the potential to directly date brittle deformation in the KKFTB and TPFZ.

The Tin Province, in southern Myanmar is relatively close to the TPFZ and forms the southern extent of the so-called Mogok-Mergui-Mandalay belt (MMMB) (fig. 4) (Gardiner et al., 2018). While limited previous studies have been conducted into the metamorphic history of the MMMB (fig. 4) (Bertrand et al., 1999; Gardiner et al., 2016), it remains unclear to what extent the exhumation history is related to activity inferred from AFT studies conducted in Thailand (Upton 1999).

This study has three aims: (1) to use samples collected from calcite veins in both the KKFTB and TPFZ areas of Thailand to unravel the timing of brittle faulting; (2) to explore the advantages and limitations of calcite LA-ICP-MS analysis combined with elemental mapping to potentially date multiple calcite growth events; and (3) to integrate the calcite data with previous (Thailand) and new (Myanmar, this study) apatite fission track (and U-Pb)

themochronology to enhance our understanding of the absolute timing of Meso-Cenozoic deformation within southeastern Asia.

[2] GEOLOGICAL SETTING

[2.1] Tectonic history of Thailand and Myanmar

Thailand and Myanmar share broadly similar tectonic histories, characterised by two major events: (1) the Indosinian collision between the Sibumasu Block and the Indochina Block and its associated volcanic arc (named Sukhothai); and (2) the collision between India and Eurasia (Ridd, Barber, Crow 2011).

Thailand can be geologically subdivided into the Sibumasu Block (in the west) and the Indochina Block (in the east). These terranes are separated by the remnants of an overthrust accretionary complex (The Inthanon Zone) and a Palaeozoic island arc (Sukhothai Arc) (Ridd, Barber, Crow., 2011) (Fig. 1). The Sibumasu block extends west into Myanmar, where it eventually becomes the West Burma Block (Searle et al., 2007). Myanmar is characterised by a series of magmatic/metamorphic belts such as the Mogok-Mandalay-Mergui Belt (MMMB) (fig. 4) (Gardiner et al. 2018).

The Sibumasu block likely represents a fragment of the northern margin of Gondwana, given the similarity of its upper Palaeozoic stratigraphy with other Gondwana-derived terranes (Ueno et al., 2010). Sibumasu probably rifted off Gondwana during the early Permian, as part of the Cimmerian ribbon continent, before colliding with Indochina (as part of Eurasia) during the Paleo-Tethys closure (Barber et al., 2011). The Sukhotai arc rifted from the Indochina block at a roughly similar time (Barr & McDonald., 1987). The Indosinian Orogeny can be divided into two stages: (1) Indosinian Stage 1, in which the Sukhotai arc re-

amalgamated with the Indochina Block, which likely occurred during the early Triassic (Barber et al 2011); and (2) Indosinian stage 2, involving the subsequent collision of the Sibumasu Block with the combined Sukhotai/Indochina Block (Ridd, et al., 2011). The timing of the latter event is poorly defined but is thought to have occurred during the late Triassic at ~220Ma, based on the timing of magmatism and contemporaneous basin inversion (Morley et al., 2013, Arboit et al., 2017).

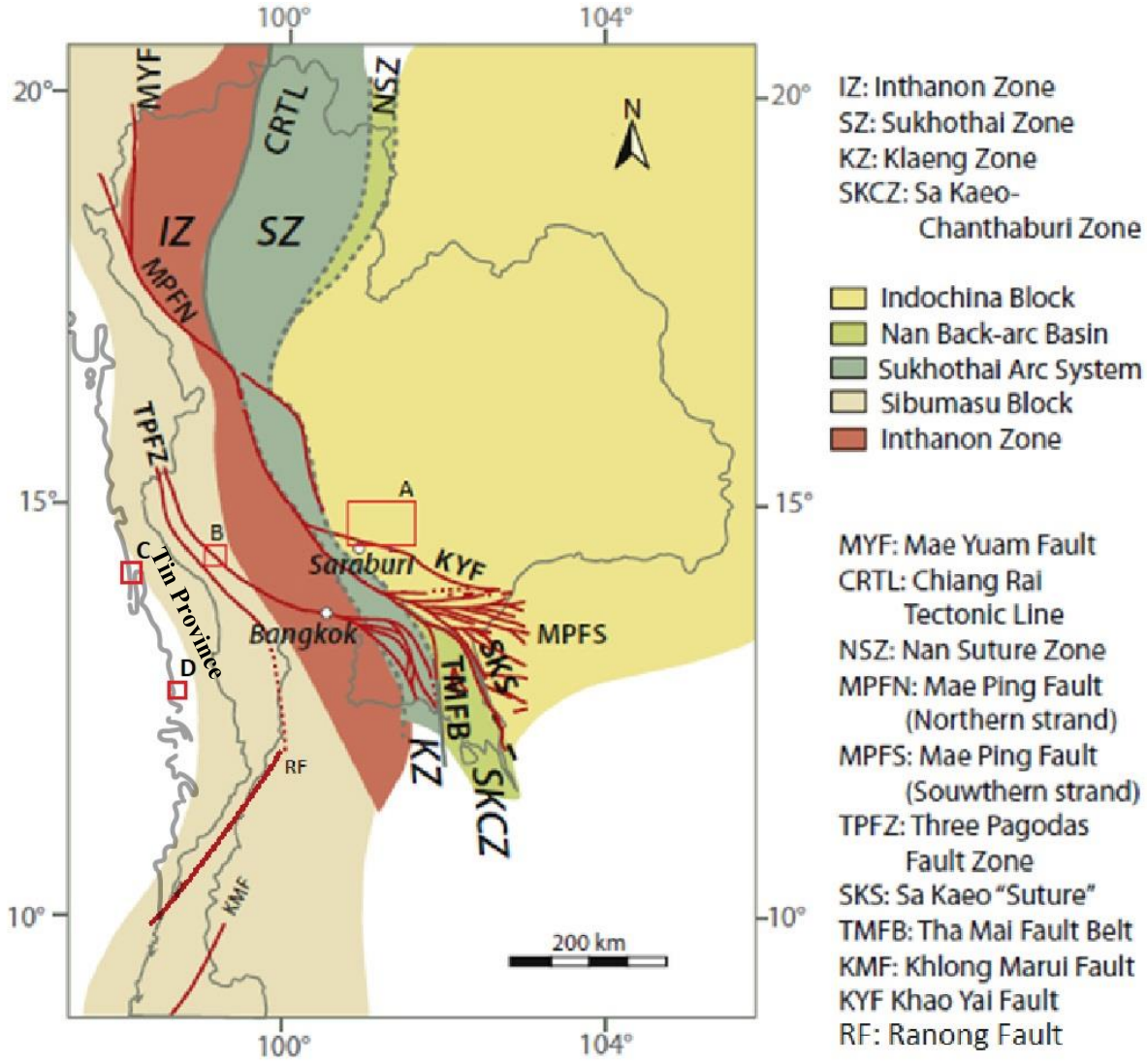

Figure 1: Simplified geological map of Thailand and southern Myanmar, showing the major terranes and fault zones. Rectangle A represents the KKFTB, from which calcite samples 7, 8, & 10 were taken. Rectangle B represents the sampling area near the TPFZ, where calcite sample 12a and slickenfibres were taken. Rectangle C shows apatite sample MY72 sampling location. Rectangle D shows apatite sample MY74 location). (Modified from Warren et al., 2014)

[2.2] Khao Kwang Fold and Thrust belt

The Khao Kwang Fold and Thrust Belt (KKFTB) (Fig. 2), in the Saraburi province of Thailand, is composed of deformed mixed siliclastic-carbonate sediments that were deposited during the Permian to early Triassic (Dew et al., 2017). Characterised by WNW-ESE to NE-SW oriented thrusts and folds, the KKFTB strikes differently compared to the largely N-S orientated Indosinian Orogeny (Morley et al., 2013). This variation from the general trend can be explained by the speculative presence of a separate terrane that was sutured to the Indochina block during Indosinian stage 1 (Morley et al., 2013). Alternatively, the KKFTB may simply represent a kink in the morphology of the Indochina Block (Arboit et al., 2014). Recent work suggests that extensive sedimentation occurred between ~250Ma and 205 Ma within piggyback basins that developed on top of thrust-sheets in the foreland of the Indosinian Orogen (Arboit et al., 2016). The timing of sedimentation in such syn-tectonic basins, combined with authigenic illite ages within the KKFTB (Hansberry et al., 2017), imply a major period of deformation that began around 250 – 240Ma and lasted until ~225Ma (Indosinian Stage 1). However, structural observations (e.g. Morley et al., 2013 and Arboit et al 2015) suggest that subsequent deformation events have occurred in the region in differing paleo-stress regimes, as demonstrated by an illite age of ~208 Ma (Hansberry et al., 2017).

Calcite twinning analysis (Arboit et al., 2015; 2017) as well as field observations of calcite vein generations (Warren et al., 2014) have identified 5 tectonic regimes that have affected the KKFTB: (1) pre Indosinian extension, with σ3 trending roughly N-S, associated with burial stylolites; (2) N-S oriented strike-slip/compression related to the Indosinian Stage 1; (3) E-W oriented strike-Slip/compression, associated with either Indosinian stage 1 or the amalgamation of a separate terrane block with the Indochina block; (4) largely N-S oriented

folding linked to the Indosinian stage II; and (5) a post Indosinian phase most likely associated with Cenozoic strike-slip activity (Arboit et al. 2015, 2017; Warren et al., 2014).

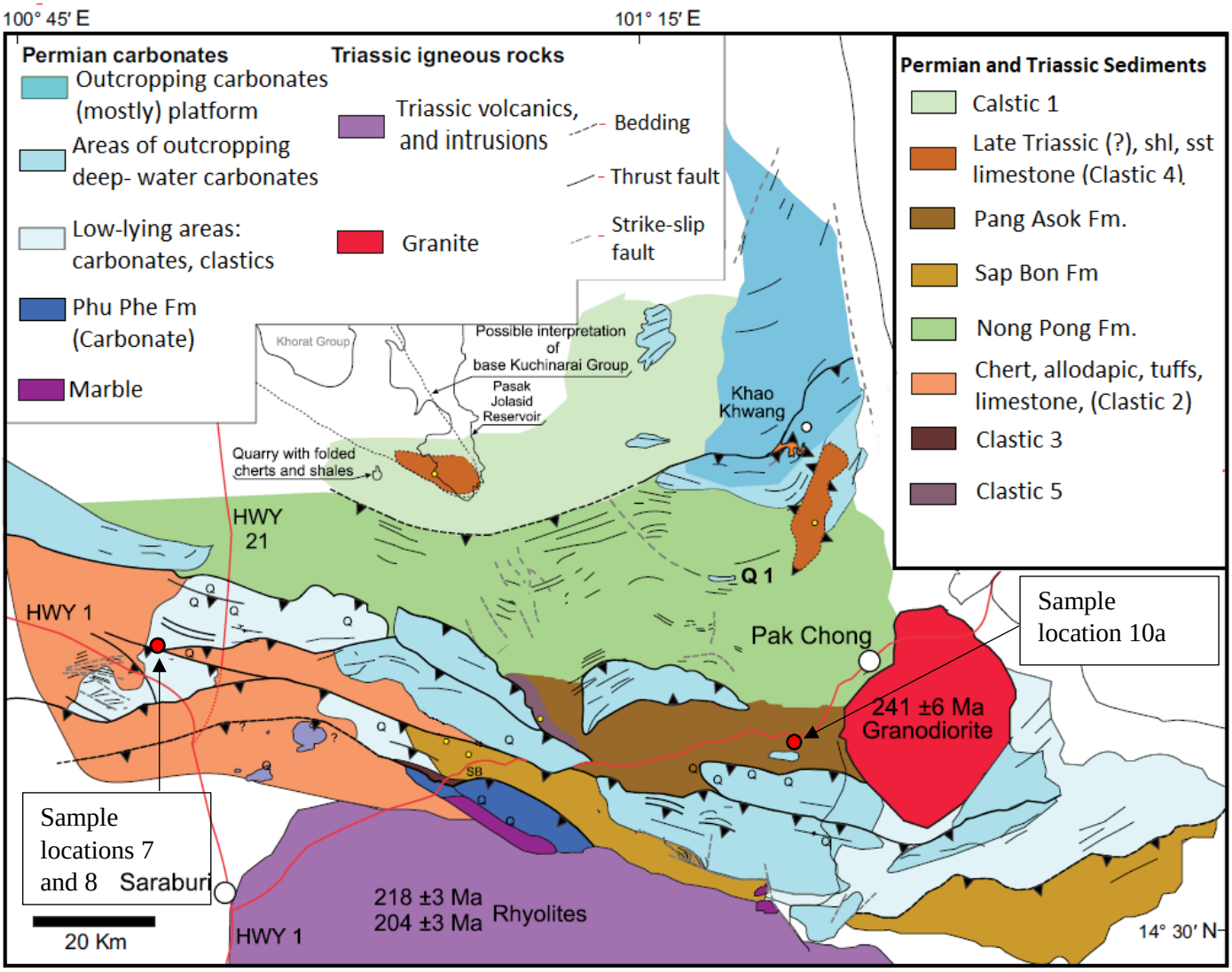

Figure 2: Geological map showing major lithological units and faults form the KKFTB (modified from Arboit et al, 2016 and Morley et al., 2013). Red circle symbols show sample locations.

[2.3] Three Pagodas Fault Zone

Situated within Kanchanaburi Province, the Three Pagodas Fault Zone (TPFZ) is characterised by a series of NW-SE trending strike-slip faults (Rhodes et al., 2005) (Fig.1 and 3) and is estimated to be more than 700km in length (Searle & Morley., 2011). Two episodes of exhumation in the area are suggested by regional apatite fission track (AFT) studies at ~39 – 32Ma and ~24 – 19Ma (Upton et al., 1999) that are both thought to be related with the

India-Eurasia collision and convergence (Rhodes et al., 2005). The first exhumation period coincides with mica Ar-Ar dates (~33 Ma) that are interpreted as being related to late Eocene – early Oligocene ductile left-lateral slip along the TPFZ (Lacassin et al. 1997).

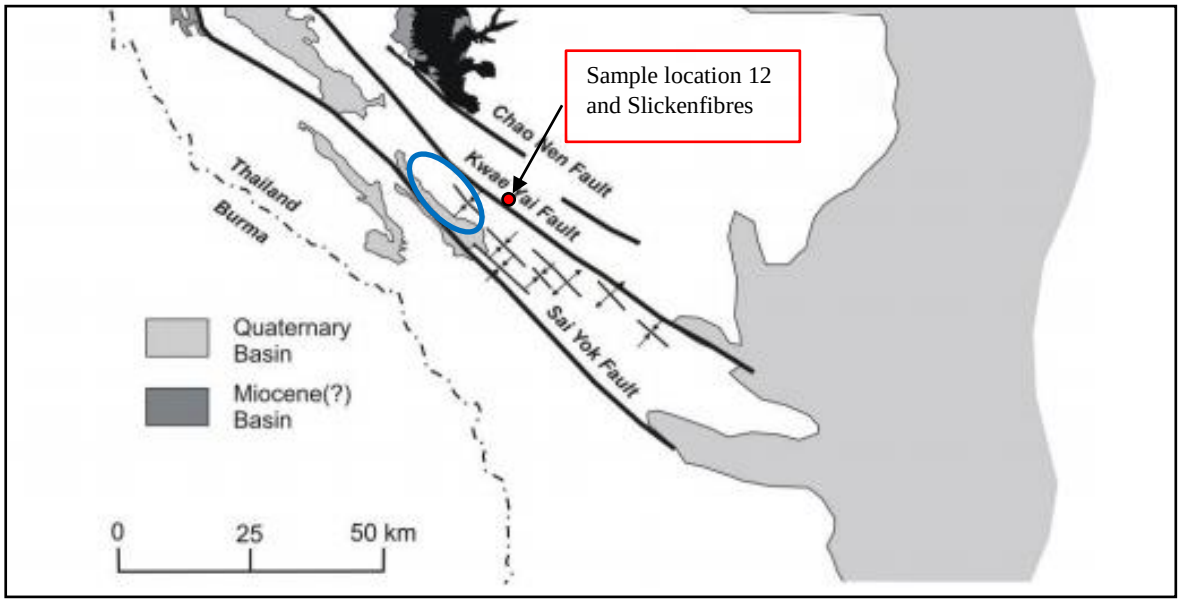

Figure 3: Map showing the major fault strands of the Three Pagodas Fault Zone. Red circle shows sample location for sample 12 and slickenfibres. Blue oval shows approximate location of the Thabsila metamorphic core complex. Modified from Rhodes et al., 2005.

In addition, the Thabsila metamorphic complex (fig. 3) represents a section of high-grade metamorphic rocks that were exhumed by movement along the TPFZ between ~36 and 32Ma (biotite Rb/Sr dates in Nantasin et al., 2012). The younger AFT ages, combined with field observations, are speculatively attributed to a period of late Oligocene – early Miocene brittle dextral faulting along the TPFZ (Upton et al., 1999, Rhodes et al., 2005) (Fig. 5).The presence of pull-apart basins with relevant ages has been used to suggest a dextral transtensional regime at ~24 – 19Ma, caused by the continued movement of India relative to the TPFZ (Rhodes et al., 2005). There is minor evidence for a Pliocene or younger reactivation event, based on observations of meander incision in high-relief areas (Rhodes et al. 2005), however there are no published absolute dates on such event.

[2.4] The Tin Province within the MMMB

The MMMB, composed of metamorphic rocks and granites, stretches from the Andaman Sea in the south to the Eastern Himalayan Syntaxis in the north (Gardiner et al., 2016).

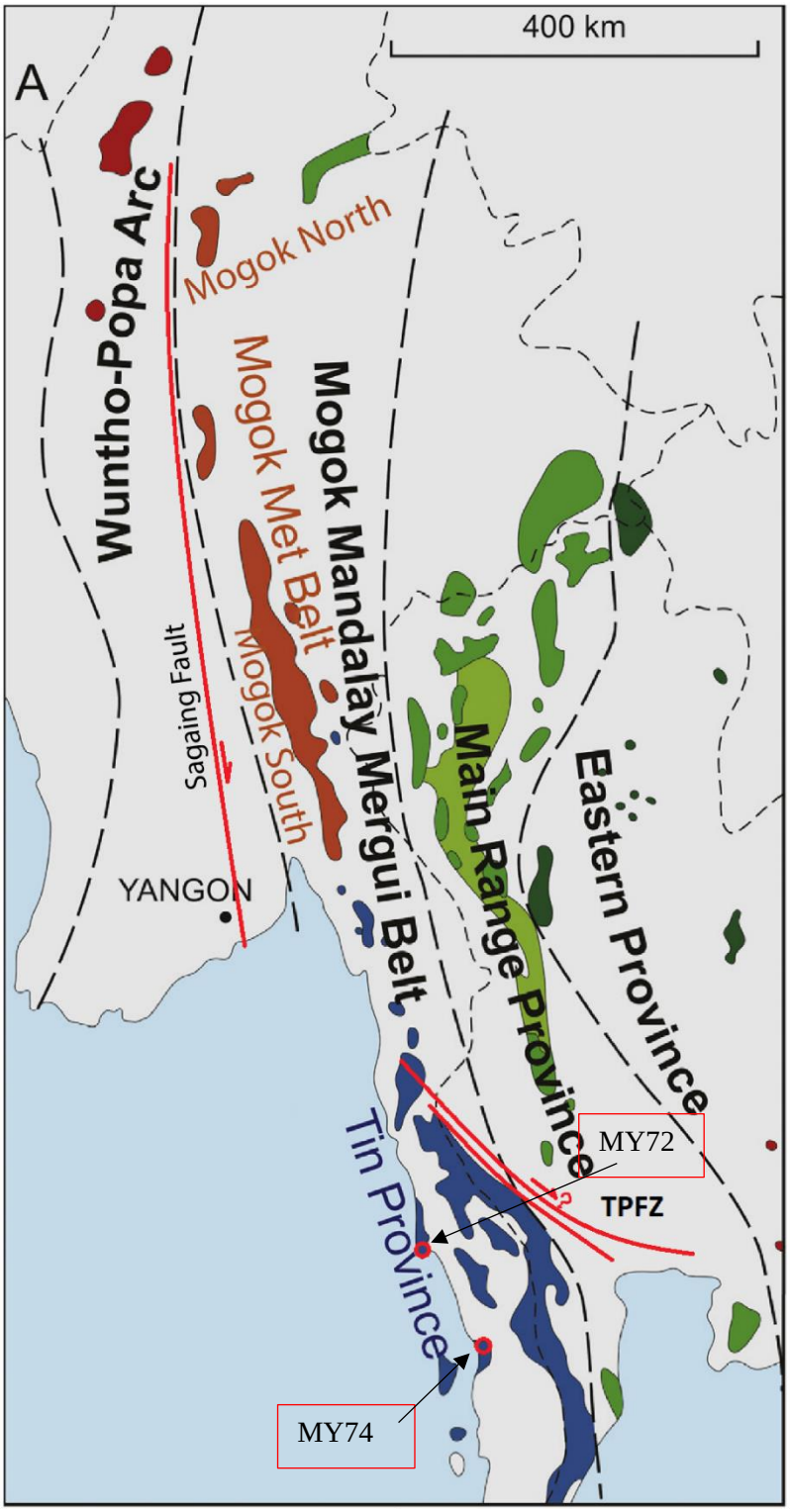

Figure 3: Schematic map showing major magmatic/metamorphic belts of Myanmar. Key faults such as the Sagaing and TPFZ are included for reference. Red circles show the locations for the apatite samples in this study (modified rom Gardiner et al., 2018)

It has been suggested that exhumation of the MMMB occurred during the Paleogene, prior to the 22 – 16Ma initiation of the Sagaing fault that dissects the area (Fig. 4) (Searle et al., 2007). The southern extend of the MMMB, labelled Tin Province, has a different isotopic signature and metamorphic history compared to the main section of the MMMB (Gardiner et al., 2016). Granitoid emplacement in the Tin province occurred at ~77 – 50Ma (Gardiner et al., 2018). The Oligocene – early Miocene timing of deformation has only been established for the Mogok belt (northern MMMB, Fig. 4), based on limited ^{40}Ar-^{39}Ar dates (Bertrand, 1999). It is currently unclear to what extent the Tin province has a similar or different exhumation history to other sections of the MMMB, such as the Mogok belt (fig. 4).

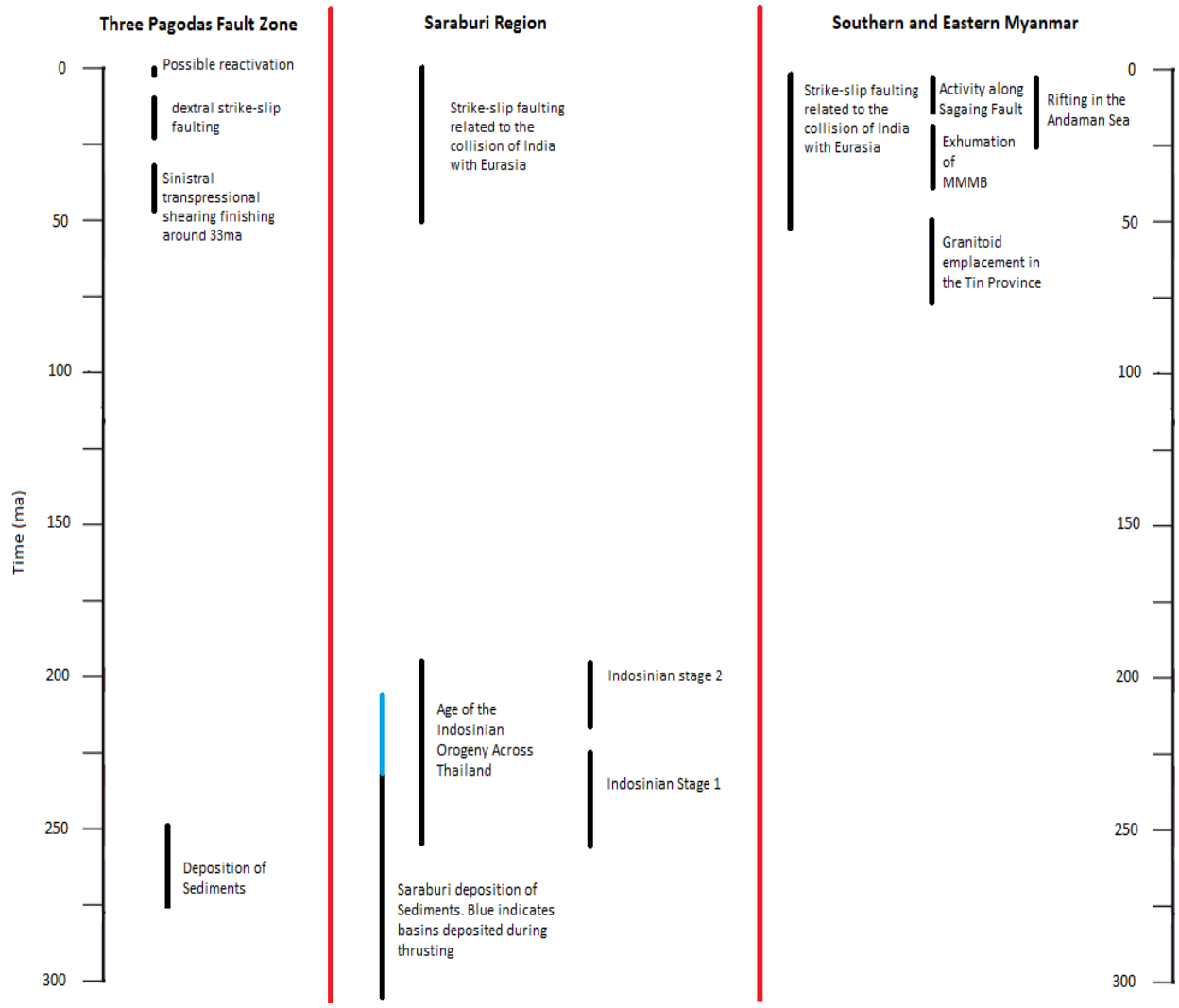

Figure 5: Schematic time-space diagram showing approximate timing of major events in the Khao Kwang Fold and Thrust belt (KKFTB), the Three Pagodas Fault zone (TPFZ), and Eastern and Southern parts of Myanmar. Data based on Arboit et al. (2016), Gardiner et al. (2016), Morley et al. (2013) and Sloan et al. (2017).

[2.4] Sample locations

[2.4.1] Calcite samples

Samples were collected from key areas in both the KKFTB and the TPFZ. Field observations suggest that the veins formed due to fluid infill during brittle faulting. Sample types include bedding parallel veins, folded veins, an overpressured `explosion` breccia, and flexural slip associated veins (including slickenfibres). Generally, the calcite veins are small, blocky to elongated, associated with syntaxial growth (from the outside of the vein inward) indicating probable crack-seal mechanisms (Bons et al., 2012). Most veins were collected directly from fault planes or associated deformation structures (Table 1, Figures 6 and 7). Samples 7b, 8a and 8b were sampled from structures in the *Khao Khad Formation*, comprising massive and bedded carbonates with a maximum depositional age of ~260Ma (Dew et al., 2017). Samples 10a and 10b were sampled from structures in the *Pang Asok Formation* (composed of limestone, shale, chert and sandstone) with a maximum depositional age of ~250Ma (Arboit et al., 2016). The TPFZ samples were taken from structures in a carbonate-rich section of the Permian *Ratburi Limestone* (DMR Thailand, 1999).

A

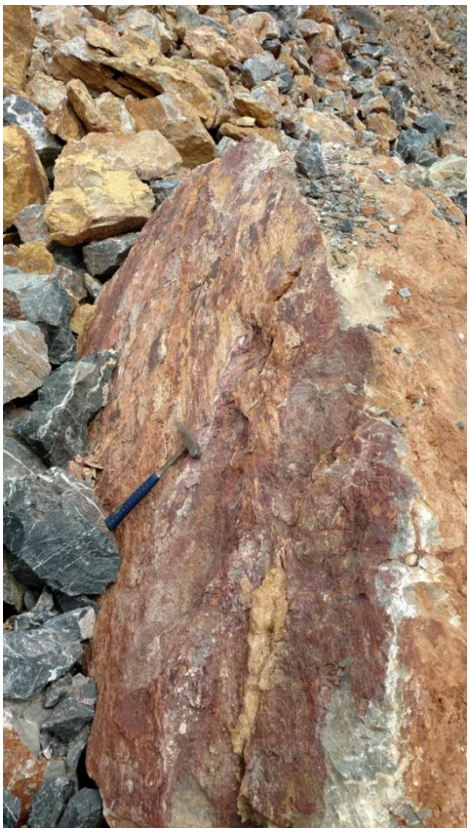

B

C

D

Figure 6: Illustrations of the sample locations in the KKFTB: (A) 7b sample location (vein to the right of the hammer); (B) sampled boulder for sample 8a with the striated slip plane exposed in reddish colour; (C) 10a sample location in (rotated) bedding parallel veins; (D) 10b sample location just opposite the cliff for 10a.

Figure 7: Illustration of the sample location in the TPFZ, where 12a was taken from the highlighted (black lines) pinch-and-swell structure and the slickenfibres were sourced from the folded striated surface near the hammer in the picture.

Sample number	Coordinates	Description (see figure x for pictures)	Vein Style
Khao Kwang Fold and Thrust belt (KKFTB)			
7b	14 2.266'N, 100 53.122'E	Sampled from in the thrust zone of the Khao Yai fault-propagation-fold. Deformation is hypothesised to be Indosinian in age.	Folded vein that runs across the bedding.
8a	14 42.783N, 100.52.250'E	Sampled in the Khao Khao quarry. Taken from a fault plane hypothesised to be Cenozoic in age.	Calcite was sourced from a red and striated boulder that displays remnants of a fault plane.
8b	14 42.783N, 100.52.250'E	Sampled from an over-pressured `explosion` brecciated limestone in the same location as 8a, thought to be Cenozoic in age.	The sample is made up of 2 well-developed calcite crystals.
10a	14 36.554N 101 23.485'E	Sampled in Pak Chong, from veins in a vertical bedding plane. Hypothesised to be Indosinian in age.	Small vein of ~1mm that cross-cuts an older (undatable) vein.
10b	14 36.554N, 101 23.478E	Sampled near sample 10a, from a folded vein, associated with flexural slip. Hypothesised to be Indosinian II.	Slightly elongate blocky crystals, displaying some evidence of growth competition. Syntaxial to stretching.
Three Pagodas Fault zone (TPFZ)			
12a	14 14.011N, 99 14.303E	Sampled in a road cutting on highway 3199 (near Chong Sadao) from a pinch-and-swell structure above a fault plane. Hypothesised to be Cenozoic.	Small (1mm), mostly blocky crystals. Some evidence of elongation/growth competition along vein boundaries. Syntaxial to stretching.
Slickenfibres	14 14.011N, 99 14.303E	Same location as 12a. Sampled from a striated calcite surface in the TPFZ. The slip plane has been subsequently folded. Hypothesized to be Cenozoic.	Individual slickenfibres from the TPFZ fault plane.

Table 1: sample descriptions and locations for calcite samples.

[2.4.2] Apatite samples

Apatites were sourced from granite samples in the Tin province of the MMMB (Myanmar) (fig. 4) (Gardiner et al 2016). The sample locations are relatively close to the TPFZ and are thus expected to have similar cooling histories to other AFT studies conducted in the region. Zircons from the same samples were dated with the U-Pb method at 64.1 ± 1.6 for MY72 and 58.7 ± 0.6 for MY74 (Gardiner et al., 2016).

Sample	Description	coordinates	U-Pb zircon age
MY72	bt + pl + kfs granite	14º08’15”N 98º07’06”E	64.1 ± 1.6
MY74	bt + pl + kfs granite	13º34’05”N 98º25’13”E	58.7 ± 0.6

Table 2: location and age data for the granitoids in the MMMB from which the apatite samples were sourced.

[3] METHODS

[3.1] Calcite U-Pb

[3.1.1] Laboratory Processing

Calcite samples were selected and cut (in ~1cm^3 blocks) to reveal internal sections that cross-cut the veins. Slickenfibres were broken off using a small flathead screwdriver. Subsequently, the calcite pieces were mounted in 1-inch (2.5cm) round mounts using epoxy resin (see appendix for details) and ground (using 2000 grit sandpaper) and polished (using 3µm polishing cloth) to reveal a smooth surface.

[3.1.2] LA-ICP-MS spot-analysis

For each calcite sample, isotopic concentrations (table 3) were measured *in-situ* using laser ablation inductively coupled plasma mass spectrometry (LA-ICP-MS) with an ASI RESOlution-LR 193nm Excimer Laser System coupled to an Agilent 7900x mass spectrometer. Spot analyses were carried out in two analytical sessions (table 3), with standards interspaced throughout. For each sample, approximately 30 to 90 spots were ablated (at 110µm spot size). The data was reduced using Iolite software (Paton et al., 2011). Glass standard NIST614 was used as the primary standard for drift corrections and normalisation of the $^{207}Pb/^{206}Pb$ ratios (Roberts et al., 2017). Subsequently, an in-house matrix-matched carbonate reference material (WC-1) of known age (254 ± 7 Ma; isotope dilution U-Pb data; Roberts et al., 2017) was used for normalisation of the $^{206}Pb/^{238}U$ ratios. In more detail, normalisation was based on the measured versus accepted ratio derived from the session-based drift-corrected mean of the WC-1 reference material (see Roberts et al., (2017) for further details). No downhole corrections were performed, instead the means for each time-resolved isotopic signal at 30s ablation (excluding the first few seconds of data) were used (Roberts et al., 2017). In addition, an in-house calcite sample from the Prague Basin with known biostratigraphic age of ~424 Ma (Farkas et al., 2016), labelled ‘Prague’)

was used as secondary standard for accuracy checks. Calcite tends to contain significant quantities of common Pb and thus requires a significant number of spots ablated for each sample to calculate an accurate U-Pb age. This age is calculated using a linear regression through the ^{238}U-^{206}Pb versus ^{207}Pb-^{206}Pb ratios for each sample on a Tera-Wasserburg Concorida plot (e.g. Chew et al., 2014). The lower intercept of this regression represents the U-Pb age of the sample, which – in the case of the calcite U-Pb method – reflects the timing of calcite growth. Tera-Wasserburg Concordia plots were made using IsoplotR (Vermeersch 2018).

[3.1.3] Calcite Elemental Mapping

Elemental mapping was conducted on selected calcite samples for which the spot U-Pb analyses returned significantly dispersed age data, aiming to reveal a link between possible age populations and elemental zonation patterns. Following U-Pb analysis, the pieces were gently re-polished using the equipment detailed in section 3.1.1. Areas surrounding previously spot-analysed calcite sections were re-ablated and mapped, in raster mode, using the ASI RESOlution-LR 193nm Excimer Laser System coupled with the Agilent 7900x mass spectrometer. Spot sizes of 91 or 134µm (depending on the size of the area to be mapped) were used in the ablation rasters. Data reduction and mapping was conducted using Iolite (Paton et al., 2011). Analytical details are given in Table 3.

Brand and Model	**RESOlution-LR 193nm Excimer Laser System**
Wavelength	193nm
Pulse Duration	20ns
Spot Size (U-Pb analysis)	110µm, (75µm - NIST614)
Spot Size (Elemental mapping)	91x91 – 134x134µm (75µm NIST612)
Repetition Rate	10Hz
Energy Attenuation	100%T (50% NIST612)
Laser Fluency	8 j/cm^2
ICPMS	
Brand and Model	Agilent 7900x
Forward Power	1350W
Torch Depth	4.5mm
Gas Flows	
Plasma (Ar) **Auxiliary (Ar)**	15L/min 1L/min
Carrier (He)	07L/min
Sample (Ar)	0.88L/min
Data Acquisition Parameters	
Data Acquisition Protocol	Time resolved analysis
Scanned Isotopes (U-Pb analysis)	43Ca, 202Hg 204Pb, 206Pb, 207Pb, 208Pb, 232Th 238U
Scanned Isotopes (elemental mapping)	23Na, 25Mg, 27Al, 29Si, 43Ca, 55Mn, 56Fe, 88Sr, 130Ba, 139La, 140Ce, 141Pr, 146Nd, 147Sm, 153Eu, 157Gd, 159Tb, 163Dy, 165Ho, 166Er, 169Tm, 172Yb, 175Lu, 202Hg, 204Pb, 206Pb, 207Pb, 208Pb, 232Th, 238U
Detector Mode	Peak Hopping, Pulse & Analog counting
Background Collection	30 (NIST612) 10 (mapping)
Ablation for Age Calculation	30
Washout	20
Standards	
Primary Standards (U-Pb analysis)	NIST614
Secondary Standards (U-Pb analysis)	WC-1, ‘Prague’
Primary Standards (elemental mapping)	NIST612

Table 3: Analytical details of calcite U-Pb analysis and calcite elemental mapping

[3.2] Apatite Fission Track and Apatite U-Pb Analysis

[3.2.1] Laboratory Processing

Samples were received as mineral separates from Nick Gardiner (Curtin University, Perth). Optical examination was conducted to locate apatite grains under a binocular microscope. The apatite crystals were then mounted in epoxy (see appendix) and ground and polished (using 2000 sandpaper and 3µm and 1µm polishing cloths). Subsequently, the samples were etched using a solution of 5%M nitric acid (HNO_3) at 20±0.5^oC for 20±0.5 seconds to reveal spontaneous fission tracks.

[3.2.2] Fission Track counting

The apatite crystals were individually imaged using a Zeiss AXIO Imager M2m Autoscan System. FastTracks software was used to measure surface track densities and confined track lengths. The fission track density in combination with the ^{238}U concentration is used to calculate a fission track age. This age represents the timing of passage through the apatite partial annealing zone (APAZ) at temperatures between ~60-120^oC (Wagner & Van den haute, 1992). The confined fission tracks are used to examine the rate of cooling through this temperature window.

[3.2.3] LA-ICP-MS Analysis

The concentration of Pb, U and Cl isotopes and other elements including REEs (table 5) were measured by laser ablation inductively coupled plasma mass spectrometry (LA-ICP-MS) using an ASI RESOlution-LR coupled with an Agilent 7900x mass spectrometer. A single 30µm spot was ablated for each grain. Standards were interspaced throughout the analytical session. The data was reduced using Iolite software (Paton, Hellstrom, Paul, Woodhead, & Hergt, 2011) using NIST610 as the primary standard to calculate the U (and other elemental) concentrations. MAD standard (Madagascar) (Chew et al., 2014) was used as the primary

standard for U-Pb analysis. The secondary standards used to check the accuracy of the results were McClure and Durango apatite (Chew et al., 2014).

[3.2.4] Apatite U-Pb analysis

Apatite tends to contain significant quantities of common Pb, rendering robust single grain AUPb age determinations (usually) impossible. The reader is referred to the calcite U-Pb section for details on age calculations. The lower intercept of the calculated regression represents the AUPb age for the sample, which represents the cessation of Pb diffusion (and thus the timing of cooling) below temperatures of 350-550ºC (Chew, Petrus, & Kamber, 2014).

Laser	
Brand and Model	RESOlution-LR 193nm Excimer Laser System
Wavelength	193nm
Pulse Duration	20ns
Spot Size	30µm
Repetition Rate	5Hz
Energy Attenuation	50%T
Laser Fluency	4 j/cm^2
ICPMS	
Brand and Model	Agilent 7900x
Forward Power	1350W
Torch Depth	4.5mm
Gas Flows	
Plasma (Ar) **Auxiliary (Ar)**	15L/min 1L/min
Carrier (He)	07L/min
Sample (Ar)	0.88L/min
Data Acquisition Parameters	
Data Acquisition Protocol	Time resolved analysis
Scanned Isotopes	29Si, 35Cl, 43Ca, 44Ca, 51V, 55Mn, 88Sr, 89Y, 90Zr, 139La, 140Ce, 141Pr, 146Nd, 147Sm, 153Eu, 157Gd, 159Tb, 163Dy, 165Ho, 166Er, 169Tm, 172Yb, 175Lu, 202Hg 204Pb, 206Pb, 207Pb, 208Pb, 232Th, 238U
Detector Mode	Peak Hopping, Pulse & Analog counting
Background Collection	30 (NIST612) 10 (mapping)
Ablation for Age Calculation	30
Washout	20
Standards	
Primary Standards	NIST610, Madagascar apatite
Secondary Standards	Durango apatite, McClure apatite

Table 4: Analytical details for LA-ICP-MS analysis used in AUPb and AFT dating.

[4] RESULTS

[4.1] Calcite U-Pb Results

[4.1.1] Calculation procedures and data accuracy

Two calcite standards were used for (1) isotopic ratio normalisation purposes (WC-1 calcite with U-Pb age of 254.4±6.48 Ma; Roberts et al., 2017) and (2) data accuracy checks (`Prague` calcite with biostratigraphic age of ~424 Ma; Farkaš et al., 2016; and U-Pb age of 422 ± 4 Ma; unpublished in-house data by S. Glorie). Prior to normalisation of the $^{206}Pb/^{238}U$ ratios, the analyses for WC-1, in two analytical sessions, returned intercept ages of 265.3 ± 1.9 Ma and 283.0 ± 2.1 Ma, respectively. WC-1 calcite contains relatively low amounts of common Pb, hindering a statistically robust determination of its common Pb isotopic ratio. Therefore, the isotopic Pb ratio for the Earth`s reservoir at ~265 and ~283 Ma (Stacey and Kramers 1975) was used to anchor the y-intercept of the regression, prior to U/Pb normalisation procedures (Roberts et al., 2017). The resulting normalisation factors for the U/Pb ratios were calculated at 0.95 for session 1 and 0.91 for session 2. These values are in good agreement with `typical` values obtained in Roberts et al., (2017). After the normalisation procedure, WC-1 calcite U-Pb ages of 253.5 ± 1.7 Ma and 255.3 ± 1.9 Ma (fig. 8) and ‘Prague’ calcite U-Pb ages of 425.6 ± 4.3 Ma and 423.9 ± 4.4 Ma (fig. 9) were obtained Both ages are in good agreement (within uncertainty) with the biostratigraphic age and previous U-Pb age determinations, detailed above.

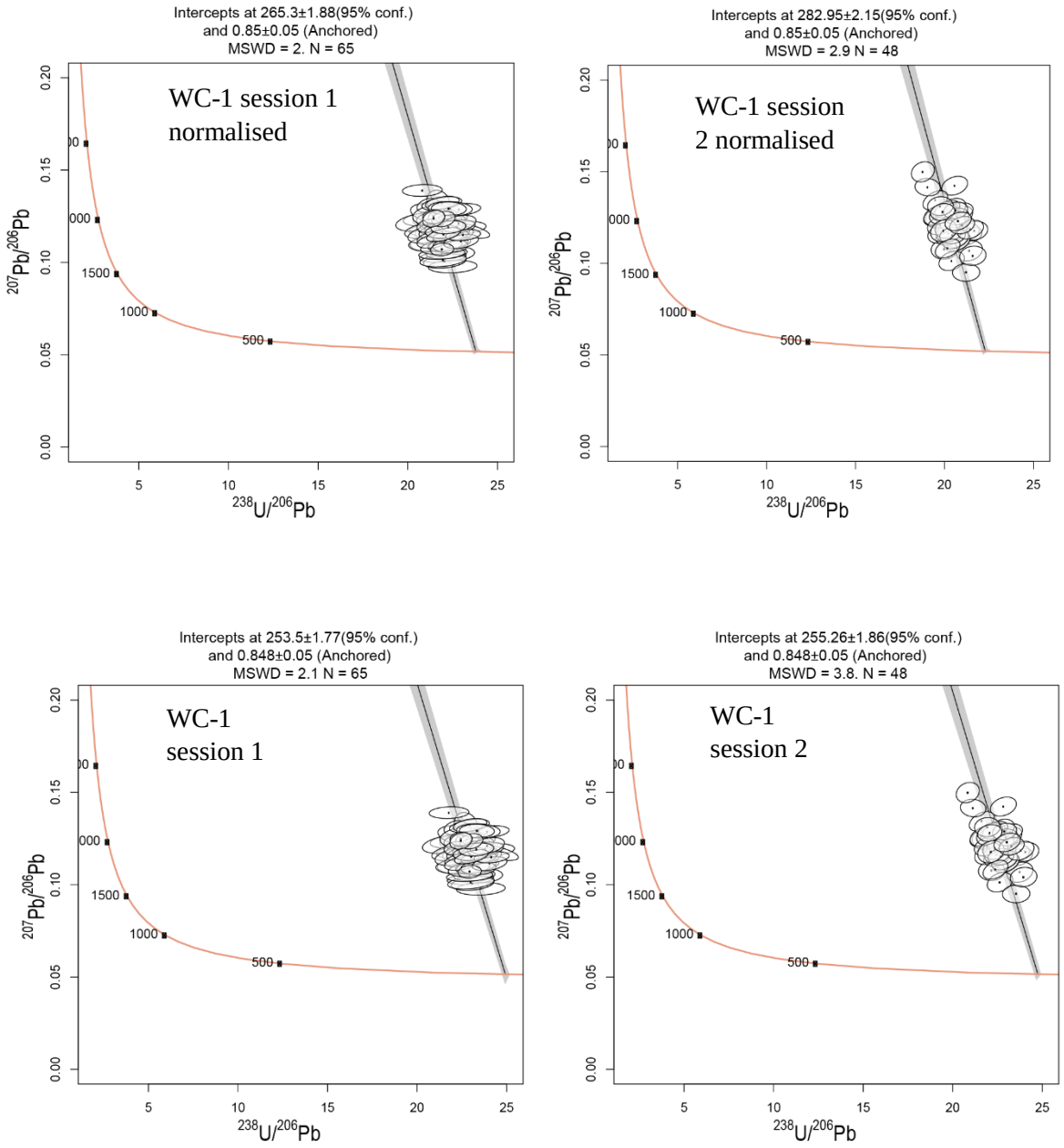

Figure 8: Tera-Wasserburg Concordia plots showing raw and normalised results for the WC-1 secondary standard. Each ellipse represents the 2σ uncertainty on the $^{207}Pb/^{206}Pb$ and $^{238}U/^{206}Pb$ ratios for individual laser spots. Uncertainties on the lower intercept ages are at 95% confidence level. The plots made using IsoplotR (Vermeesch, 2018)

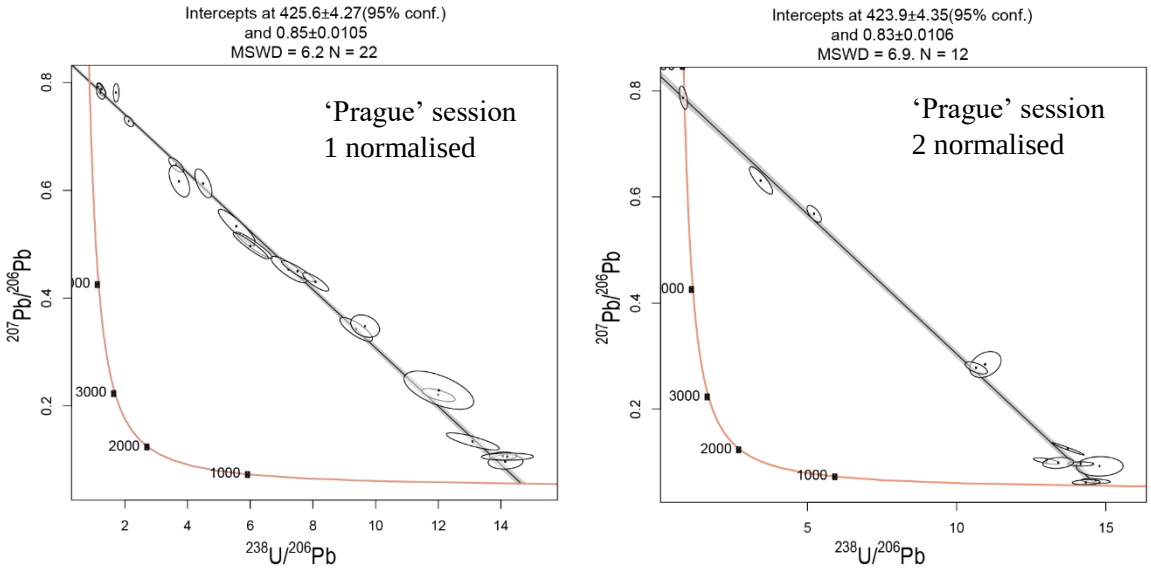

Figure 9: Tera-Wasserburg Concordia plots showing normalised results for the `Prague` secondary standard in two analytical sessions. See caption for Figure 8 for further details.

[4.1.2] Khao Kwang Fold and Thrust Belt

Of the eight samples collected in the KKFTB, seven yielded significant radiogenic Pb to calculate a calcite U-Pb age. Three samples, however, were discarded due to scatter that meant an accurate regression was impossible. The calcite data for the four other samples are reported in the Concordia plots below (Fig. 10). The data vary in complexity with some returning rather precise and consistent Late Triassic calcite U-Pb ages of 215.8 ± 5.3 Ma (for sample 7b) and 216.8±2.2 Ma (for sample 10b). Sample 8b shows three possible age populations (colour coded in Fig. 10) of (1) Oligocene (27.6±4.2 Ma), (2) Early Cretaceous (135.1 ± 10.4 Ma) and (3) Late Triassic (209.8 ± 5.1 Ma) ages. For sample 8a, an imprecise age of 11.01 ± 10.14 Ma was obtained.

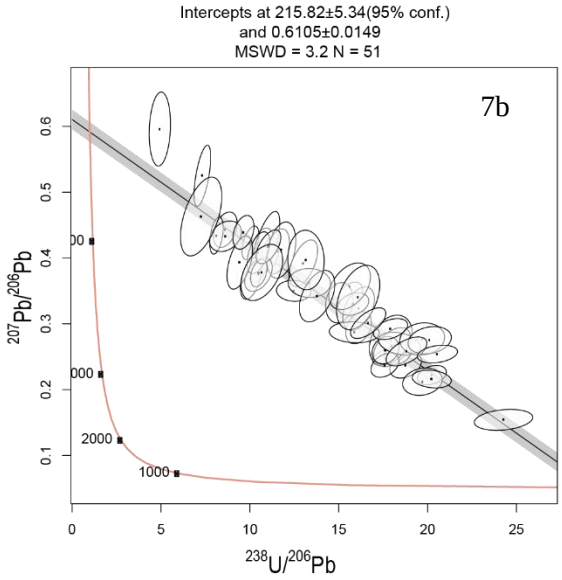

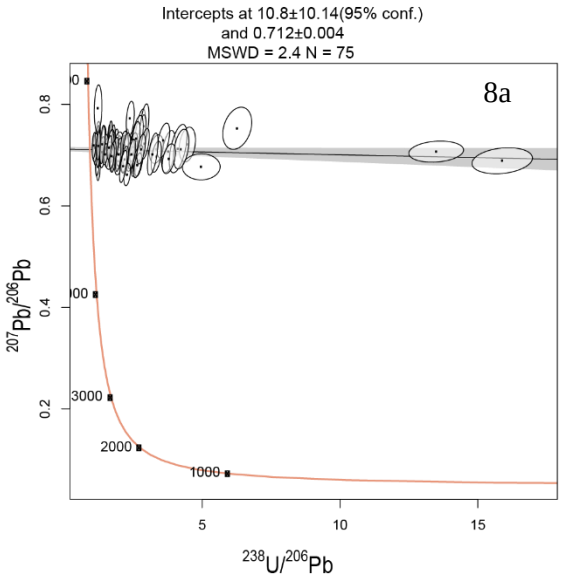

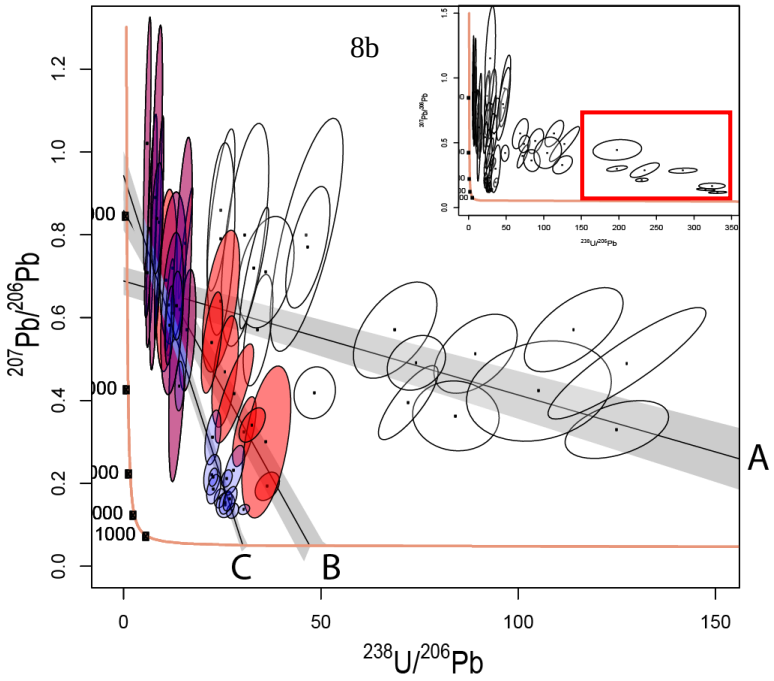

A
Intercepts at 27.56±2.06(95% conf.)
and 0.689±0.033
MSWD = 4.5 N = 29

B
Intercepts at 135.06±5.04(95% conf.)
and 0.859±0.047
MSWD = 1.8 N = 25

C
Intercepts at 209.81±5.13(95% conf.)
and 0.943±0.028
MSWD = 3.8 N = 27

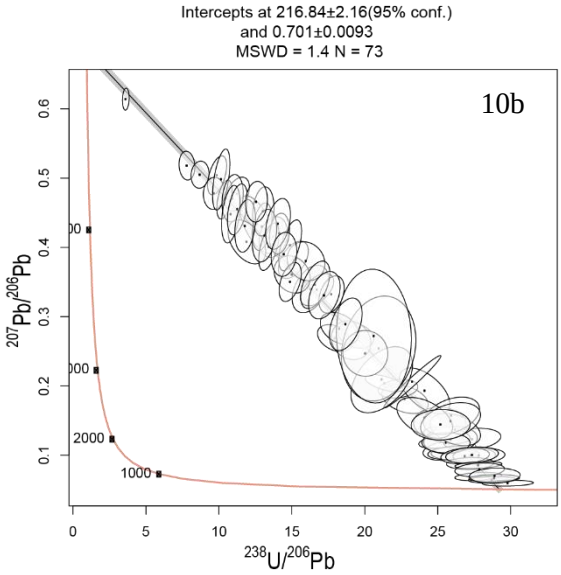

Figure 10: Tera-Wasserburg Concordia plots showing normalised results for the unknowns from the KKFTB. Each ellipse represents the 2σ uncertainty on the $^{207}Pb/^{206}Pb$ and $^{238}U/^{206}Pb$ ratios for individual laser spots. Uncertainties on the lower intercept ages are at 95% confidence level. 8b: top right shows all data poits, red rectangle shows discarded high U/Al spots. Plots made using isoplotR (Vermeesch 2018

[4.1.3] Three Pagodas Fault Zone

For the samples taken in the TPFZ, six samples suffered from high common Pb in proportion to U and were discarded. The successful samples (sample 12a and a series of slickenfibres) reveal rather complex data. Sample 12a returned ages ranging from the late Pliocene to the Eocene. The slickenfibre data also returned a range of ages, with the oldest being 148.1 ± 22.6 Ma and the youngest being 57.8 ± 5.8Ma. U/Pb analyses for the host rock of the slickenfibres gave an age of 248.8 ± 6.3 Ma, and therefore, all analysed slickenfibre samples returned ages that are significantly younger than the age of the host rock. Mean squared weighted deviates (MSWD) vary with most being higher than 2.5. These high MSWD values, reflecting significant data scatter, suggest that the age results should be treated with some caution.

Intercepts at 1.28±1.50(95% conf.)
A and 0.635±0.0076
MSWD = 3.5 N = 16

Intercepts at 23.98±1.05(95% conf.)
B and 0.635±0.0112
MSWD = 4 N = 33

Intercepts at 44.78±2.41(95% conf.)
C and 0.642±0.0066
MSWD = 3.2 N = 45

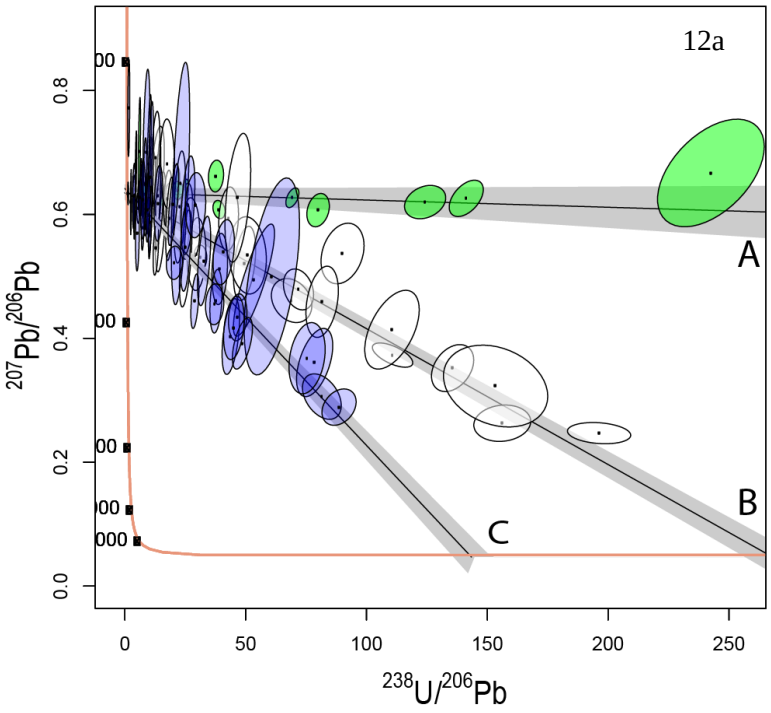

Intercepts at 248.83±6.34(95% conf.)
and 0.842±0.0023
MSWD = 12 N = 30

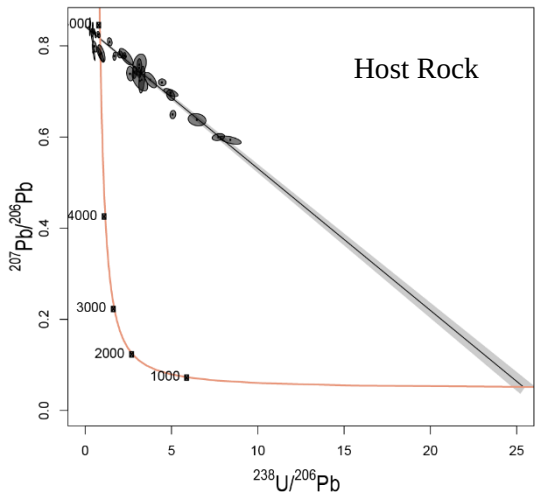

Intercepts at 94.75±6.02(95% conf.)
and 0.65±0.0052
MSWD = 9.3 N = 21

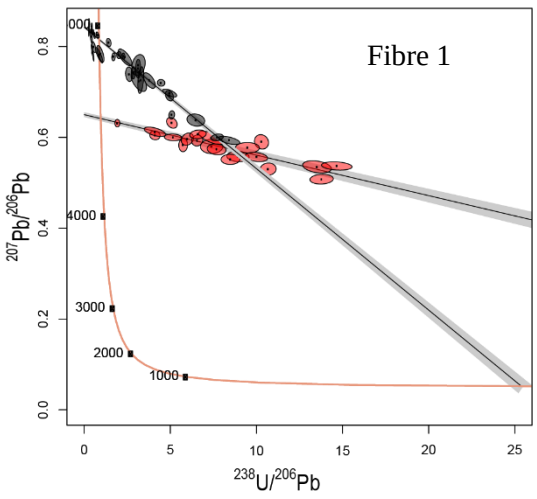

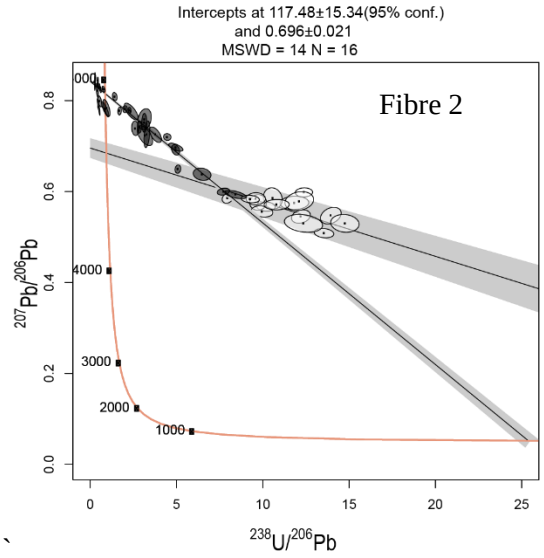
Intercepts at 117.48±15.34(95% conf.)
and 0.696±0.021
MSWD = 14 N = 16
Fibre 2
$^{207}Pb/^{206}Pb$
$^{238}U/^{206}Pb$

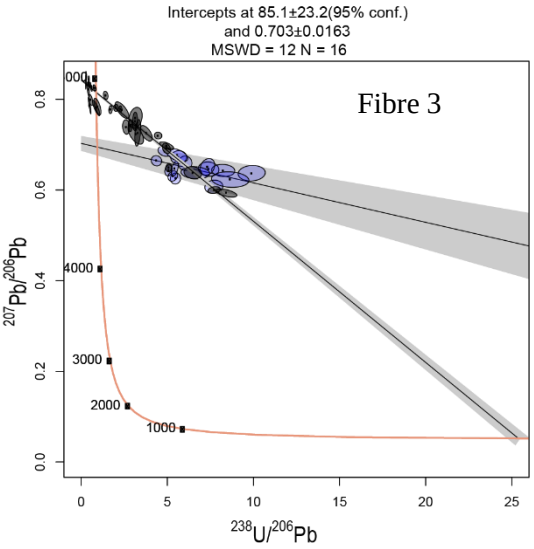
Intercepts at 85.1±23.2(95% conf.)
and 0.703±0.0163
MSWD = 12 N = 16
Fibre 3
$^{207}Pb/^{206}Pb$
$^{238}U/^{206}Pb$

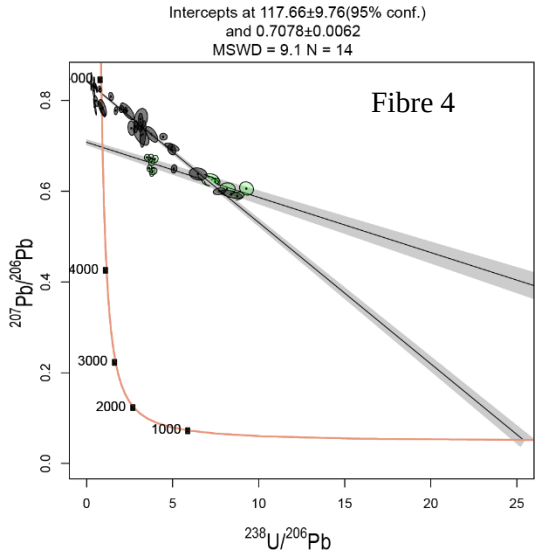
Intercepts at 117.66±9.76(95% conf.)
and 0.7078±0.0062
MSWD = 9.1 N = 14
Fibre 4
$^{207}Pb/^{206}Pb$
$^{238}U/^{206}Pb$

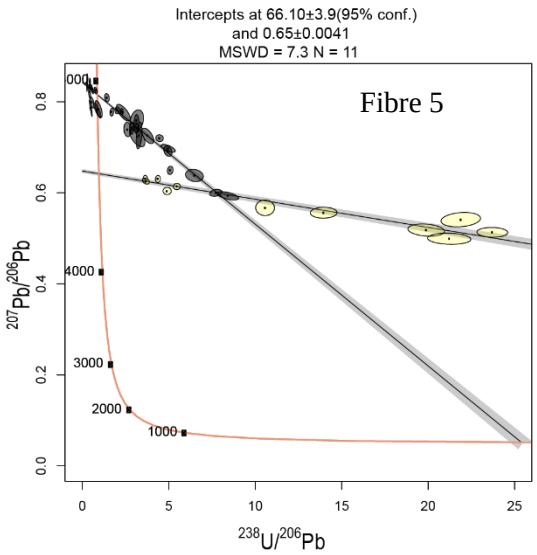
Intercepts at 66.10±3.9(95% conf.)
and 0.65±0.0041
MSWD = 7.3 N = 11
Fibre 5
$^{207}Pb/^{206}Pb$
$^{238}U/^{206}Pb$

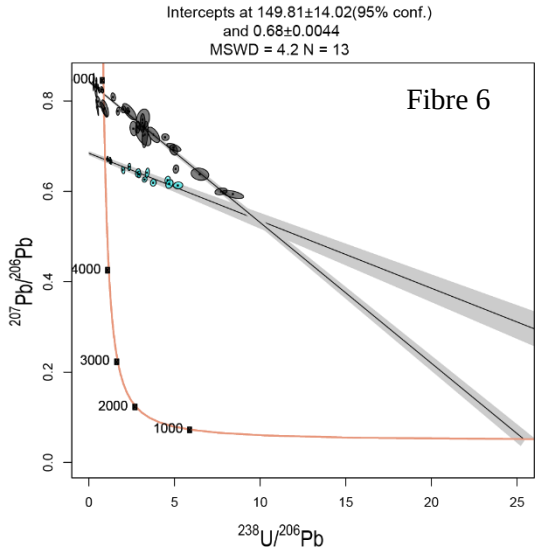
Intercepts at 149.81±14.02(95% conf.)
and 0.68±0.0044
MSWD = 4.2 N = 13
Fibre 6
$^{207}Pb/^{206}Pb$
$^{238}U/^{206}Pb$

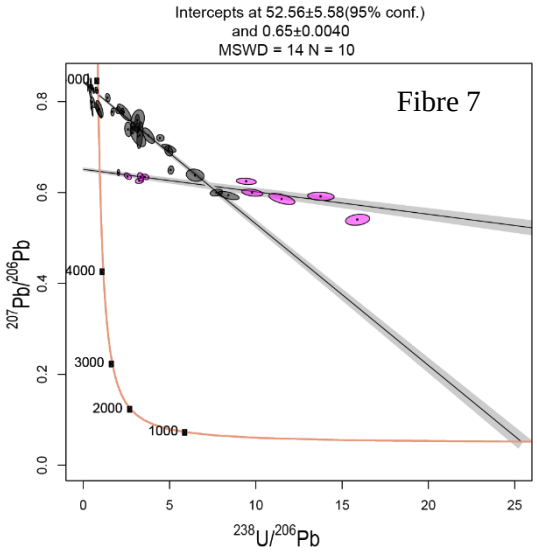
Intercepts at 52.56±5.58(95% conf.)
and 0.65±0.0040
MSWD = 14 N = 10
Fibre 7
$^{207}Pb/^{206}Pb$
$^{238}U/^{206}Pb$

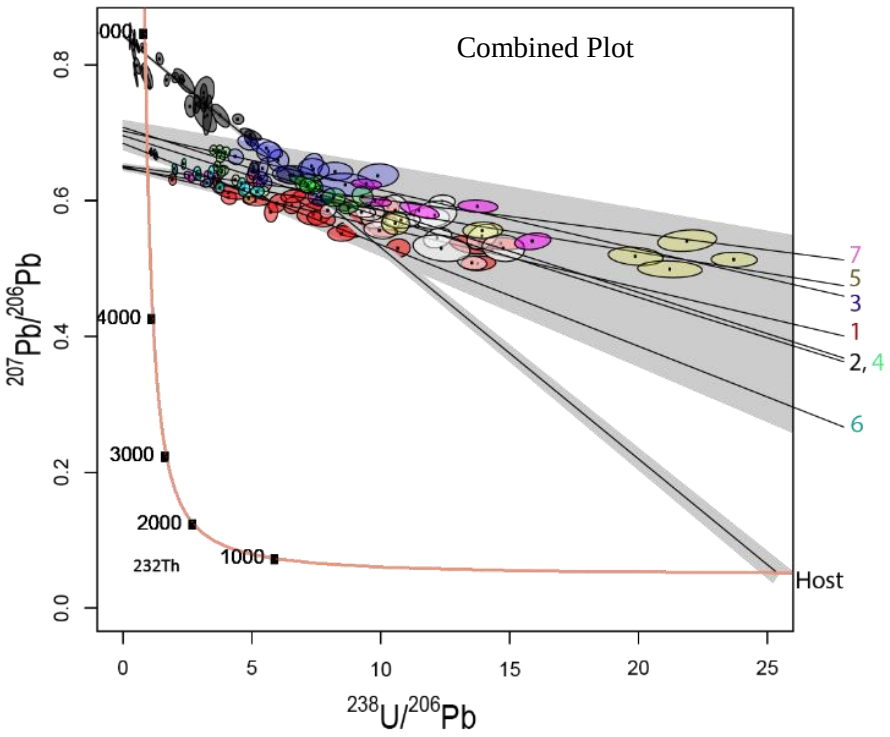

Figure 11: Tera-Wasserburg Concordia plots showing the results for the TPFZ. All slickenfibre plots have the host rock regression line superimposed for reference. In the combined plot (bottom panel), the regression line for each fibre is numbered with the slickenfibre names. Each ellipse represents the 2σ uncertainty on the $^{207}Pb/^{206}Pb$ and $^{238}U/^{206}Pb$ ratios for individual laser spots. Uncertainties on the lower intercept ages are at 95% confidence level. The colours separate the data associated with different age populations preserved in the same piece of calcite. Plots were constructed with IsoplotR (Vermeesch et al. 2018)

[4.1.4] Elemental mapping

Elemental maps, obtained for key samples with highly dispersed age data, show a wide array of variation in elemental concentrations. Generally, two types of useful patterns are detected: (1) a pattern of consistent zonation between different elements, that corresponded to different age populations or (2) high Al, Si, or U zones that corresponded to contaminants (i.e. dirt) in cracks.

Elemental maps for sample 8b show higher uranium and aluminium concentrations that can be associated with optically visible cracks running along the surface (Fig. 12: A, B). Additionally, higher Mn was associated with the younger age population.

Elemental maps for sample 12a show an apparent correlation between zones enriched in some of the LREEs (such as Ce and La) with the oldest U-Pb age population for that sample (see figure 11: 12a).

In order to better quantify the differences in elemental concentrations between the different age populations, the concentration in Mn (for sample 8b) and Ce (for sample 12a) was measured from the elemental maps at each spot location. The results are presented in `Box and whisker plots` and demonstrate a clear correlation between Ce concentration and calcite U-Pb age population for sample 12a (Fig. 13). For sample 8b, the ~27Ma population appears to have a higher Mn content compared to the ~209Ma population. The analyses related to the ~130Ma population have Mn concentrations in between those for the other two populations (Fig 12).

A

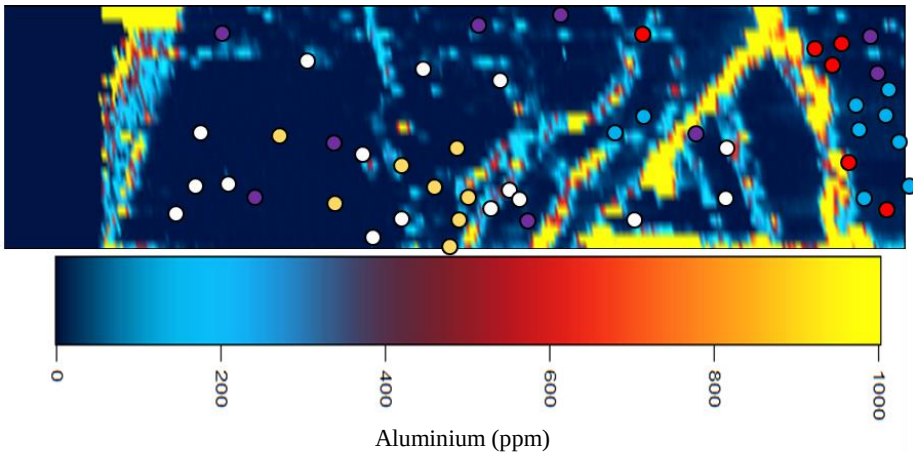

B

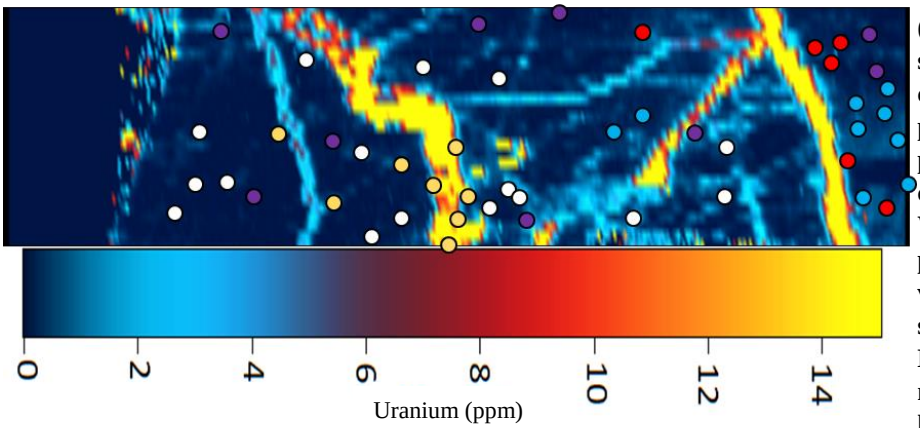

C

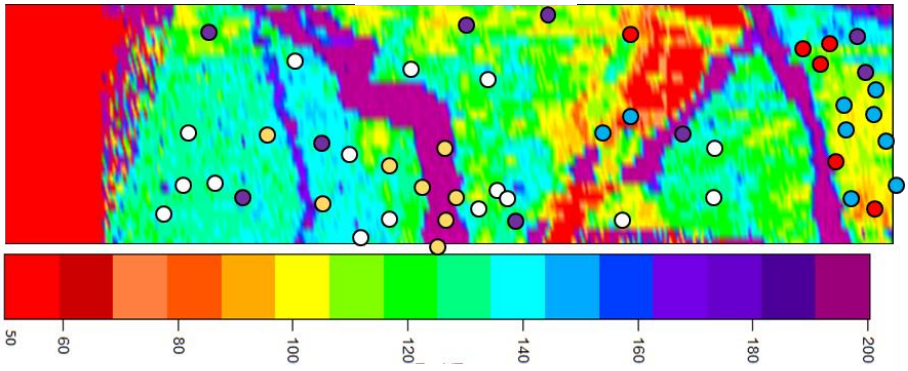

Figure 12: (A) Al elemental map for sample 8b. (B) U elemental map for sample 8b. (C) Mn elemental map of sample 8b. Common to all elemental maps: yellow symbols = discarded high U/Al analyses, purple symbols = high common Pb analyses, white symbolds = ~ 27Ma population, red symbols = ~130Ma population, blue symbols = ~209Ma population.

(D) Box and whisker plots showing measured Mn concentrations versus age populations. The populations are colour - coded to match Tera-Wasserburg Concordia plots. X symbols show mean values, coloured box show 1 standard deviation. Horizontal line shows median values. Upper and lower bounds show maximum and minimum values for each population.

(E) Photograph of sample 8b with interpreted cracks (black lines) and interpreted crystal boundary (blue line).

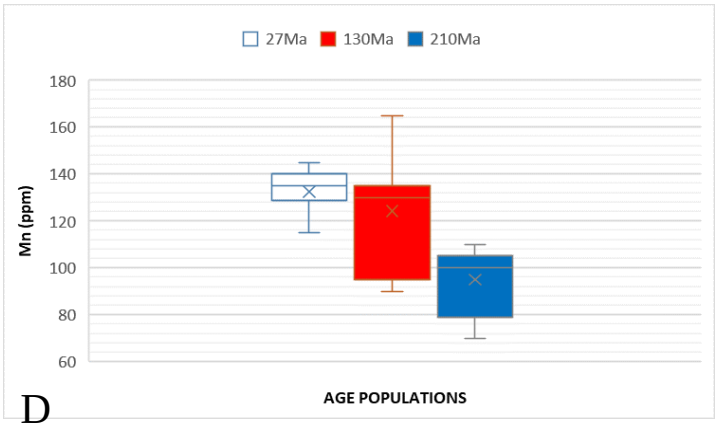

D

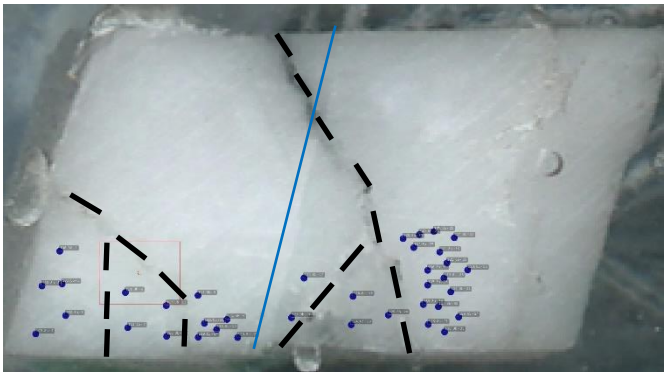

E

12a

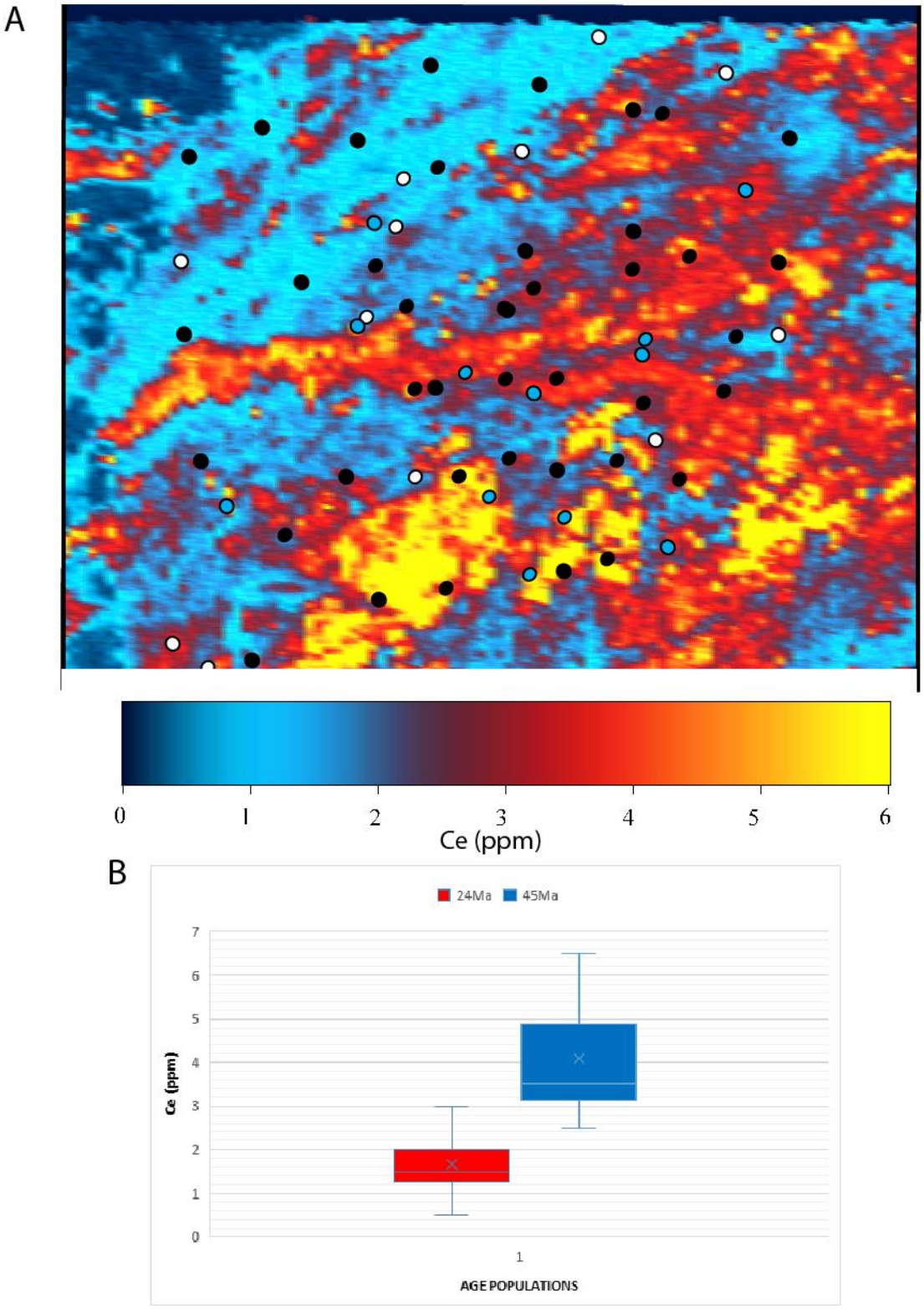

Figure 13: Ce elemental map and box and whisker plot for sample 12a. (A) Ce elemental map with LA-ICP-MS spots superimposed. (The symbols are colour-coded to match the colours used in the Tera-Wasserburg Concordia plots). White symbols = ~24Ma population, blue symbols = ~45Ma population, black symbols = high common Pb spots. (B) Box and whisker plot of age population v Ce concentration for sample 12a.

[4.2] Apatite U-Pb Results

[4.2.1] Data accuracy

To check the accuracy of the apatite U-Pb results, secondary standards (Durango and McClure apatites) were interspaced between the unknown apatite samples during analysis. Durango apatite returned a U-Pb age of 34±4Ma, and McClure apatite returned a U-Pb age of 516±10Ma. Both calculated ages are within uncertainty in agreement with previously published ages (31.44±0.18 for Durango, and 524.6±3.2 for McClure; Mcdowell et al., 2005; Schoene and Bowring, 2006). These results indicate that the obtained apatite U-Pb ages in this study can be used with confidence.

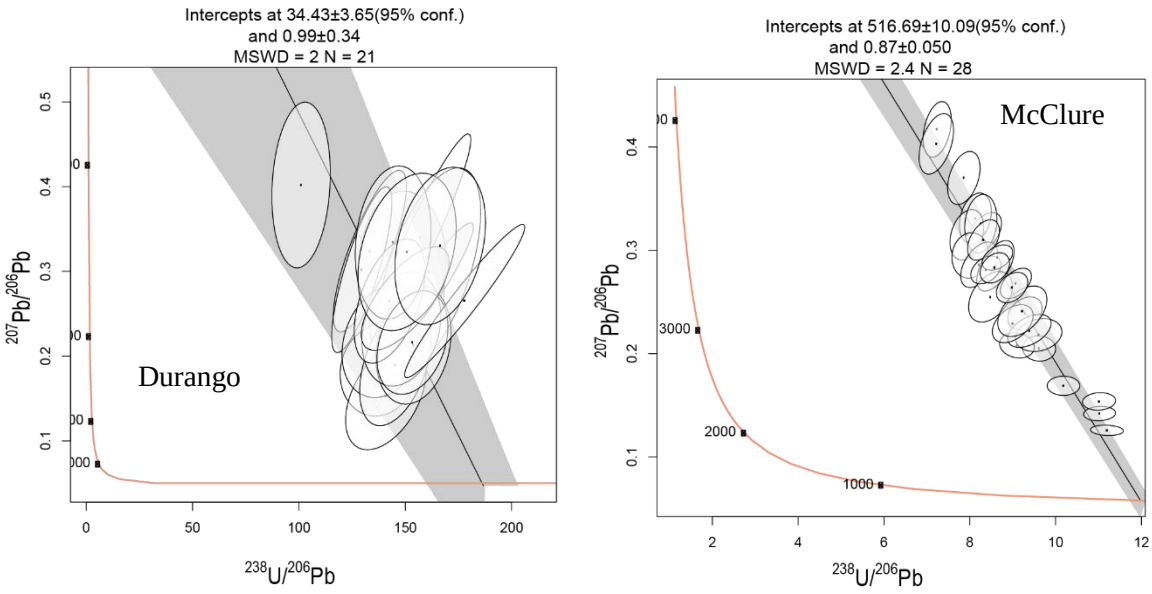

Figure 14: Tera-Wasserburg Concordia plots showing the results for the apatite standards. Each ellipse represents the 2σ uncertainty on the $^{207}Pb/^{206}Pb$ and $^{238}U/^{206}Pb$ ratios for individual laser spots. Uncertainties on the lower intercept ages are at 95% confidence level.

[4.2.2] Tin Belt (Myanmar)

Two apatite samples, taken in proximity to the TPFZ, were analysed. The MSDW values are within the expected range for a single population, suggesting that the isochron linear

regressions are appropriate and the lower intercept ages are good representations of the apatite U-Pb ages for the samples. The obtained apatite U-Pb ages (MY72 = 60.4 ± 4.8 Ma, and MY74 = 58.0 ± 2.5) are in excellent agreement (within uncertainty) to the previously published zircon ages for the same granites (MY72 = 64.1 ± 1.6 Ma, and MY74 = 58.7 ± 0.6 Ma; Gardiner et al., 2016).

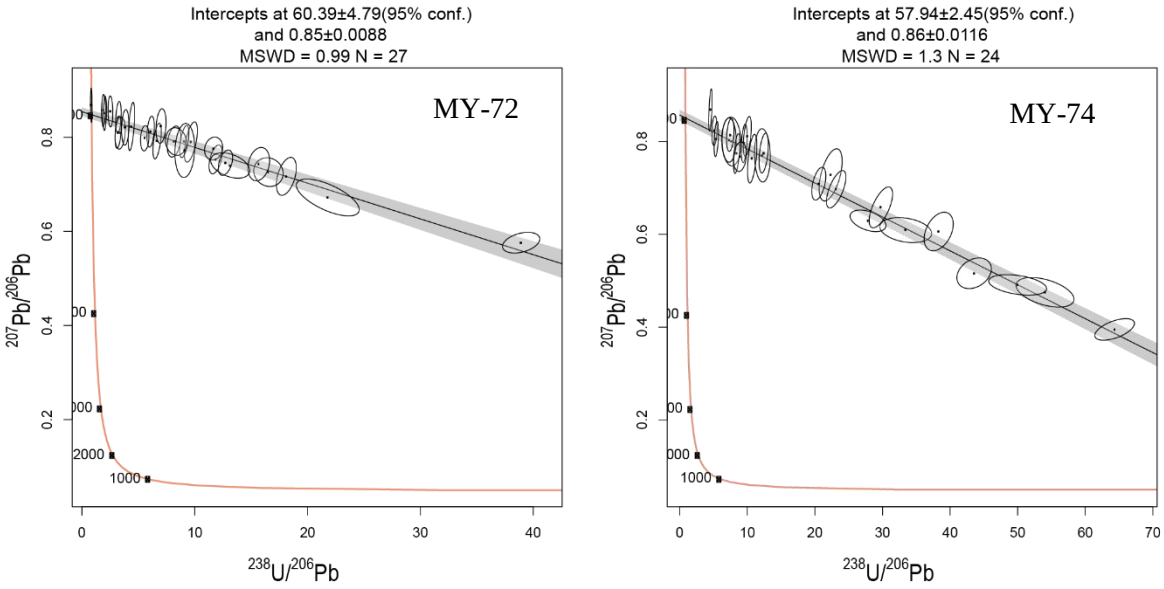

Figure 15: Tera-Wasserburg Concordia plots showing the results for the Myanmar apatites. Each ellipse represents the 2σ uncertainty on the $^{207}Pb/^{206}Pb$ and $^{238}U/^{206}Pb$ ratios for individual laser spots. Uncertainties on the lower intercept ages are at 95% confidence level.

[4.3] Apatite Fission Track (AFT) results

[4.3.1] Data Accuracy

Single grain-AFT ages for unknown samples were corrected with a zeta calibration factor based on Durango apatite measurements (Vermeesch, 2017). The obtained mean AFT age of 30.4 ± 1.3 Ma (Figure 8) is in good agreement (within uncertainty) to the published $^{40}Ar/^{39}Ar$ age of 31.44 ± 0.18 Ma (McDowell et al., 2005), suggesting fission track counting results and LA-ICP-MS analysis yield reliable results.

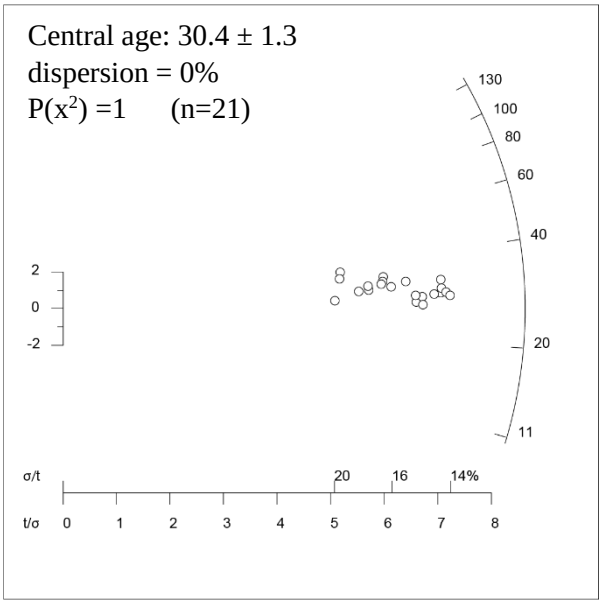

Figure 16: Radial plot showing AFT central ages for the Durango apatite standard. Single grain AFT ages weighted against precision (t/σ) such that more precise single grain ages exert greater weighting on the final central age calculation.

[4.3.2] Radial Plots

Resulting radial plots (fig. 17), showing apatite central ages are given below. For sample MY72 an AFT age of 26 ± 3Ma was obtained with low single-grain age dispersion. The single-grain age data shows no correlation with different elemental proxies for enhanced annealing (eU, Th, or Cl) (fig 17: MY72), suggesting that the central AFT age is an appropriate estimate for the AFT cooling age. Sample MY74 shows significant single-grain age dispersion, indicating the presence of two age populations. The older peak of 56 ± 4 Ma overlaps with the respective apatite U-Pb age (58.7 ± 0.6 - Gardiner et al., 2016). The younger peak yields an AFT age of 19 ± 1 Ma. The single-grain analyses related to the younger populations correlate with relatively higher eU and Th concentrations (fig. 17: MY74-eU, MY74-Th), compared to those for the grains in the older population. No correlations were found with respect to the Cl (fig. 17: MY74-Cl) concentrations in this sample. The mean confined track length for sample MY74 is 11.62 ± 1.4µm (1σ) (Table 5, fig. 18). MY72 did not contain sufficient confined tracks to gain a representative sample.

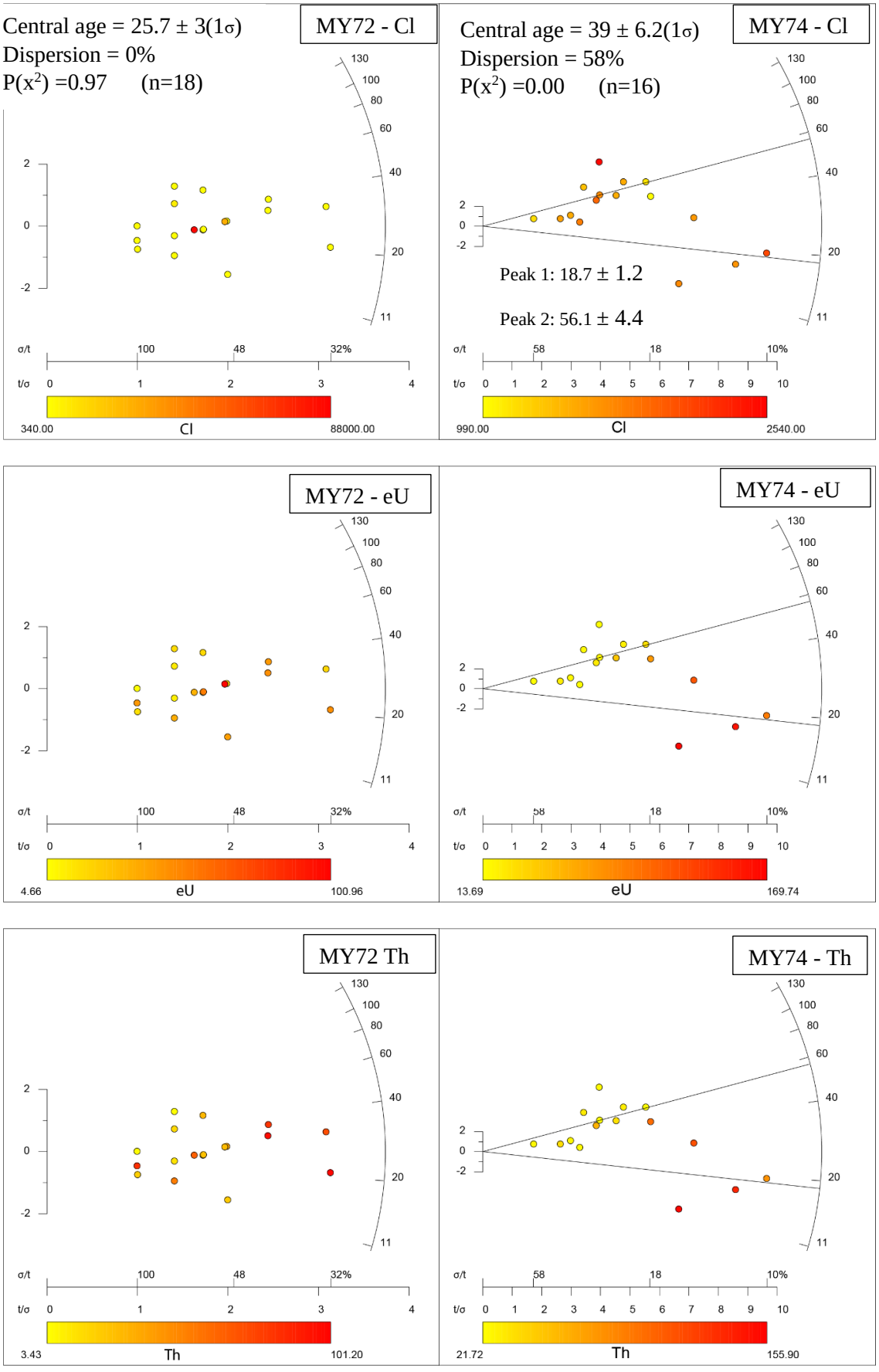

Figure 17: Radial plots showing AFT central ages for the Myanmar apatite samples. Single grain AFT ages weighted against precision (t/σ) such that more precise single grain ages exert greater weighting on the final age peak. Samples plotted with respect to Chlorine (Cl), effective Uranium (eU) (calculated using eU = [U] + 0.235[Th] (Flowers et al., 2009) and Thorium (Th) concentration for each apatite grain.

Sample	ρ_s(x10^5/cm^2)	Ns	n	^{35}Cl (ppm)	1σ (ppm)	^{238}U (ppm)	1σ (ppm)	t (Ma)	1σ (Ma)	nl	MTL (µm)	1σ (µm)	Disp (%)	P(χ^2)
MY72	1.83	166	18	577.3	272.6	17.53	10.02	26.4	3.2	N/A	N/A	N/A	0	0.98
MY74	4.90	478	16	1626.25	376.6	41.46	43.83	39	6.2	18	11.62	1.41	40	0

Table 5: AFT results. ρs represents the average surface density of spontaneous fission tracks. Ns represents the total number of spontaneous fission tracks counted in all grains analysed in the sample. n is the number of grains analysed in the sample. ^{35}Cl (ppm) represents average concentration of 35Cl in analysed grains, with uncertainty given as 1σ. 238U represents average concentration of 238U in analysed grains, with uncertainty given as 1σ. T represent population AFT age with uncertainty given as 1σ. nl is the number of confined tracks measured from all grains in a sample. MTL is the mean track length of confined tracks per sample, with uncertainty quoted as 1σ. Disp. represents the percentage of dispersion of single grain AFT ages calculated with Radial Plotter. P(χ2) is the chi-squared probability that all grains in a sample belong to a single age population.

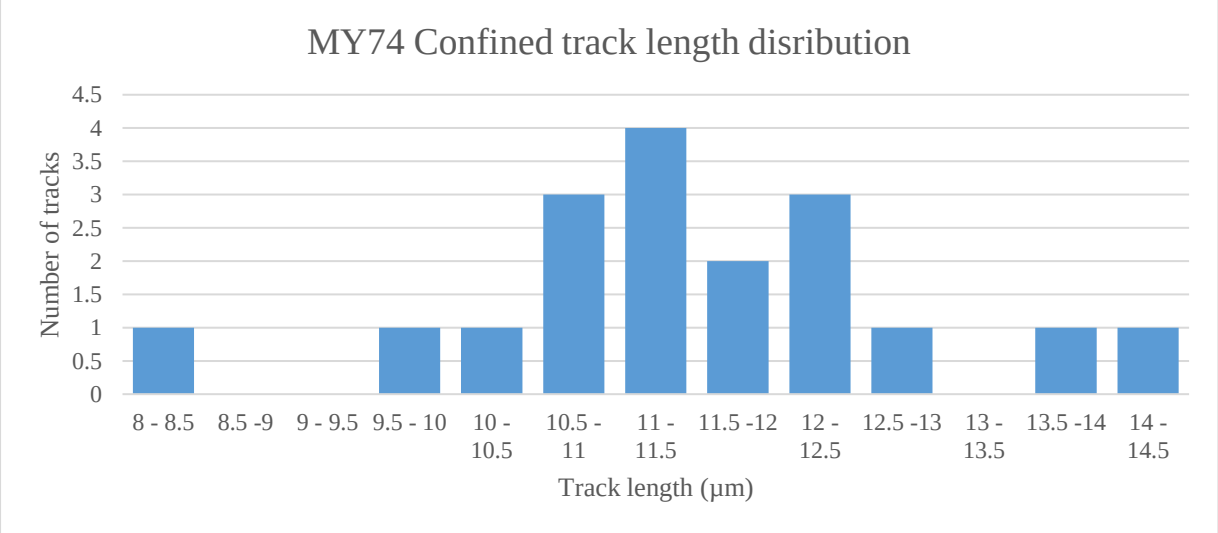

Figure 18: Confined track length distribution for apatite sample MY74.

[5] DISCUSSION

[5.1] Calcite U-Pb dates

[5.1.1] Relationship between U-Pb dates, calcite growth and (brittle) deformation

With any dating method, it is crucial to understand the process being dated. Tectonic veins form due to the opening and subsequent filling of fractures (Bons et al. 2012). Tectonically induced fractures can occur in two ways; either due to 'opening' where displacement is perpendicular to the fracture plane (extensional), or due to some form of shearing (Bons et al. 2012). For the calcite dates to be accurately associated with the timing of faulting, calcite infilling should occur relatively quickly after fracture opening. Crack seal-textures, in which veins periodically open and new calcite precipitates through the centre, are associated with rapid precipitation occurring at the time of fracture opening (Roberts & Walker, 2016). Syntaxial and stretching vein growth is associated with this mechanism while antitaxial vein growth is generally associated with slow precipitation (Bons et al., 2012). Veins from this study tend to have blocky textures, with little to no younging toward the centre (syntaxial) or toward the edges (antitaxial). This would imply that they fall somewhere on the syntaxial/stretching continuum (Bons et al., 2012) and probably represent crack-seal veins.

Based on experiments on Pb diffusion using synthetic calcite, Cherniak (1997) suggests that the isotopic Pb composition in 1mm calcite crystals will be preserved at 300°C (or colder) for longer than the age of the earth, and at 400^{o}C, it will be preserved for at least ~280Ma. Larger crystals should be affected more slowly by volume diffusion, allowing for the timing of calcite growth to be preserved at higher temperatures. Therefore, volume diffusion after calcite growth should have little influence on the U-Pb systematics when dating brittle faulting, as temperatures are likely below 300-400^{o}C in the brittle part of the crust (Scholz, 1989). Hydrothermal fluids are unlikely to induce volume Pb diffusion unless they remain at high temperatures for millions of years (Cherniak, 1997) and are more likely to simply

precipitate more calcite i.e. by crack seal mechanism (Roberts and Walker, 2016; Bons et al., 2012). Hence, given the field-relations of the sampled calcite with prominent brittle structures, the calcite U-Pb dates likely constrain the timing of calcite growth during fluid circulation associated with (brittle) fault activity.

[5.1.2] Limitations of the applied calcite U-Pb methodology

Given the current lack of a matrix-matched primary standard, the U-Pb isotopic ratio needs to be normalised against secondary standards (see section 4.1.1). There is inherent uncertainty in this process that is currently not fully propagated to the total uncertainty of the analysed samples (as this uncertainty is yet to be appropriately quantified; Roberts et al., 2017).

In addition, the calculated common Pb compositions (based on the upper intercept $^{207}Pb/^{206}Pb$ ratios) for the samples in this study are usually significantly different from expected values based on the Pb evolution model of the Earth (Stacey and Kramers, 1975). The differing common Pb values are theorised to be related to the inherited isotopic Pb composition of the surrounding host-rock or the source-rock where the fluids were generated. A similar explanation was suggested for anomalous initial Pb intercepts found in titanite (Kirkland et al., 2017). Therefore, open system behaviour between host rock and the precipitating fluid that forms the calcite veins, is likely. The extent of potential host-rock (or older calcite in general) inheritance is further discussed below.

Furthermore, the extent of dispersion of single-spot analyses needs to be evaluated. Overdispersion (highlighted by high MSWD values on the regression lines) may be due to heterogeneous initial common Pb compositions. However, modelling conducted by Rasbury and Cole (2009) has suggested that initial common Pb should not significantly affect the accuracy of the isochron, assuming there is a large number and significant spread of data points along the regression line. Alternatively, the higher than natural MSWD`s may be

associated with undetected zoning between U and Pb or suggest that multiple age populations are present that cannot (easily) be separated due to limited age differences.

These methodological limitations are considered in further discussion of the calcite U-Pb results for this thesis.

[5.1.3] Khao Kwang Fold and Thrust Belt

Sample 7b was taken from a thrust fault in a fault propagation fold of the Khao Yai Fault. It has been assumed previously that this structure developed during the Indosinian Orogeny (Morley et al., 2011). The obtained calcite U-Pb date of 215.8 ± 5.3Ma agrees with this interpretation and constrains the timing of calcite growth to the Indosinian II deformation phase (roughly ~220 – 190Ma; Morley et al., 2013). Hence, the timing of brittle fault displacement in the Khao Yai Fault is interpreted to be contemporaneous with the Indosinian stage II. This sample had relatively low calcite surface area and, therefore, analysis of more sections of 7b may reduce the uncertainty in the age.

Sample 8a was sampled from a fault plane with structural characteristics of a (Cenozoic) strike-slip fault. The obtained calcite U-Pb age (10.8 ± 10.1Ma, fig. 11: 8a) should be treated with caution due to its ~100% uncertainty and potential limitations in dating young samples. However, Richards et al (1998) has shown agreement between U-series dating and U-Pb dating of a ~250Ka calcite speleothem, demonstrating that U-Pb dating of calcite can provide useful dates for very young samples. Unlike the sample used by Richards et al (1998), however, 8a contains relatively high common Pb, and the isochron relies heavily on only two data points. Therefore, no solid conclusions can be drawn for this sample, besides that calcite growth or recrystallization has likely occurred in the last 20 Ma. This supports the hypothesis that the strike-slip fault, from which 8a was sampled, has likely been active during the

Neogene, and is probably related to hypothesised contemporaneous activity along the Mae Ping Fault (fig. 1; Arboit et al., 2017; Morley et al., 2013).

Sample 8b was taken from the same location as sample 8a, from a large crystal in an explosion breccia. Elemental maps of sample 8b demonstrate significant increases in U and Al along visible cracks (figs. 12: A, B). Particularly the high Al concentration suggests that the cracks are filled with a different mineral phase (such as clay minerals) and, therefore, the data associated with those cracks was not included in further interpretations. In addition, the elemental maps revealed a zone of high U (up to 1500% increase) that is not always obviously related to surface cracks. These high uranium spots were also treated as outliers (likely different mineral inclusions) and removed from the data-set. The data for sample 8b demonstrates the importance of using elemental mapping, as the extent of these inclusions is not always apparent purely from optical examination.

The calcite sample is composed of two crystals that are joint by a 60-120^{o} cleavage fracture (fig. 12: E). The ~209Ma and ~130Ma age populations correlate with one crystal, while the ~27Ma spots largely plot on the other (fig. 12: E). Additionally, the ~209Ma population appears to correlate with zones of low Mn concentrations compared to the ~27Ma population (fig. 12: C). The ~27Ma zone may, therefore, possibly represent re-precipitated calcite that is enriched in Mn.

The ~27Ma age population for sample 8b corresponds with apatite fission track ages (~39-19 Ma) in the vicinity (Upton 1999), as well as with Ar-Ar dates on Cenozoic structures such as the TPFZ (Lacassin et al., 1997). Therefore, following the interpretation given for the AFT and Ar-Ar dates, sample 8b likely records Cenozoic deformation that can be linked to the far-field effects of the India-Eurasia collision (Rhodes et al., 2005). The ~209Ma age population in sample 8b corresponds with a ~208Ma authigenic illite age in the KKFTB (fig. 19;

Hansberry et al. 2017), demonstrating that parts of the calcite sample preserve U-Pb ages that correspond to fault movement associated with Indosinian stage 2 deformation (Morley et al., 2013). It is therefore envisaged that the calcite initially grew during the Indosinian Orogeny and that parts were subsequently recrystallised during a Cenozoic deformation phase. Given the clear separation of both age populations, and for the reasons given above, it`s unlikely that the age-disparity is related to volume diffusion. Additionally, few data points reveal a calcite age population of ~130Ma that doesn`t correlate with any known regional tectonic event and that likely represents a mixing age between the ~209Ma and ~27Ma calcite growth events. The position of the ~130Ma spots along cracks associated with the crystal boundary (fig. 12: E) supports that parts of both crystals were blasted together in the ~130Ma spots, homogenising the different ratios, and leading to a mixing age that is nearly exactly the median between the two other populations. The ~130Ma age population is hence not discussed further.

Sample 10b was sourced from a vein that formed in relation to flexural slip and folding. The sample gave the most precise age (216.8 ± 2.2 Ma) of all analysed samples in this study, with an uncertainty of just 1% on the isochron intercept age. Note that the uncertainty on the normalisation was not propagated (section 4.1.1) and, therefore, the total uncertainty may be larger by ~20-30%. If the calcite in this sample was affected by significant heterogeneity in initial Pb, Pb/U loss/gain, or recrystallization, a much larger age dispersion would be expected (Rasbury & Cole, 2009). Thus, this vein almost certainly precipitated soon after fracture opening and did not recrystallise subsequently. This age correlates with the 215.8 ± 5.3Ma age of sample 7b (fig. 19) and dates flexural slip in relation to folding during the Indosinian stage 2 (Morley et al., 2013).

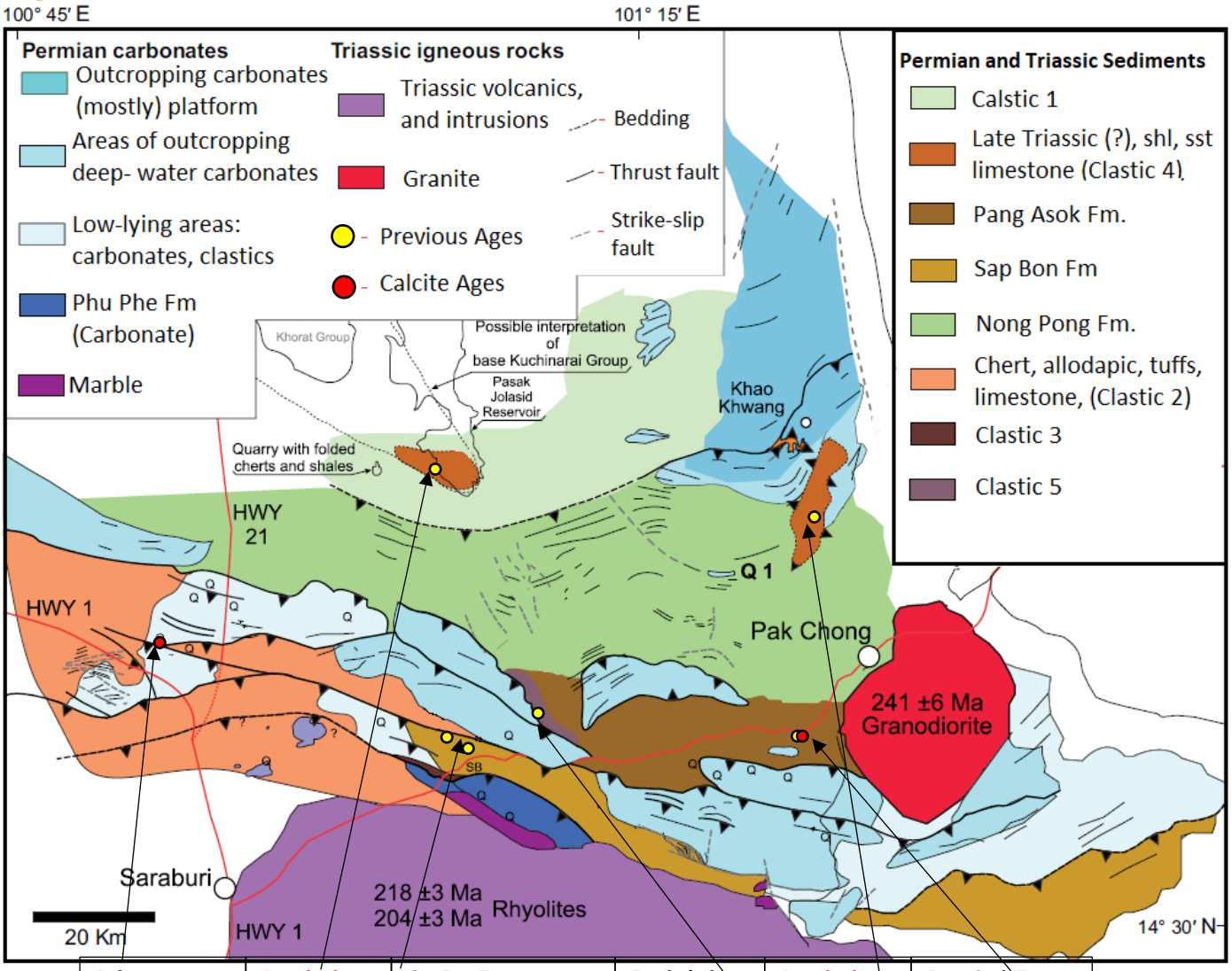

Indosinian ages: (7b): 216±5Ma (8b): 210±5Ma Younger ages: (8b): 135±10.4 (8b): 28±4Ma (8a): 11±10Ma	Piggyback basin depositional age: 224±4Ma (Arboit et al., 2017)	Sap Bon Formation depositional age: 275±4Ma (Arboit et al., 2017)	Brittle fault movement: 208±4.6Ma (Hansberry et al., 2016)	Piggyback basin depositional age: 217±4Ma (Arboit et al., 2017)	Pang Asok Fm. depositional age: 251±3Ma (Arboit et al., 2017) deformation ages (10b): 217±2Ma

Figure 19: geological map showing major formations of the KKFTB. With data from this study, Arboit et al., 2016 and Hansberry et al., 2017 included (Modified from Arboit et al., 2016. Original - Morley et al., 2013)

[5.3] Three Pagodas Fault Zone:

Successful age determinations were obtained for samples from vein-filled pinch-and-swell structures, found on the fault plane of the TPFZ (sample 12a), and slickenfibres collected from a folded section of the same fault (fig. 7). Stable isotope analysis conducted on veins from the same location reveals very negative $\delta^{18}O_{PDB}$ (-18 to -24%) values, interpreted to represent an allochthonous, deep, hot fluid, that underwent open system behaviour with its surroundings (Nazrul, 2015). The open system behaviour may suggest that inherited common and radiogenic Pb from the host rock was incorporated into the fluid and subsequently precipitated in the calcite (discussed further in relation to the slickenfiberes). This represents a potential limitation of U-Pb calcite dating that may impact samples without good constraints on the initial common Pb ratio.

Sample 12a preserves three populations. A very young age of ~1.3Ma is associated with an individual vein. The other two age populations of ~24Ma and ~45Ma can be distinguished by LREE zonation (fig. 13: A). The ~24Ma population correlates closely with the onset of the ~24 – 18Ma period of regional uplift/denudation (Upton 1999, Rhodes et al., 2005) near the TPFZ. The older population (~45Ma) correlates with areas of higher Ce and other LREEs. Additionally, there is a mild inverse correlation with the HREEs. Ce/Yb ratios have been used previously to distinguish between different calcite generations (Maskenskaya et al., 2013). Similarly, Barker (2007) proposed that Ce changes may be related to fluid changes. Furthermore, REE distributions have been proposed as a proxy for fluid properties, similar to $\delta^{18}O$. In more detail, correlations of Ce concentrations with $\delta^{18}O$ ratios have been drawn recently (Roberts, 2018). Therefore, the higher Ce calcite likely represents a different fluid event, that is partially preserved in the ~24Ma calcite vein.

The ~45Ma high Ce calcite may be associated with the proposed ~39 – 32Ma episode of ductile deformation in the TPFZ (Rhodes et al., 2005). Given that ductile deformation does

not occur at the surface (Sholtz, 1989), it is possible that the ~45Ma isochron represents a translation of the dextral shear to brittle faulting at the surface.

The young population (~1.3Ma) for this sample suffers from limitations previously discussed for sample 8a, and thus the absolute age should be treated with caution. This age may relate to recent <5Ma reactivation, associated with the presence of high topographic relief and meander incision (Rhodes et al., 2005) or possibly be related to a late stage of rifting in the Andaman Sea (Sloan et al., 2017).

The slickenfibre data shows a wide range of ages, from ~148Ma to ~53Ma. This significant range is problematic, given that the calcite crystals that make up the slickenfibres should theoretically grow during a single fault movement (Bons et al., 2012). The host-rock was dated at ~250Ma (see figure 8), which is only slightly younger than the expected Permian deposition age (DMR Thailand, 1999). For the host rock data, a $^{207}Pb/^{206}Pb$ intercept of 0.84 was obtained, which suggests that it was in equilibrium with expected $^{207}Pb/^{206}Pb$ values (Stacey and Kramers, 1975). The slickenfibres data, however, suggest $^{207}Pb/^{206}Pb$ intercepts of ~0.65 to ~0.7, indicating the presence of inherited radiogenic Pb. Therefore, the Pb isotopes, measured in the slickenfibre calcite, seem to be affected by open-system behaviour (see section 5.1.1). In addition, the large scatter in $^{207}Pb/^{206}Pb$ ratios for individual analyses (high MSWD values) may be associated with an initial heterogeneity in common Pb (Rasbury & Cole., 2009), and, therefore, supports open-system behaviour. Furthermore, the older fibres lack good constraints on the lower intercept in the Tera-Wasserburg plots (Fig. 11), which may suggest that the younger fibres with more radiogenic Pb have more accurate age constraints. The age range for the slickenfibres can be explained by different proportions of host rock contamination (i.e. mixing of the carbonate host rock with new calcite that precipitated as slickenfibres leading to a larger data spread and older ages) and, therefore, the younger fibres more accurately represent the timing of deformation.

An alternative (less likely) explanation for the range of ages could be related to aseismic creep. In this process, multiple small-scale fault slip events lead to the dissolution and sealing of microcracks after the slickenfibre formation event. This explanation was posited by Goodfellow et al (2017) as a possible explanation for age discrepancies between different calcite slickenfibres. Aseismic creep, however requires a major seismic event to initiate at the timing of the oldest slickenfibre dates (Çakir et al., 2012). However, there is no evidence in support of a late Jurassic – Early Cretaceous (~149-117Ma) deformation event in the study area. Hence, an explanation in terms of aseismic creep is unlikely for the studied samples in the TPFZ.

The youngest slickenfibres (~66Ma and ~53Ma) are only slightly older than the age of the high-Ce calcite in the same outcrop (~45Ma). Given the most likely scenario of open-system behaviour between host rock and slickenfibre growth, the timing of slip could still be (slightly) later than the youngest slickenfibre date (as there may still be some host-rock contamination present). Hence, the timing of fault slip and associated calcite recrystallization in the slickenfibres may be contemporaneous with the high-Ce fluid alteration event (at ~45 Ma). This event may be linked to a major period of right-lateral shear along the nearby Ranong fault (Fig. 1) at ~48-40 Ma (^{40}Ar-^{39}Ar ages - Watkinson et al., 2011). It has been suggested that the Ranong fault is the southern continuation of the TPFZ through the Gulf of Thailand (Morley, 2002), which may explain a similar deformation history. Subsequent left-lateral shear along the TPFZ at ~24Ma (Rhodes et al., 2005) can then be correlated with the calcite recrystallization (low-Ce calcite) at ~24Ma. These ages match with the two groups of fission track ages at ~39 - 32Ma and ~24 - 19Ma in both Thailand (Upton, 1999) and Myanmar (this work) and may reflect the timing of escape tectonics in response to the India-Eurasia collision (Rhodes et al., 2005) and subsequent rifting in the Andaman Sea (Morley & Searle., 2017).

[5.4] Myanmar apatites

The central age of apatite sample MY72 (~26Ma) is in good agreement with the 24 – 19Ma exhumation ages for the TPFZ (Rhodes et al., 2005) and can be correlated with the timing of low-Ce calcite growth (~24Ma in sample 12a).

Sample MY74 showed two peaks of ~18Ma and ~56Ma. The older AFT age corresponds to the apatite and zircon U-Pb age and is thus related to the crystallisation and post-magmatic cooling of the granitoid from which the sample was taken. The difference in effective uranium and thorium between the two populations are thought to reflect a difference in annealing rates (e.g. Hendriks & Redfield, 2005). In more detail, studies have indicated that damage caused by the release of α-particles may lead to radiation enhanced annealing of fission tracks (Hendricks & Redfield, 2005). α-particles are predominantly released by the decay of U and Th and the effective U content is used as a proxy for radiation enhanced annealing (Flowers et al., 2009). Therefore, it is hypothesised that sample MY74 entered the APAZ soon after crystallization. The sample spent an extended period in the APAZ before being further exhumed during the Neogene (~18Ma). The different radiation enhanced annealing behaviour between the apatite populations resulted in the partial preservation of the ~56 Ma AFT ages for low eU grains and the presence of a secondary (~18Ma) event, recorded in the high eU grains. This ~18Ma age correlates with the final stages of the proposed 24 – 18Ma period of exhumation (Upton, 1999), as well as with significant rifting in the Andaman sea, contemporaneous with sea-floor spreading in the Sewell and Alcock rises at around 20Ma (Morley and Searle, 2017).

[6] CONCLUSIONS

(1) U-Pb dating and elemental mapping of calcite precipitated in tectonic veins can be used to constrain the timing of tectonic events. There are, however limitations. Stable isotope

analysis, Cathodoluminescence imaging and fluid inclusion analysis are among the techniques that could potentially enhance our understanding of the U-Pb calcite dates.

(2) REE concentrations, may be a useful proxy for investigating different calcite generations and precipitating fluid, but further research is required to establish the mechanisms behind this.

(3) The KKFTB deformed during the mid-Late Triassic. In more detail, regional faulting and folding occurred at ~216Ma and 209Ma associated with the Indosinian Orogeny stage II.

(4) Calcite and apatite data from this study, integrated with previous dating results, suggest a two-stage brittle deformation history for the TPFZ at ~52-45Ma and at~24Ma-18Ma.

(5) A period of exhumation was dated in the Tin Province (Myanmar) at ~26Ma-18Ma, agreeing with previous AFT studies in Thailand.

[7] ACKNOWLEDGEMENTS

I'd like to thank my supervisor Stijn Glorie for giving me this opportunity and for taking me to China. I'd like to thank Jack Gillespie for helping me with calcite U-Pb analysis and elemental mapping. I'd like to thank Gilby Jepson, Angus Nixon, and Alex Otasavic for helping me with apatite U-Pb and AFT analysis. I'd like to thank everyone who helped, especially Sarah Gilbert from Adelaide Microscopy for helping me on the LA-ICP-MS and polishing machine. I'd like to thank Chris Morley and Nick Gardiner for providing samples. Lastly, I'd like to thank Alec Walsh for helping me throughout the year, sorry I broke your 1-inch epoxy mould.

[8] REFERENCES

ARBOIT, F., COLLINS, A.S., KING, R., MORLEY, C.K., HANSBERRY, R., (2014). Structure of the Sibumasu–Indochina collision, central Thailand: a section through the Khao Khwangfold-thrust belt. *J. Asia Earth Sci*. 95, 182–191.

ARBOIT, F., AMROUCH, K., COLLINS, A. S., KING, R., MORLEY, C. K. Determination of the tectonic evolution from fractures, faults, and calcite twins on the southwestern margin of the Indochina Block. Tectonics 34 (8), 1576-1599

ARBOIT, F., COLLINS, A.S., MORLEY, C., KING, R., AMROUCH, K., (2016). Detrital zircon analysis of the southwest Indochina terrane, central Thailand: unravelling the Indosinian orogeny. *Geol. Soc. Am. Bull*. 128, 1024–1043.

ARBOIT, F., AMROUCH, K., MORLEY, C., COLLINS, A.S., KING, R., (2017). Palaeostress magnitudes in the Khao Khwang fold-thrust belt, new insights into the tectonic evolution of the Indosinian orogeny in central Thailand. *Tectonophysics.*710-711. 266-276

BARBER, A. J., RIDD, M. F., CROW, M. J., (2011) The Origin, Movement and assembly of the pre-Tertiary tectonic units of Thailand. in Ridd, M.F., et al., eds., *The geology of Thailand*: London, Geological Society, 71–136

BARKER, S. L. L., (2007) Dynamics of fluid flow and fluid chemistry during crustal shortening. Australian National University

BARKER, S. L. L., COX, S. F., (2011) Oscillatory zoning and trace element incorporation in hydrothermal minerals: insights from calcite growth experiments. Geofluids. 11, 48– 56

BARR, S. M., MACDONALD, A, S., (1988). Nan River suture zone, northern Thailand. Geology. 15, 907–910.

BERTRAND, G., RANGIN, C. MULASKI, H., TIN AUNG HAN., MYINT, O., THEIN, M., MAW, W (1999). Cenozoic metamorphism along the Shan Scarp (Myanmar): Evidences for ductile shear along the Sagaing fault or the northward migration of the Hymalayan Syntaxis? *geophysical research letters*, VOL. 26, NO.7, PAGES 915-918

BONS, P. D., ELBURG, M A., GOMEZ-RIVAS, E., (2012). A review of the formation of tectonic veins and their microstructures. *Journal of Structural Geology* **43**: 33-62.

BOOTH, J.E., SATTAYARAK, N., 2011. Subsurface Carboniferous – Cretaceous geology of Northeast Thailand. In: Ridd, M.F., Barber, A.J., Crow, M.J. (Eds.), *The Geology of Thailand*. Geological Society, London, pp. 184–222

BROOKS, C., I. WENDT, and S. R. HART (1972), Realistic use of 2-error regression treatments as applied to rubidium-strontium data, Rev.Geophys., 10, 551–577

ÇAKIR, Z., ERGINTAV, S., OZENER, H., DOGUN, U., AKOGLU, A. M., MEGHRAOUI, M., REILINGER, R., (2012) Onset of aseismic creep on major strike-slip faults. *Geology*. 40 (12): 1115-1118

CHERNIAK, D. J. (1997). An experimental study of strontium and lead diffusion in calcite, and implications for carbonate diagenesis and metamorphism. *Geochimica et Cosmochimica Acta* 61(19): 4173-4179.

CHEW, D., PETRUS, J., & KAMBER, B. (2014). U–Pb LA–ICPMS dating using accessory mineral standards with variable common Pb. *Chemical Geology, 363*, 185-199.

DEW, R. E. C., KING, R., COLLINS, A. S., MORLEY, C. K., ARBOIT, F., GLORIE, S. (2017). Stratigraphy of deformed Permian carbonate reefs in Saraburi Province, Thailand. *Journal of the Geological Society of London*., 175, 163-175

DMR. (1999). *Geological Map of Thailand , Scale 1:1 Million. Department of Mineral Resources*, Bangkok.

DONELICK, R., O'SULLIVAN, P. B., KETCHAM, R. A., (2005) Apatite Fission-Track Analysis.*Reviews in Mineralogy & Geochemistry*. 58. 49-94

FARKAŠ, J., FRYDA, J., & HOLMDEN, C. (2016). Calcium isotope constraints on the marine carbon cycle and CaCO 3 deposition during the late Silurian (Ludfordian) positive δ 13 C excursion. *Earth and Planetary Science Letters, 451*, 31-40

FLOWERS, R. M., KETCHAM, R. A., SHUSTER, D. L., FARLEY, K. L., (2009) Apatite (U–Th)/He thermochronometry using a radiation damage accumulation and annealing model. *Geochimica et Cosmochimica Acta*. 73. 2347–2365

GARDINER, N.J., ROBB, L.J., MORLEY, C.K., SEARLE, M.P., CAWOOD, P.A., WHITEHOUSE, M.J., KIRKLAND, C.L., ROBERTS, N.M.W., TIN AUNG MYINT, (2016). The tectonic and metallogenic framework of Myanmar: a Tethyan mineral system. *Ore Geology Reviews* 79, 26–45.

GARDINER, N.J., SEARLE, M.P., MORLEY, C.K., ROBB, L.J., WHITEHOUSE, M.J., ROBERTS, N.M.W., KIRKLAND, C.L., SPENCER, C.J., (2018) The crustal architecture of Myanmar imaged through zircon U-Pb, Lu-Hf and O isotopes: Tectonic and metallogenic implications, *Gondwana Research*. 62, 27-60.

GILLESPIE, J., GLORIE, S., XIAO, W.-J., ZHANG, Z., COLLINS, A. S., EVANS, N. J., . . . DE GRAVE, J. (2017). Mesozoic reactivation of the Beishan, southern Central Asian Orogenic Belt: Insights from low-temperature thermochronology. *Gondwana Research, 43*, 107-122.

GLEADOW, A., HARRISON, M., KOHN, B., LUGO-ZAZUETA, R., & PHILLIPS, D. (2015). The Fish Canyon Tuff: A new look at an old low-temperature thermochronology standard. *Earth and Planetary Science Letters, 424*, 95-108.

GLORIE, S., ALEXANDROV, I., NIXON, A., JEPSON, G., GILLESPIE, J., & JAHN, B.- M. (2017). Thermal and exhumation history of Sakhalin Island (Russia) constrained by apatite U-Pb and fission track thermochronology. *Journal of Asian Earth Sciences, 143*, 326-342

GOODFELLOW, B. W., VIOLA, G., BINGEN, B., NURIEL, P., KYLANDER-CLARK, A, C, L., (2017). Palaeocene faulting in SE Sweden from U–Pb dating of slickenfibre calcite. *Terra Nova* 29(5): 321-28.

HANSBERRY, R. L., ZWINGMANN2, H., LOEHR, R., COLLINS, A, S., KING, R, C., MORLEY, C, K., DRYSDALE, R., (2017). Constraining the timing of shale detachment faulting: A geochemical approach. *Lithosphere* 9(3): 431-440.

HENDRIKS, B.W.H., REDFIELD, T.F., (2005) Apatite fission track and (U-Th)/He data fromFennoscandia: An example of underestimation of fission track annealing in apatite. Earth and Planetary Science Letters. 236. 443– 458

KIRKLAND, C. L., FOUGEROUSE, D., REDDY, S. M., HOLLIS, J., SAXEY, D. W., (2018). Assessing the mechanisms of common Pb incorporation into titanite. *Chemical Geology* 483: 558-566.

LACASSIN, R., REPLUMAZ, A., AND LELOUP, P. H. (1998) Hairpin river loops and slip-sense inversion on southeast Asian strike-slip faults: *Geology*, v.26, p. 703-706

LEE, Y-J., MORSE, J. W., (1998). Calcite precipitation in synthetic veins: implications for the time and fluid volume necessary for vein filling. *Chemical Geology*. 156. 151–170

LI, Q., PARRISH, R.R., HORSTWOOD, M.S.A., and MCARTHUR, J.M., (2014). U–Pb dating of cements in Mesozoic ammonites. *Chemical Geology* 376: 76-83.

MASKENSKAYA, O. M., DRAKE, H., ÅSTRÖM, M. E., (2013). Geochemistry of Calcite Veins: Records of Fluid Mixing and Fluid-Rock Interaction. *Procedia Earth and Planetary Science* **7**: 566-569.

MCDOWELL, F. W., MCINTOSH, W. C., & FARLEY, K. A. (2005). A precise 40 Ar–39 Ar reference age for the Durango apatite (U–Th)/He and fission-track dating standard. *Chemical Geology, 214*(3), 249-263

MORLEY, C. K. (2002). A tectonic model for the Tertiary evolution of strike–slip faults and rift basins in SE Asia. *Tectonophysics* **347**(4): 189-215.

MORLEY, C. K., RIDD, M. F., (2011). The Khao Yai Fault on the southern margin of the Khorat Plateau, and the pattern of faulting in Southeast Thailand. *Proceedings of the Geologists' Association* 122 143–156

MORLEY, C.K., AMPAIWAN, P., THANUDAMRONG, S., KUENPHAN, N., WARREN, J., (2013). Development of the Khao Khwang Fold and Thrust Belt: Implications for the geodynamic setting of Thailand and Cambodia during the Indosinian Orogeny. *Journal of Asian Earth Sciences* **62**: 705-719.

MORLEY, C. K., SEARLE, M. P., (2017). Regional tectonics, structure and evolution of the Andaman–Nicobar Islands from ophiolite formation and obduction to collision and back-arc spreading. in Bandopadhyay, P. C. & Carter, A. (eds). *The Andaman–Nicobar Accretionary Ridge: Geology, Tectonics and Hazards*. Geological Society, London, Memoirs, 47, 51–74

NANTASIN, P., HAUZENBERGER, C., LIU, X., KRENN, K., DONG, Y., THÖNI, M., WATHANAKUL, P.,(2012). Occurrence of the high grade Thabsila metamorphic complex within the lowgrade Three Pagodas shear zone, Kanchanaburi Province, western Thailand:Petrology and geochronology. *Journal of Asian Earth Sciences*. 60. 68-87

NAZRUL, M. (2015). Fluid evolution through different deformation stages: a carbonate outcrop-based study in the western highland of thailand. University of Leads, U.K

NURIEL, P., WEINBERGER, R., KYLANDER-CLARK, A. R. C., HACKER, B. R., & CRADDOCK, J. P. (2017). The onset of the Dead Sea Transform based on calcite age-strain analyses. *Geology* 45 587-590

PATON, C., HELLSTROM, J., PAUL, B., WOODHEAD, J., & HERGT, J. (2011). Iolite: Freeware for the visualisation and processing of mass spectrometric data. *Journal of Analytical Atomic Spectrometry, 26*(12), 2508-2518

RASBURY, E. T. AND J. M. COLE (2009). Directly dating geologic events: U-Pb dating of carbonates. R*eviews of Geophysics* **47**(3).

RICHARDS, D. A., BOTTRELL, S. H., CLIFF, R. A., STROHLE, K., ROWE, P., 1998. U-Pb dating of a speleothem of Quaternary age. *Geochimica et Cosmochimica Acta* **62**(23): 3683-3688.

RIDD, M. F., MORLEY, C. K., (2011) The Khao Yai Fault on the southern margin of the Khorat Plateau, and the pattern of faulting in Southeast Thailand. *Proceedings of the Geologists' Association*. 122. 143–156

RIDD, M. F., BARBER, A. J., CROW, M. J., (2011) Introduction to the Geology of Thailand. in Riddp, M.F., et al., eds., *The geology of Thailand*: London, Geological Society, p. 71–36

ROBERTS, N, M, W. (2018). Progress in Crustal deformation and fluid-flow using U-Pb carbonate geochronology. Proceedings of the 15th International Conference on Gondwana to Asia IAGR. 69 -70.

ROBERTS, N. M. W., RASBURY, E. T., PARRISH, R, P., SMITH, C. J., HORSTWOOD., M. S. A., CONDON, J., (2017). A calcite reference material for LA-ICP-MS U-Pb geochronology.

Geochemistry, Geophysics, Geosystems **18**(7): 2807-2814.
ROBERTS, N. M. W. AND R. J. WALKER (2016). U-Pb geochronology of calcite-mineralized faults: Absolute timing of rift-related fault events on the northeast Atlantic margin. *Geology* 44(7): 531-534.
RHODES, B. CHARUSIRI, P. KOSUWAN, S. LAMJUAN, A. (2005). Tertiary Evolution of the Three Pagodas Fault, Western Thailand. *Proceedings of the International Conference on Geology, Geotechnology and Mineral Resources of Indochin*a, Khon Kaen, Thialand. Pp 498-505
SCHEONE, B., BOWRING, S. A., (2006). U–Pb systematics of the McClure Mountain syenite: hermochronological constraints on the age of the 40Ar/39Ar standard MMhb. *Contrib Mineral Petrol*. 151. 5. 615-630
SCHOLZ, C. H., (1989) The Mechanics of Faulting. *Annual Review of Earth and Planetary Sciences*. 17. 309-334
SEARLE, M.P., NOBLE, S.R., COTTLE, J.M., WATERS, D.J., MITCHELL, A.H.G., TIN HLAING, HORSTWOOD, M.S.A., (2007). Tectonic evolution of the Mogok metamorphic belt, Burma (Myanmar) constrained by U-Th-Pb dating of metamorphic and magmatic rocks. *Tectonics* 26
SEARLE, M. P., MORLEY, C. K., (2011) Tectonic and thermal evolution of Thailand in the regional context of SE Asia. in Ridd, M.F., et al., eds., *The geology of Thailand*: London, Geological Society, p. 71–136
SLOAN, R.A., ELLIOTT, J. R., SEARLE, M. P., MORLEY, C. K., (2017) in Barber, A. J., Khin Zaw & Crow, M. J. (eds). *Myanmar: Geology, Resources and Tectonics*. Geological Society, London, Memoirs, 48, 19–52
STACEY, J. S. AND J. D. KRAMERS (1975). Approximation of terrestrial lead isotope evolution by a two-stage model. *Earth and Planetary Science Letters* **26**(2): 207-221.
UENO, K., MIYAHIGASHI, A., CHAROENTITIRAT, T., (2010). The Lopingian (Late Permian) of mid-oceanic carbonates in the Eastern Palaeotethys: stratigraphical outline and foraminiferal faunal succession. *Geol. J*. 45: 285–307
UPTON, D., BRISTOW, C., HURFORD, A.J., CARTER, A., (1997). Cenozoic tectonic denudation in northwestern Thailand: Provisional results from apatite fission-track analysis. In: *The International Conference on Stratigraphy and Tectonic Evolution of Southeast Asia and the South Pacific*, Bangkok, Thailand, pp. 421 - 431.
UPTON, D., HURFORD, A., BRISTOW, C., AND CARTER, A., (1999). Constructing Tertiary thermal histories in Thailand, in anonymous, ed., *European Union of Geosciences conference*; EUG 10, Cambridge publications, p. 58.
VERMEESCH, P., 2018, IsoplotR: a free and open toolbox for geochronology. *Geoscience Frontiers*, doi: 10.1016/ j.gsf.2018.04.001 (in press).
WAGNER, G. A., & VAN DEN HAUTE, P. (1992). *Fission-track dating*. Amsterdam, Netherlands: Springer.
WARREN, J., MORLEY, C., CHAROENTITIRAT, T., CARTWRIGHT, I., AMPAIWAN, P., KHOSITCHAISRI, P., MIRZALOO, M., AND YINGYUEN, J.,. (2014). Structural and fluid evolution of Saraburi Group sedimentary carbonates, central Thailand: A tectonically driven fluid system. *Marine and Petroleum Geology* 55: 100-121.
WATKINSON, I., C. ELDERS, AND R. HALL. (2008). The kinematic history of the Khlong Marui and Ranong Faults, southern Thailand. *Journal of Structural Geology* 30(12): 1554-1571.
WATKINSON, I., ELDERS, C., BATT, G., JOURDAN, F., HALL, R., MCNAUGHTON, N, J., (2011). The timing of strike-slip shear along the Ranong and Khlong Marui faults, Thailand. *Journal of Geophysical Research: Solid Earth* 116(B9).
WIGLEY, T. M. L., PLUMMER, L. N., (1976). Mixing of carbonate waters. *Geochimica et Cosmochimica acta*. 40. 989-995
WOODHEAD, J., HERGT, J., (2007). Strontium, Neodymium and Lead Isotope Analyses of NIST Glass Certified Reference Materials: SRM 610, 612, 614. *Geostandards and geotechnical Research*. 25 (2-3). 262-266.
YAO, C.-H. (2016). Escape tectonics along major shear zones in Western Thailand induced by India-Asia convergence: constraints from basement thermochronology. Masters thesis, University of Ghent.

[9] APPENDIX A CALCITE AND APATITE DATA

Calcite U-Pb raw (unnormalized) data tables:

Analytical session 1

	238_206	238_206_Prop2SE	207_206	207_206_Prop2SE	ErrorCorrelation_38_6vs7_6
NIST612 - 1.d	3.815338	0.041487	0.905	0.0017	0.21979
NIST612 - 2.d	3.81971	0.040853	0.9026	0.00175	0.52021
NIST612 - 3.d	3.728283	0.04031	0.9109	0.00145	0.37625
NIST612 - 4.d	3.731343	0.040376	0.907	0.00165	0.47407
NIST612 - 5.d	3.645643	0.039208	0.9072	0.00155	0.39075
NIST612 - 6.d	3.650968	0.039322	0.9052	0.00175	0.50368
NIST612 - 7.d	3.675525	0.039853	0.9058	0.00155	0.48215
NIST612 - 8.d	3.68053	0.039962	0.9071	0.00175	0.54075
NIST612 - 9.d	3.621876	0.039354	0.909	0.0015	0.41863
NIST612 - 10.d	3.608024	0.039054	0.9087	0.0017	0.68492
NIST612 - 11.d	3.542331	0.038272	0.9082	0.0018	0.42805
NIST612 - 12.d	3.521127	0.037815	0.9094	0.00175	0.46666

NIST612 - 13.d	3.517411	0.037735	0.9088	0.00155	0.41661
NIST612 - 14.d	3.529827	0.038002	0.9066	0.0017	0.69588
NIST612 - 15.d	3.650968	0.039322	0.9113	0.00175	0.42243
NIST612 - 16.d	3.620958	0.038678	0.9083	0.0014	0.50683
NIST614 - 1.d	1.228803	0.01359	0.8733	0.00325	0.50898
NIST614 - 2.d	1.241157	0.013864	0.8671	0.00335	0.58508
NIST614 - 3.d	1.220107	0.014142	0.8666	0.0033	0.5066
NIST614 - 4.d	1.240387	0.013847	0.8711	0.0033	0.49135
NIST614 - 5.d	1.239311	0.013823	0.8702	0.00345	0.52369
NIST614 - 6.d	1.247505	0.014006	0.8751	0.0033	0.34254
NIST614 - 7.d	1.222643	0.013454	0.8733	0.00355	0.48843
NIST614 - 8.d	1.222793	0.014205	0.8752	0.00375	0.47216
NIST614 - 9.d	1.239004	0.013816	0.8712	0.00325	0.43639
NIST614 - 10.d	1.235025	0.013728	0.8692	0.00295	0.4648
NIST614 - 11.d	1.238697	0.013809	0.8743	0.0033	0.40218
NIST614 - 12.d	1.233502	0.013694	0.869	0.00355	0.56335

NIST614 - 13.d	1.239465	0.013826	0.8716	0.0032	0.44813
NIST614 - 14.d	1.234111	0.014469	0.8739	0.00375	0.61834
NIST614 - 15.d	1.245485	0.014737	0.8747	0.004	0.62683
NIST614 - 16.d	1.223541	0.013473	0.8641	0.00325	0.41627
NIST612 - 25.d	3.455425	0.07164	0.9093	0.0024	0.29347
NIST612 - 26.d	3.472222	0.072338	0.9085	0.00245	0.42847
NIST612 - 27.d	3.567606	0.076367	0.9072	0.0024	0.49078
NIST612 - 28.d	3.537319	0.075076	0.9054	0.00235	0.39812
NIST612 - 29.d	3.547357	0.075502	0.9065	0.00255	0.56928
NIST612 - 30.d	3.567606	0.076367	0.9101	0.00255	0.62293
NIST612 - 31.d	3.657644	0.08027	0.9098	0.00235	0.47716
NIST612 - 32.d	3.688676	0.081638	0.9078	0.00255	0.51957
NIST612 - 33.d	3.508772	0.073869	0.9043	0.00255	0.5788
NIST612 - 34.d	3.522367	0.074442	0.9083	0.0025	0.53876
NIST612 - 35.d	3.563792	0.076204	0.9078	0.0025	0.46623
NIST612 - 36.d	3.567606	0.076367	0.9056	0.0025	0.44802

NIST612 - 37.d	3.619254	0.078594	0.9078	0.00245	0.38817
NIST612 - 38.d	3.629764	0.079051	0.9052	0.00235	0.37751
NIST612 - 39.d	3.610108	0.078197	0.9057	0.00255	0.41292
NIST612 - 40.d	3.650968	0.079977	0.9022	0.00265	0.48245
NIST614 - 25.d	1.241619	0.026208	0.8742	0.0039	0.42096
NIST614 - 26.d	1.228049	0.026392	0.8688	0.00395	0.47381
NIST614 - 27.d	1.233654	0.026633	0.8726	0.004	0.57172
NIST614 - 28.d	1.236552	0.026759	0.8723	0.0035	0.40986
NIST614 - 29.d	1.244245	0.026318	0.8666	0.0038	0.45692
NIST614 - 30.d	1.22549	0.026282	0.8745	0.00385	0.34847
NIST614 - 31.d	1.256124	0.026823	0.8671	0.0042	0.53355
NIST614 - 32.d	1.217434	0.025938	0.8716	0.0041	0.52206
NIST614 - 33.d	1.244865	0.026345	0.8705	0.0038	0.39648
NIST614 - 34.d	1.22835	0.026405	0.8713	0.0037	0.31017
NIST614 - 35.d	1.237471	0.026033	0.8714	0.0039	0.49399
NIST614 - 36.d	1.23259	0.026587	0.8657	0.00405	0.59541

NIST614 - 37.d	1.239772	0.026898	0.8651	0.00425	0.42438
NIST614 - 38.d	1.230921	0.026515	0.8758	0.00385	0.549
NIST614 - 39.d	1.242082	0.026998	0.8754	0.00385	0.6244
NIST614 - 40.d	1.227596	0.026372	0.8708	0.00355	0.33811
NIST612 - 13.d	3.505082	0.085999	0.9102	0.0024	0.44446
NIST612 - 14.d	3.517411	0.086605	0.9073	0.00245	0.69481
NIST612 - 15.d	3.625816	0.085453	0.9118	0.00255	0.50725
NIST612 - 16.d	3.608545	0.08464	0.9081	0.00225	0.45393
NIST612 - 17.d	3.501401	0.085819	0.9091	0.0025	0.49844
NIST612 - 18.d	3.479471	0.084747	0.9075	0.00245	0.46289
NIST612 - 19.d	3.557453	0.088588	0.9062	0.0025	0.47342
NIST612 - 20.d	3.532321	0.087341	0.9065	0.00245	0.40721
NIST612 - 21.d	3.518649	0.086666	0.9074	0.0025	0.48899
NIST612 - 22.d	3.543586	0.087899	0.9081	0.00235	0.34817
NIST612 - 23.d	3.641661	0.086201	0.9098	0.00255	0.50765
NIST612 - 24.d	3.615329	0.084959	0.9076	0.00255	0.42378

NIST612 - 25.d	3.526093	0.087033	0.9072	0.00235	0.28342
NIST612 - 26.d	3.512469	0.086362	0.9062	0.00245	0.42841
NIST612 - 27.d	3.566334	0.089031	0.9056	0.00235	0.45011
NIST612 - 28.d	3.534818	0.087465	0.9042	0.00235	0.39323
NIST614 - 13.d	1.236552	0.029817	0.8722	0.0036	0.44912
NIST614 - 14.d	1.23259	0.030386	0.8745	0.0041	0.61954
NIST614 - 15.d	1.24502	0.030226	0.8745	0.00435	0.63015
NIST614 - 16.d	1.227144	0.030118	0.8639	0.00365	0.40027
NIST614 - 17.d	1.244555	0.030204	0.8713	0.004	0.3978
NIST614 - 18.d	1.22534	0.030029	0.8734	0.0042	0.55765
NIST614 - 19.d	1.235941	0.029787	0.8729	0.00385	0.51542
NIST614 - 20.d	1.233654	0.030438	0.8675	0.00385	0.45451
NIST614 - 21.d	1.243781	0.030166	0.8659	0.00485	0.5516
NIST614 - 22.d	1.213592	0.030193	0.87	0.006	0.39597
NIST614 - 23.d	1.251251	0.03053	0.8755	0.004	0.60848
NIST614 - 24.d	1.216841	0.029614	0.8725	0.0042	0.5965

NIST614 - 25.d	1.24471	0.030211	0.873	0.004	0.44655
NIST614 - 26.d	1.226091	0.030066	0.8679	0.0039	0.456
NIST614 - 27.d	1.233654	0.029677	0.8715	0.00395	0.57518
NIST614 - 28.d	1.236247	0.029802	0.8708	0.0035	0.41092
NIST612 - 37.d	3.682427	0.062377	0.9059	0.00165	0.2886
NIST612 - 38.d	3.68053	0.062313	0.9046	0.00145	0.36462
NIST612 - 39.d	3.621876	0.059031	0.9053	0.00175	0.47166
NIST612 - 40.d	3.656307	0.061496	0.9034	0.00185	0.53336
NIST612 - 41.d	3.676335	0.062847	0.909	0.00125	0.30076
NIST612 - 42.d	3.646973	0.062512	0.9041	0.0018	0.45643
NIST612 - 43.d	3.542331	0.059604	0.9055	0.0017	0.4822
NIST612 - 44.d	3.559986	0.060199	0.9065	0.0015	0.43967
NIST612 - 45.d	3.624502	0.061744	0.9061	0.00185	0.56998
NIST612 - 46.d	3.625816	0.061131	0.9101	0.0015	0.46239
NIST612 - 47.d	3.660322	0.061631	0.9079	0.0017	0.45424
NIST612 - 48.d	3.67242	0.062039	0.9073	0.00165	0.36614

NIST612 - 49.d	3.812429	0.065406	0.9087	0.00165	0.39759
NIST612 - 50.d	3.759398	0.064306	0.905	0.0016	0.43788
NIST612 - 51.d	3.623188	0.061043	0.9083	0.00195	0.44992
NIST612 - 52.d	3.652301	0.061361	0.9088	0.00205	0.57293
NIST612 - 53.d	3.671072	0.062667	0.9094	0.0019	0.55212
NIST612 - 54.d	3.648304	0.061892	0.9044	0.0017	0.52929
NIST614 - 37.d	1.234263	0.021328	0.8628	0.00355	0.46103
NIST614 - 38.d	1.235178	0.021359	0.8752	0.0035	0.58533
NIST614 - 39.d	1.241927	0.021593	0.8753	0.0036	0.62561
NIST614 - 40.d	1.227295	0.021088	0.8703	0.0033	0.3116
NIST614 - 41.d	1.231679	0.021238	0.8746	0.00385	0.45427
NIST614 - 42.d	1.238237	0.021465	0.8697	0.00395	0.51212
NIST614 - 43.d	1.247038	0.021771	0.8715	0.0036	0.59346
NIST614 - 44.d	1.223242	0.020948	0.8638	0.00445	0.49146
NIST614 - 45.d	1.240233	0.021534	0.8709	0.0043	0.3341
NIST614 - 46.d	1.229559	0.021165	0.8724	0.0034	0.44473

NIST614 - 47.d	1.235025	0.021354	0.8778	0.00355	0.50048
NIST614 - 48.d	1.235178	0.021359	0.867	0.0037	0.53344
NIST614 - 49.d	1.221001	0.021617	0.8702	0.0039	0.35467
NIST614 - 50.d	1.241619	0.021583	0.8725	0.00375	0.38764
NIST614 - 51.d	1.242854	0.021626	0.8719	0.00365	0.37741
NIST614 - 52.d	1.226994	0.021077	0.871	0.0032	0.34888
NIST614 - 53.d	1.236247	0.021396	0.869	0.00305	0.47425
NIST614 - 54.d	1.23335	0.021296	0.8707	0.0038	0.48952
7a - 1.d	4.273504	0.16436555	0.356	0.0055	0.073705
7a - 2.d	9.174312	1.178352	0.383	0.009	-0.00936
7a - 3.d	73.04602	1.7074305	0.352	0.0145	0.14517
7a - 4.d	5.91716	0.1925703	0.402	0.02	0.11766
7a - 5.d	14.64129	0.439453	0.422	0.016	0.47257
7a - 6.d	9.99001	0.30938095	0.453	0.018	0.49602
7a - 7.d	28.6533	1.395719	0.413	0.022	0.29632
7a - 8.d	5.494505	0.3471803	0.433	0.0255	0.16465
7a - 9.d	16.33987	0.61408	0.471	0.0235	0.61634
7a - 10.d	4.424779	0.16641865	0.447	0.0215	0.49279
7a - 11.d	9.569378	0.36171335	0.352	0.012	0.34527
7a - 12.d	7.407407	0.20027435	0.4	0.0185	0.56346
7a - 13.d	1.628664	0.047745865	0.353	0.0055	0.039056

7a - 14.d	4.201681	0.1147518	0.3478	0.00435	0.097742
7a - 15.d	2.518892	0.09834465	0.357	0.008	0.30568
7a - 16.d	4.878049	0.1665675	0.445	0.024	0.46672
7a - 17.d	4.317789	0.0932165	0.351	0.0085	0.027336
7a - 18.d	6.265664	0.19040395	0.357	0.011	0.21157
7a - 19.d	6.410256	0.2465483	0.422	0.0155	0.41003
7a - 20.d	41.841	1.1379355	0.523	0.017	0.48301
7a - 21.d	3.174603	0.08062485	0.361	0.0115	0.34958
7a - 22.d	16.39344	1.61247	0.521	0.035	0.06665
7a - 23.d	4.1841	0.14005355	0.458	0.0245	0.33962
7a - 24.d	7.132668	0.24928725	0.413	0.0205	0.20349
7a - 25.d	9.433962	0.48949805	0.443	0.0215	0.40314
7a - 26.d	5.882353	0.20761245	0.491	0.0245	0.5752
7a - 27.d	25.25253	0.892766	0.489	0.0165	0.024284
7a - 28.d	7.347539	0.2213439	0.381	0.0095	0.33269
7a - 29.d	7.886435	0.2798814	0.389	0.009	0.28923
7a - 30.d	4.587156	0.220941	0.394	0.016	0.023506
7a - 31.d	5.617978	0.20515085	0.414	0.0225	0.73786
7a - 32.d	3.10559	0.08197985	0.361	0.0075	0.38539
7a - 33.d	3.755163	0.0775569	0.347	0.0075	0.41286
7a - 34.d	5.91716	0.2100767	0.351	0.021	-0.03976
7a - 35.d	2.624672	0.06888905	0.409	0.0135	0.52802
7a - 36.d	4.830918	0.2217088	0.456	0.023	0.44462
7a - 37.d	1.324503	0.02543748	0.337	0.0055	0.25679
7a - 38.d	13.22751	0.621133	0.469	0.033	0.25975

7a - 39.d	7.936508	0.40942305	0.458	0.0145	0.5894
7a - 40.d	2.659574	0.09549005	0.584	0.0335	0.64799
7a - 41.d	11.11111	0.41358025	0.511	0.0275	0.40154
7a - 42.d	3.984064	0.27777335	0.375	0.0065	0.21024
7a - 43.d	5.347594	0.17158055	0.44	0.0215	0.56515
7a - 44.d	1.612903	0.09495315	0.392	0.0085	0.1122
7a - 45.d	5.376344	0.21678805	0.618	0.0365	0.51508
7a - 46.d	41.32231	1.7075335	0.5	0.021	0.27585
7a - 47.d	2.55102	0.05856935	0.402	0.0135	0.47871
7a - 48.d	7.204611	0.25434145	0.346	0.0135	0.16591
7a - 49.d	3.731343	0.13226775	0.378	0.013	0.42688
7a - 50.d	1.173709	0.045460555	0.3754	0.0044	0.073334
7a - 51.d	5.882353	0.46712805	0.378	0.0065	-0.10525
7a - 52.d	0.387597	0.03229974	0.3762	0.0035	-0.0485
7a - 53.d	1.589825	0.1137395	0.383	0.005	0.015693
7a - 54.d	2.906977	0.07182935	0.365	0.0105	0.33729
10a(old) - 1.d	2.717391	0.11076325	0.791	0.025	0.31738
10a(old) - 2.d	29.49853	1.696818	0.54	0.0365	0.86218
10a(old) - 3.d	25.57545	1.079271	0.502	0.0125	-0.14803
10a(old) - 4.d	8	0.384	0.701	0.021	-0.04764
10a(old) - 5.d	13.51351	1.004383	0.567	0.0255	0.047039

10a(old) - 6.d	11.41553	0.4756469	0.648	0.023	0.24912
10a(old) - 7.d	3.401361	0.2429543	0.845	0.0385	0.20493
10a(old) - 8.d	4.716981	0.36712355	0.711	0.0235	-0.02621
10a(old) - 9.d	6.622517	0.3508618	0.771	0.04	0.93005
10a(old) - 10.d	23.31002	1.90175	0.799	0.0465	0.72558
10a(old) - 11.d	5.747126	0.19817675	0.822	0.0335	0.63776
10a(old) - 12.d	5.681818	0.1775568	0.786	0.025	0.33536
10a(old) - 13.d	1.176471	0.06920415	0.81	0.0285	0.28408
10a(old) - 14.d	1.814882	0.06587595	0.872	0.031	0.47238
10a(old) - 15.d	1.6	0.11008	0.731	0.0125	0.12091
10a(old) - 16.d	24.93766	1.772377	0.652	0.023	0.21784
10a(old) - 17.d	0.806452	0.045525495	0.843	0.0235	0.001079
10a(old) - 18.d	5.91716	0.6127235	0.71	0.06	0.07637
10a(old) - 19.d	3.649635	0.12653845	0.863	0.0165	0.036356
10a(old) - 20.d	2.427184	0.1649543	0.89	0.055	0.75365
10a(old) - 21.d	2.087683	0.16779915	0.794	0.044	0.087978
10a(old) - 22.d	18.83239	1.6136985	0.515	0.0215	-0.1193

10a(old) - 23.d	4.716981	0.3782485	0.777	0.0305	0.21058
10a(old) - 24.d	1.552795	0.1133251	0.92	0.045	0.53915
10a(old) - 25.d	1.811594	0.0623556	0.882	0.0235	0.49346
10a(old) - 26.d	7.751938	0.4206478	0.684	0.029	0.06747
10a(old) - 27.d	12.98701	1.011975	0.71	0.07	0.53437
10a(old) - 28.d	1.831502	0.0805056	0.864	0.028	0.60196
10a(old) - 29.d	3.344482	0.2069328	0.851	0.045	0.41592
10a(old) - 30.d	9.174312	0.84168	0.97	0.065	0.8763
10a(old) - 31.d	9.433962	0.8899965	0.752	0.029	0.02444
10a(old) - 32.d	3.597122	0.28466435	0.875	0.0305	0.51437
10a(old) - 33.d	2.262443	0.2533732	0.925	0.038	0.65768
10a(old) - 34.d	26.59574	2.228101	0.592	0.033	0.28106
10a(old) - 35.d	2.824859	0.2114654	0.881	0.0485	0.45537
10a(old) - 36.d	14.97006	0.7955645	0.82	0.05	0.42883
10a(old) - 37.d	3.367003	0.2324026	0.795	0.0345	0.62938
10a(old) - 38.d	76.33588	3.2049415	0.742	0.0295	0.28321
10a(old) - 39.d	16.58375	0.9075685	0.63	0.0405	0.28346

10a(old) - 40.d	5.347594	0.5147415	0.758	0.0265	-0.00574
10a(old) - 41.d	2.364066	0.10898175	0.831	0.039	0.77706
10a(old) - 42.d	10.31992	0.3940526	0.536	0.026	0.13612
10a(old) - 43.d	18.34862	0.707011	0.538	0.018	-0.34475
10a(old) - 44.d	6.329114	0.36051915	0.596	0.0315	0.088228
8B - 1.d	23.64066	1.4251465	0.86	0.08	0.74643
8B - 2.d	8.264463	0.34150675	0.646	0.04	0.91276
8B - 3.d	11.06195	0.4894667	0.631	0.0455	0.74382
8B - 4.d	65.78947	4.328255	0.57	0.0475	0.52985
8B - 5.d	32.57329	1.538478	0.57	0.055	0.54743
8B - 6.d	34.48276	2.9131985	0.71	0.055	0.34568
8B - 7.d	220.3614	3.39914	0.213	0.0055	0.22107
8B - 8.d	68.96552	3.0915575	0.395	0.0365	0.81385
8B - 9.d	13.5318	0.4669295	0.435	0.0245	0.16329
8B - 10.d	8.62069	0.4830559	0.83	0.105	0.80046
8B - 11.d	11.76471	1.1764705	0.61	0.08	0.35715
8B - 12.d	44.64286	2.2919325	0.77	0.06	0.60937
8B - 13.d	10.41667	1.0850695	0.69	0.09	0.29352
8B - 14.d	31.15265	1.3586825	0.341	0.017	0.5219
8B - 15.d	14.9925	0.752997	0.78	0.055	0.9384
8B - 16.d	109.0513	5.113635	0.571	0.0415	0.63236
8B - 17.d	11.29944	0.4021833	0.58	0.0295	0.58535

8B - 18.d	25	0.5625	0.212	0.0085	0.32714
8B - 19.d	21.73913	0.4725898	0.215	0.009	0.28522
8B - 20.d	12.93661	0.577378	0.629	0.034	0.12556
8B - 21.d	5.747126	0.39635355	1.02	0.125	0.69912
8B - 22.d	70.92199	3.017957	0.491	0.027	0.21908
8B - 23.d	301.7502	5.007925	0.1391	0.0036	-0.43593
8B - 24.d	121.9512	8.179655	0.49	0.055	0.90175
8B - 25.d	309.5975	7.188795	0.167	0.009	0.010982
8B - 26.d	8.196721	0.604676	0.84	0.055	0.35973
8B - 27.d	29.41176	2.465398	0.8	0.11	0.58528
8B - 28.d	46.2963	2.143347	0.419	0.0255	0.10293
8B - 29.d	23.58491	1.446244	0.79	0.095	0.30363
8B - 30.d	11.16071	0.45464965	0.581	0.039	0.46758
8B - 31.d	5.847953	0.3248863	0.709	0.0445	0.56614
8B - 32.d	31.64557	1.502163	0.72	0.06	0.8872
12a - 1.d	0.08680556	0.002637	0.6518	0.00295	0.13149
12a - 2.d	2.754821	0.106247	0.649	0.008	0.24416
12a - 3.d	43.66812	1.716215	0.594	0.0185	0.14099
12a - 4.d	4.098361	0.235152	0.708	0.0215	0.076211
12a - 5.d	0.3731343	0.016708	0.652	0.00235	0.03019
12a - 6.d	0.2881844	0.009966	0.6508	0.00235	-0.022646
12a - 7.d	0.1398601	0.007433	0.675	0.0105	0.087823
12a - 8.d	0.04401408	0.001356	0.6531	0.00225	-0.040709
12a - 9.d	0.2277904	0.010378	0.6524	0.0025	0.0065407
12a - 10.d	9.345794	0.917111	0.6147	0.005	-0.6451

12a - 11.d	0.9174312	0.092585	0.6466	0.0034	-0.23973
12a - 12.d	2.188184	0.155615	0.6426	0.00405	-0.23573
12a - 13.d	1.282051	0.098619	0.651	0.0055	0.033445
12a - 14.d	20.66116	1.323339	0.539	0.019	-0.55175
12a - 15.d	0.3194888	0.010718	0.645	0.005	0.13824
12a - 16.d	0.6493506	0.027408	0.624	0.006	0.013212
12a - 17.d	0.7251632	0.02603	0.6302	0.0045	-0.10811
12a - 18.d	7.446016	0.332659	0.597	0.007	0.05311
12a - 19.d	3.521127	0.105386	0.6332	0.00425	0.21497
12a - 20.d	1.351351	0.136961	0.6416	0.00325	-0.24721
12a - 21.d	1.757469	0.063318	0.6435	0.00365	-0.027186
12a - 22.d	30.03003	0.991983	0.656	0.017	0.41833
12a - 23.d	0.04	0.0016	0.6561	0.00225	0.10151
12a - 24.d	1.848429	0.093959	0.65	0.01	0.10672
12a - 25.d	0.1137656	0.003171	0.6505	0.00225	-0.05955
12a - 26.d	1.136364	0.071023	0.6359	0.00395	-0.24129
12a - 27.d	104.9318	3.413312	0.373	0.008	-0.63046
12a - 28.d	29.5858	1.09415	0.531	0.008	-0.020682
12a - 29.d	17.27116	0.909794	0.605	0.0185	0.098242
12a - 30.d	35.21127	1.549792	0.455	0.0135	0.087421
12a - 31.d	24.09639	1.045145	0.609	0.017	0.28586
12a - 32.d	185.8736	5.355095	0.247	0.007	-0.19466
12a - 33.d	1.538462	0.16568	0.772	0.032	0.30048
12a - 34.d	12.82051	1.150559	0.669	0.03	0.45092
12a - 35.d	44.24779	1.566294	0.434	0.0155	0.17019

12a - 36.d	77.22008	3.279617	0.306	0.015	-0.39423
12a - 37.d	28.08989	1.578084	0.536	0.024	0.093223
12a - 38.d	65.35948	3.417489	0.461	0.0145	-0.23776
12a - 39.d	4.784689	0.366292	0.6317	0.00275	-0.26941
12a - 40.d	14.02525	0.895019	0.588	0.033	0.51346
12a - 41.d	147.929	4.814257	0.263	0.012	0.10073
12a - 42.d	12.98701	0.56502	0.64	0.0235	0.17833
12a - 43.d	16.89189	0.71334	0.625	0.019	0.26606
12a - 44.d	71.42857	3.061225	0.368	0.0235	0.24595
12a - 45.d	38.75969	1.802777	0.539	0.0215	0.31508
12a - 46.d	27.70083	1.726506	0.615	0.0215	0.095046
12a - 47.d	46.08295	1.698911	0.392	0.017	0.58008
12a - 48.d	104.712	4.605137	0.414	0.026	0.50525
12a - 49.d	83.96306	2.890416	0.289	0.012	0.29009
12a - 50.d	26.10966	1.397515	0.578	0.02	-0.10598
12a - 51.d	19.01141	0.885513	0.616	0.027	0.68447
12a - 52.d	85.32423	3.640113	0.537	0.02	0.25833
12a - 53.d	39.84064	1.428549	0.637	0.025	0.3237
12a - 54.d	16.66667	1.222222	0.682	0.0295	-0.060691
12a - 55.d	42.73504	1.73497	0.417	0.021	0.29938
12a - 56.d	0.3745318	0.022444	0.712	0.034	0.082617
12a - 57.d	68.07352	2.548702	0.479	0.0135	-0.25804
12a - 58.d	46.94836	1.873526	0.521	0.0245	0.37573
12a - 59.d	7.518797	0.423992	0.87	0.065	0.89109
12a - 60.d	10.30928	0.743969	0.657	0.0205	0.17997

12a - 61.d	0.3703704	0.010974	0.6589	0.0036	-0.026755
10b - 1.d	24.44988	0.747246	0.107	0.006	0.25613
10b - 2.d	11.64144	0.413346	0.498	0.0195	0.55921
10b - 3.d	23.90057	0.628361	0.1196	0.00395	0.36441
10b - 4.d	21.55172	0.650268	0.181	0.0085	-0.36934
10b - 5.d	17.0068	0.491693	0.269	0.008	-0.35133
10b - 6.d	18.34862	0.505008	0.273	0.0075	-0.27017
10b - 7.d	26.30887	0.657549	0.0693	0.00245	0.30558
10b - 8.d	24.8139	0.677303	0.1022	0.00395	-0.031848
10b - 9.d	21.09705	0.556357	0.196	0.0055	0.20499
10b - 10.d	23.80952	0.736962	0.146	0.0095	-0.027216
10b - 11.d	22.83105	0.703697	0.193	0.0135	-0.56612
10b - 12.d	25.90674	0.805391	0.123	0.0065	0.25714
10b - 13.d	25.31646	0.769108	0.181	0.01	-0.12485
10b - 14.d	23.69668	0.701916	0.199	0.0095	0.45008
10b - 15.d	24.27184	0.648035	0.129	0.005	-0.33485
10b - 16.d	24.57002	0.664055	0.1032	0.0039	0.20834
10b - 17.d	25.80645	0.699272	0.0992	0.00475	0.11401
10b - 18.d	11.97605	0.509162	0.433	0.017	-0.62397
10b - 19.d	24.5098	0.750913	0.122	0.008	0.15949
10b - 20.d	24.8139	0.708089	0.137	0.0095	-0.36571
10b - 21.d	18.05054	0.553898	0.266	0.0115	-0.13201
10b - 22.d	24.21308	0.674214	0.118	0.006	-0.011058
10b - 23.d	14.30615	0.419565	0.382	0.011	0.47966

10b - 24.d	15.40832	0.510445	0.34	0.014	0.40485
10b - 25.d	17.30104	0.538787	0.283	0.0095	-0.35691
10b - 26.d	9.354537	0.266897	0.504	0.0115	0.50339
10b - 27.d	15.84786	0.464636	0.339	0.0095	0.51321
10b - 28.d	13.0039	0.397388	0.415	0.012	0.21511
10b - 29.d	14.22475	0.505859	0.361	0.011	-0.19343
10b - 30.d	10.66098	0.34097	0.477	0.01	0.40829
10b - 31.d	15.12859	0.526411	0.38	0.0115	-0.128
10b - 32.d	9.149131	0.297158	0.478	0.0095	0.058419
10b - 33.d	3.427005	0.093955	0.614	0.0065	0.11501
10b - 34.d	7.39645	0.221565	0.518	0.0085	-0.091934
10b - 35.d	8.244023	0.251467	0.505	0.008	0.08535
10b - 36.d	0.5643341	0.014172	0.6523	0.0028	0.37359
10b - 37.d	1.55521	0.039908	0.6314	0.00395	0.13576
10b - 38.d	0.7107321	0.024247	0.6455	0.0031	0.03374
10b - 39.d	22.07506	0.560405	0.1195	0.003	0.19185
10b - 40.d	0.295421	0.007418	0.6738	0.00235	0.17395
10b - 41.d	1.412429	0.037904	0.6247	0.00375	0.17614
10b - 42.d	20.24291	0.553197	0.204	0.005	-0.56868
10b - 43.d	26.35046	0.729064	0.0995	0.00455	0.12301
10b - 44.d	27.20348	0.666027	0.0645	0.00195	0.15143
10b - 45.d	22.02643	0.80052	0.206	0.0155	0.97885
10b - 46.d	24.57002	0.784792	0.157	0.011	0.36797
10b - 47.d	25.7732	0.664258	0.0881	0.0035	0.088459
10b - 48.d	22.83105	0.781886	0.154	0.012	-0.47758

10b - 49.d	24.15459	1.196061	0.22	0.0265	0.56683
10b - 50.d	24.5098	0.841023	0.149	0.011	0.34434
10b - 51.d	20.04008	0.863451	0.209	0.0195	0.44886
10b - 52.d	11.28668	0.528665	0.408	0.013	-0.44
10b - 53.d	23.86635	0.825924	0.144	0.009	0.028871
10b - 54.d	25.45177	0.680182	0.0991	0.0047	0.2142
10b - 55.d	25.90674	0.738275	0.1001	0.0048	0.22634
10b - 56.d	26.31579	0.657895	0.0858	0.0021	0.34435
10b - 57.d	28.22467	0.716969	0.0597	0.00175	0.1327
10b - 58.d	19.84127	1.043242	0.254	0.031	0.15863
10b - 59.d	26.39916	0.696916	0.0788	0.00415	0.16776
10b - 60.d	18.97533	0.630111	0.247	0.0135	-0.016972
10b - 61.d	27.34482	0.710352	0.0667	0.0022	0.12908
10b - 62.d	19.53125	1.049042	0.272	0.0395	-0.044158
10b - 63.d	27.38226	0.712299	0.0705	0.00445	0.094491
12bSlick - 1.d	4.926108	0.2062656	0.5999	0.00305	-0.10239
12bSlick - 2.d	7.042254	0.29756	0.599	0.006	-0.68478
12bSlick - 3.d	6.309148	0.1970365	0.6065	0.00395	0.16413
12bSlick - 4.d	8.1103	0.2236417	0.5515	0.0046	0.015852
12bSlick - 5.d	7.342144	0.22371435	0.5735	0.0049	-0.15667
12bSlick - 6.d	14.0056	0.36289025	0.5369	0.00375	-0.20283

12bSlick-7.d	3.921569	0.1230296	0.6044	0.00405	-0.09475
12bSlick-8.d	3.921569	0.25374855	0.6122	0.00425	-0.57297
12bSlick-9.d	1.838235	0.0591344	0.6311	0.00345	-0.01412
12bSlick-10.d	1.976285	0.0624912	0.7364	0.00335	-0.46305
12bSlick-11.d	1.358696	0.05630465	0.8089	0.00365	-0.24125
12bSlick-12.d	1.930502	0.05590255	0.7811	0.0032	0.01073
12bSlick-13.d	1.628664	0.04244077	0.7772	0.0036	0.15036
12bSlick-14.d	1.828154	0.09358005	0.6923	0.00465	-0.71667
12bSlick-15.d	3.610108	0.1433617	0.725	0.007	-0.60119
12bSlick-16.d	6.19195	0.2108714	0.638	0.0055	-0.15846
12bSlick-17.d	1.824818	0.05993925	0.6631	0.00235	0.43264
12bSlick-18.d	0.518672	0.014796145	0.8303	0.0029	-0.62578
12bSlick-19.d	3.748126	0.09833915	0.6111	0.0035	0.21999
12bSlick-20.d	0.529101	0.05039055	0.7985	0.005	-0.53212
12bSlick-21.d	4.739336	0.16845985	0.6975	0.0036	-0.63882
12bSlick-22.d	9.165903	0.2268372	0.584	0.0055	0.015371
12bSlick-23.d	9.514748	0.2534852	0.5561	0.005	-0.21025

12bSlick - 24.d	10.31992	0.29820195	0.5711	0.0047	0.03334
12bSlick - 25.d	8.857396	0.215747	0.5835	0.00335	-0.17858
12bSlick - 26.d	4.62963	0.16075105	0.6851	0.00445	-0.25848
12bSlick - 27.d	0.392157	0.02768166	0.822	0.0065	-0.60495
12bSlick - 28.d	5.405405	0.18991965	0.672	0.006	0.025778
12bSlick - 29.d	6.329114	0.3404903	0.638	0.0055	-0.11981
12bSlick - 30.d	5.319149	0.2546401	0.677	0.006	-0.5041
12bSlick - 31.d	0.46729	0.03384575	0.786	0.0075	-0.90129
12bSlick - 32.d	3.012048	0.1587676	0.759	0.0095	0.22583
12bSlick - 33.d	8.264463	0.44395875	0.623	0.007	-0.11687
12bSlick - 34.d	0.900901	0.08522035	0.784	0.0075	-0.65125
8a - 1.d	1.085776	0.034188395	0.712	0.013	0.17021
8a - 2.d	1.879699	0.04946577	0.705	0.0135	0.30947
8a - 3.d	1.865672	0.0591724	0.688	0.011	0.29752
8a - 4.d	2.475248	0.0827125	0.707	0.0145	0.28395
8a - 5.d	1.349528	0.035513885	0.726	0.013	0.42582
8a - 6.d	2.493766	0.09950185	0.728	0.0205	0.58482
8a - 7.d	0.572738	0.01476128	0.697	0.0075	0.38678
8a - 8.d	4.739336	0.2807664	0.677	0.0105	0.011672

8a - 9.d	5.988024	0.2151386	0.753	0.017	0.27782
8a - 10.d	15.17451	0.44901805	0.689	0.0105	0.2075
8a - 11.d	0.833333	0.025694445	0.712	0.0105	0.14154
8a - 12.d	1.422475	0.04451558	0.713	0.0115	0.20055
8a - 13.d	1.31406	0.041442115	0.706	0.0125	0.33664
8a - 14.d	3.937008	0.13175025	0.713	0.0195	0.53718
8a - 15.d	4.042037	0.11436645	0.712	0.016	0.39815
8a - 16.d	12.8866	0.4068578	0.707	0.0085	0.15892
8a - 17.d	1.061571	0.039442665	0.715	0.0115	0.29763
8a - 18.d	2.192982	0.0553055	0.716	0.01	0.39578
8a - 19.d	3.184713	0.101424	0.712	0.0115	0.31079
8a - 20.d	2.78319	0.0658422	0.722	0.0125	0.54865
8a - 21.d	1.886792	0.06229975	0.724	0.009	0.21762
8a - 22.d	3.424658	0.09382625	0.729	0.014	0.52728
8a - 23.d	2.277904	0.05967175	0.772	0.014	0.31528
8a - 24.d	3.180662	0.07587455	0.697	0.0125	0.46798
8a - 25.d	3.616637	0.09810045	0.693	0.012	0.43009
8a - 26.d	2.070393	0.06429795	0.691	0.011	0.15646
8a - 27.d	0.90009	0.02470994	0.718	0.008	0.34108
8a - 28.d	3.058104	0.079492	0.702	0.017	0.59146
8a - 29.d	2.386635	0.0626563	0.716	0.0115	0.4697
8a - 30.d	2.48139	0.06157295	0.732	0.014	0.41639
8a - 31.d	1.615509	0.048282575	0.723	0.0115	0.38013
8a - 32.d	1.912046	0.047526955	0.702	0.0095	0.5211
8a - 33.d	1.658375	0.045378415	0.711	0.014	0.51121

8a - 34.d	1.552795	0.0687184	0.699	0.011	0.14887
8a - 35.d	2.283105	0.05994455	0.7	0.013	0.49357
8a - 36.d	2.518892	0.06344815	0.686	0.012	0.40482
8a - 37.d	1.876173	0.04752032	0.701	0.0135	0.60884
8a - 38.d	1.605136	0.047664565	0.717	0.013	0.23786
8a - 39.d	2.074689	0.0581085	0.719	0.0115	0.24154
8a - 40.d	2.145923	0.0575623	0.711	0.0135	0.44879
8a - 41.d	1.408451	0.0386828	0.702	0.0085	0.40312
8a - 42.d	1.017294	0.02742451	0.719	0.0105	0.3467
8a - 43.d	1.175088	0.033830385	0.718	0.011	0.31073
8a - 44.d	1.769912	0.043856215	0.714	0.0085	0.49422
8a - 45.d	1.162791	0.05678745	0.792	0.019	0.13178
8a - 46.d	1.312336	0.03702785	0.721	0.0155	0.48625
8a - 47.d	1.686341	0.044078045	0.697	0.0125	0.43908
8a - 48.d	2.331002	0.0570525	0.702	0.012	0.54186
8a - 49.d	1.633987	0.038713745	0.698	0.01	0.40966
8a - 50.d	2.087683	0.05448025	0.692	0.0105	0.49603
8a - 51.d	2.57732	0.06310445	0.689	0.0125	0.52538
8a - 52.d	2.531646	0.0608877	0.68	0.01	0.57695
8a - 53.d	2.656042	0.06349105	0.712	0.012	0.51273
8a - 54.d	2.167317	0.049321255	0.662	0.009	0.36151
8a - 55.d	2.03666	0.0559978	0.678	0.013	0.61085
8a - 56.d	0.952381	0.0770975	0.689	0.007	0.096519
8a - 57.d	0.471698	0.02002492	0.6847	0.00475	-0.01014
8a - 58.d	1.55521	0.03869885	0.715	0.0095	0.43121

7b - 1.d	15.17451	0.575664	0.287	0.0065	-0.0857
7b - 2.d	15.12859	0.3547552	0.33	0.007	0.28081
7b - 3.d	11.91895	0.3977719	0.35	0.0065	-0.05919
7b - 4.d	17.60563	0.48043545	0.27	0.007	-0.29193
7b - 5.d	4.716981	0.244749	0.596	0.023	0.13212
7b - 6.d	18.83239	0.5142555	0.277	0.01	0.098872
7b - 7.d	19.23077	0.49926035	0.275	0.0085	0.20752
7b - 8.d	17.12329	0.3958294	0.292	0.0065	0.4032
7b - 9.d	10.55966	0.2843415	0.417	0.0105	0.57322
7b - 10.d	14.92537	0.47894855	0.357	0.0145	0.40996
7b - 11.d	12.7551	0.4880779	0.362	0.009	-0.01863
7b - 12.d	23.20186	0.6729075	0.154	0.0065	0.23767
7b - 13.d	17.98561	0.4690492	0.258	0.009	0.56771
7b - 14.d	19.64637	0.4631756	0.254	0.0055	0.27926
7b - 15.d	14.08451	1.9837335	0.229	0.012	-0.58778
7b - 16.d	18.79699	1.731302	0.287	0.012	-0.02114
7b - 17.d	16.39344	0.4971782	0.329	0.0075	0.035623
7b - 18.d	10.20408	0.4789671	0.378	0.0175	0.44236
7b - 19.d	10	0.6	0.341	0.007	0.21473
7b - 20.d	9.21659	0.24209475	0.439	0.0105	0.34955
7b - 21.d	15.38462	0.4970414	0.34	0.02	0.39678
7b - 22.d	15.92357	0.40569595	0.301	0.0095	0.63272
7b - 23.d	13.17523	0.40792875	0.342	0.016	0.45858
7b - 24.d	12.57862	0.4192872	0.397	0.0185	-0.03524

7b - 25.d	4.310345	0.4087396	0.368	0.015	0.13336
7b - 26.d	19.92032	0.6150695	0.351	0.0155	0.41838
7b - 27.d	19.34236	0.44895225	0.216	0.0055	-0.19328
12b - 1.d	16.6113	1.0071635	0.199	0.006	0.37492
12b - 2.d	20.4918	0.839828	0.201	0.0065	0.29136
12b - 3.d	7.692308	0.4733728	0.18	0.0065	0.23222
12b - 4.d	43.66812	1.239488	0.1395	0.0044	0.075976
12b - 5.d	40.45307	1.0636935	0.163	0.007	0.25697
12b - 6.d	15.40832	0.9377945	0.1046	0.0028	0.30123
12b - 7.d	38.31418	1.3945775	0.131	0.006	-0.30393
12b - 8.d	64.51613	1.519251	0.1274	0.00445	-0.24901
12b - 9.d	23.98082	1.035143	0.1078	0.0032	0.084315
12b - 10.d	34.75843	0.845704	0.146	0.006	0.2505
12b - 11.d	80.45052	1.715156	0.0863	0.00445	0.085416
12b - 12.d	55.55556	2.469136	0.114	0.008	-0.06512
12b - 13.d	58.07201	1.635594	0.146	0.0085	0.004497
12b - 14.d	58.71991	1.896415	0.1313	0.00465	0.1884
12b - 15.d	24.93766	0.839547	0.198	0.0085	0.16621
12b - 16.d	8.064516	0.3577003	0.373	0.013	0.11703
12b - 17.d	22.98851	0.7134365	0.168	0.011	0.49341
12b - 18.d	62.5	2.34375	0.1239	0.0048	-0.05006
12b - 19.d	58.13953	2.1971335	0.1127	0.00395	0.068576
12b - 20.d	32.67974	1.0679655	0.205	0.01	0.1783
12b - 21.d	24.5098	0.7208765	0.161	0.0085	0.32167

12b - 22.d	42.55319	1.267542	0.146	0.008	0.1837
12b - 23.d	68.21282	1.8844605	0.124	0.005	0.4177
12b - 24.d	41.66667	1.128472	0.1208	0.00435	0.24228
12b - 25.d	52.8262	1.3394915	0.1207	0.0043	0.008948
12b - 26.d	64.68305	1.673559	0.143	0.005	-0.10008
12b - 27.d	36.10108	1.238124	0.1556	0.00415	-0.04214
12b - 28.d	24.15459	1.0793715	0.172	0.007	-0.24611
12b - 29.d	30.21148	0.95837	0.1321	0.0044	0.35834
12b - 30.d	37.59398	1.130646	0.1514	0.00475	0.32498
12b - 31.d	30.03003	1.397794	0.1123	0.0038	0.14011
12b - 32.d	33.89831	1.2640045	0.173	0.006	0.017494
12b - 33.d	27.39726	0.6380185	0.2175	0.0046	0.40624
12b - 34.d	27.17391	0.923027	0.1573	0.0043	0.042668
12b - 35.d	37.31343	1.3922925	0.1268	0.004	0.15008
12b - 36.d	27.85515	1.396637	0.171	0.005	-0.20521
12b - 37.d	41.49378	1.1191265	0.1111	0.0037	0.18706
12b - 38.d	37.24395	0.832267	0.1099	0.00405	-0.11139
12b - 39.d	20.16129	0.670688	0.151	0.0065	0.20844
12b - 40.d	10.43841	0.4140498	0.128	0.006	0.22375
12b - 41.d	23.47418	1.3775925	0.128	0.006	-0.1875
12b - 42.d	72.51632	1.656464	0.1027	0.00385	0.3188
12b - 43.d	35.84229	1.28467	0.107	0.005	0.18768
12b - 44.d	59.80861	1.7169935	0.1032	0.00345	0.2694
12b - 45.d	42.01681	1.5006	0.116	0.005	-0.16149
12b - 46.d	13.40483	0.4671923	0.125	0.005	0.23636

12b - 47.d	24.44988	1.0760335	0.131	0.0055	-0.13149
12b - 48.d	16.10306	0.6871675	0.124	0.0055	0.25151
12b - 49.d	46.04052	1.2718375	0.1084	0.00335	-0.06798
12b - 50.d	32.67974	1.3349565	0.129	0.0042	-0.03186
12b - 51.d	37.50938	0.9145195	0.1225	0.00485	0.17976
12b - 53.d	30.30303	1.331497	0.188	0.0055	0.11475
12b - 54.d	39.68254	2.047115	0.127	0.0055	-0.23428
13a - 1.d	0.115473	0.005333646	0.8462	0.0071	0.070094
13a - 2.d	0.083264	0.006239596	0.838	0.011	0.1695
13a - 3.d	0.088889	0.00537284	0.849	0.01	0.13908
13a - 4.d	0.075415	0.004038046	0.849	0.014	0.23118
13a - 5.d	0.08489	0.004972314	0.843	0.015	0.22699
13a - 6.d	0.039216	0.002921953	0.85	0.016	0.14581
13a - 7.d	0.076687	0.003940212	0.8414	0.0078	0.15996
13a - 8.d	0.015314	0.001477455	0.845	0.0095	0.019127
13a - 9.d	0.02457	0.001931796	0.8532	0.0094	0.018645
13a - 10.d	0.02331	0.0015214	0.8499	0.0059	0.077667
13a - 11.d	0.021008	0.001853683	0.859	0.012	0.12051
13a - 12.d	0.023923	0.001888693	0.8513	0.008	0.22811
13a - 13.d	0.084034	0.01059247	0.835	0.012	-0.03375
13a - 14.d	0.092593	0.01286008	0.8421	0.0086	-0.08091
13a - 15.d	1.17096	0.04936132	0.791	0.023	0.53295
11aS(2) - 1.d	0.019493	0.001633931	0.841	0.01	0.00724

11aS(2) - 2.d	0.022936	0.00136773	0.8381	0.0079	0.15616
11aS(2) - 3.d	0.012594	0.001332411	0.835	0.013	0.021323
11aS(2) - 4.d	0.006897	0.000760999	0.837	0.011	0.20886
11aS(2) - 5.d	0.10352	0.004929508	0.8341	0.0069	0.16033
11aS(2) - 6.d	0.220264	0.01261426	0.8352	0.0073	-0.13734
11aS(2) - 7.d	0.149477	0.006702997	0.86	0.013	0.43666
11aS(2) - 8.d	0.114548	0.004986033	0.8417	0.008	0.037706
11aS(2) - 9.d	0.018382	0.001520599	0.843	0.01	0.13119
11aS(2) - 10.d	0.018519	0.001303155	0.844	0.012	0.23542
11aS(2) - 11.d	0.022573	0.001783449	0.8409	0.0098	-0.05284
11aS(2) - 12.d	0.061728	0.002857796	0.8407	0.0088	0.27059
11aS(2) - 13.d	0.089606	0.003773718	0.8454	0.0074	0.10045
11aS(2) - 14.d	0.117233	0.004672839	0.8444	0.0085	0.2014
11aS(2) - 15.d	0.154321	0.00690634	0.8383	0.0082	0.38615
11aS(2) - 16.d	0.263366	0.01040423	0.833	0.013	0.25428
11aS(1) - 1.d	0.344828	0.01664685	0.832	0.018	0.36611

11aS(1) - 2.d	0.591716	0.02871048	0.84	0.02	0.21526
11aS(1) - 3.d	0.142046	0.009684917	0.849	0.019	0.16793
11aS(1) - 4.d	1.055966	0.04683271	0.81	0.026	0.23923
11aS(1) - 5.d	0.105597	0.008474491	0.856	0.023	0.035387
11aS(1) - 6.d	0.27933	0.01872601	0.85	0.024	0.26789
11aS(1) - 7.d	0.78064	0.03778274	0.812	0.024	0.36894
11aS(1) - 8.d	1.089325	0.04746512	0.798	0.016	0.12238
11aS(1) - 9.d	0.448632	0.02012704	0.845	0.016	0.3598
11aS(1) - 10.d	0.378788	0.02008724	0.835	0.021	0.25947
10aY - 1.d	20.57613	1.524158	0.456	0.044	0.25695
10aY - 2.d	3.717472	0.3178508	0.745	0.053	0.39731
10aY - 3.d	3.095975	0.2204564	0.833	0.038	0.27951
10aY - 4.d	9.920635	0.8267196	0.677	0.077	0.69833
10aY - 5.d	7.092199	0.5532921	0.81	0.21	0.99184
10aY - 6.d	2.97619	0.611182	0.776	0.089	-0.23781
10aY - 7.d	9.345794	1.57219	1.19	0.25	0.94592
10aY - 8.d	122.549	9.16114	0.335	0.037	0.16383
10aY - 9.d	60.97561	4.833432	0.526	0.065	0.39092
10aY - 10.d	7.352941	1.081315	0.81	0.1	0.72099
10aY - 11.d	10.30928	1.169093	0.348	0.048	0.14118

13aSlick - 1.d	0.087413	0.003667661	0.8471	0.0064	0.11929
13aSlick - 2.d	0.021186	0.001346596	0.8485	0.0038	0.22634
13aSlick - 3.d	0.046168	0.002344638	0.8477	0.0097	0.16481
13aSlick - 4.d	0.011494	0.000647378	0.8475	0.0037	0.10015
13aSlick - 5.d	0.031417	0.00138183	0.8471	0.0041	0.022269
13aSlick - 6.d	0.057604	0.00252182	0.8499	0.0054	0.26473
13aSlick - 7.d	0.011947	0.000628061	0.849	0.0038	0.032828
13aSlick - 8.d	0.093809	0.003608024	0.8529	0.0078	0.11777
13aSlick - 9.d	0.07728	0.003165245	0.8534	0.0066	0.14505
13aSlick - 10.d	0.060459	0.004020885	0.8595	0.0066	0.21876
13d - 1.d	0.002874	0.000338552	0.8516	0.0061	0.096247
13d - 2.d	0.067613	0.003337233	0.8528	0.0064	-0.08765
13d - 3.d	0.031056	0.002025385	0.846	0.0062	0.08743
13d - 4.d	0.03096	0.002683818	0.8532	0.0071	0.038487
13d - 5.d	0.006173	0.000495351	0.8471	0.0071	-0.18995
13d - 6.d	0.05618	0.006627951	0.8546	0.0077	0.10561
13d - 7.d	0.033223	0.003311222	0.8437	0.0074	-0.05906
13d - 8.d	0.002825	0.000406971	0.851	0.0082	0.020239
13d - 9.d	0.111857	0.005380138	0.8572	0.008	0.11701

13b - 1.d	0.006329	0.000600865	0.8551	0.0067	-0.13263
13b - 2.d	0.040984	0.005878796	0.8549	0.007	0.088678
13b - 3.d	0.015649	0.001420451	0.8487	0.0062	0.058128
13b - 4.d	0.015432	0.001762308	0.8498	0.0073	0.094053
13b - 5.d	0.002747	0.000309443	0.8536	0.0079	-0.18459
13b - 6.d	0.058617	0.003332834	0.8499	0.0069	-0.01816
13b - 7.d	0.017271	0.001431806	0.8503	0.0067	0.14234
13b - 8.d	0.012225	0.000866805	0.8471	0.0065	0.15903
13b - 9.d	0.003663	0.000348858	0.8461	0.0064	-0.02165
13b - 10.d	0.006452	0.00074922	0.8481	0.0083	0.17857
13b - 11.d	0.006645	0.000441496	0.8469	0.0072	-0.0473

Analytical session 2

N612 - 1.d	3.571429	0.04655612	0.9064	0.00275	0.65677
N612 - 2.d	3.602954	0.04673261	0.9069	0.00265	0.46382
N612 - 3.d	3.53857	0.045703405	0.9057	0.00265	0.365
N612 - 4.d	3.601008	0.04668214	0.9097	0.0027	0.48947
N612 - 5.d	3.614284	0.047026965	0.9069	0.0027	0.53403
N612 - 6.d	3.602305	0.046715775	0.9067	0.0026	0.42346
N612 - 7.d	3.509634	0.045574865	0.9066	0.0026	0.21484
N612 - 8.d	3.946174	0.05138855	0.9073	0.0027	0.49327
N612 - 9.d	3.459011	0.04486783	0.9075	0.0026	0.49355
N612 - 10.d	3.501401	0.04536128	0.9065	0.00265	0.48924
N612 - 11.d	3.545722	0.04588833	0.907	0.00265	0.31723
N612 - 12.d	3.568115	0.04646978	0.9081	0.0027	0.45234
N612 - 13.d	3.558212	0.046212195	0.9046	0.0027	0.41714
N612 - 14.d	3.685006	0.047527435	0.9092	0.0027	0.4108
N612 - 15.d	3.654971	0.04742378	0.9084	0.0027	0.55212
N612 - 16.d	3.518649	0.04580929	0.9078	0.0026	0.36692
N612 - 17.d	3.816648	0.04952713	0.9062	0.00265	0.41738
N612 - 18.d	3.399048	0.04390341	0.9069	0.00265	0.53723
N612 - 19.d	3.412969	0.044263765	0.9085	0.00265	0.28839
N612 - 20.d	3.466205	0.04505465	0.9062	0.00265	0.17547
N612 - 21.d	3.484321	0.045526835	0.9053	0.00265	0.3135
N612 - 22.d	3.480682	0.04543181	0.909	0.00265	0.39289

N612 - 23.d	3.637686	0.046976305	0.909	0.0028	0.42231
N612 - 24.d	3.842016	0.04944965	0.9043	0.0028	0.37296
N612 - 25.d	3.570154	0.046522885	0.9091	0.00295	0.29036
N612 - 26.d	3.752486	0.04857997	0.9063	0.0028	0.46586
N612 - 27.d	3.449465	0.04462054	0.9064	0.0027	0.38434
N612 - 28.d	3.481894	0.04546345	0.9074	0.0027	0.23918
N612 - 29.d	3.443526	0.04446702	0.9054	0.0028	0.37336
N612 - 30.d	3.399048	0.04390341	0.9035	0.00295	0.55109
N612 - 31.d	3.423368	0.0445339	0.9056	0.0028	0.35045
N612 - 32.d	3.487967	0.04501387	0.9049	0.0027	0.41127
N612 - 33.d	3.824677	0.04973572	0.9049	0.0028	0.54145
N612 - 34.d	3.627789	0.046721025	0.9088	0.0027	0.38279
N612 - 35.d	3.57769	0.046079505	0.9062	0.00265	0.40339
N612 - 36.d	3.527337	0.04603579	0.9065	0.00275	0.40514
N612 - 37.d	3.489184	0.045654005	0.9061	0.003	0.27937
N612 - 38.d	3.495281	0.04520287	0.9085	0.0029	0.36161
N612 - 39.d	3.462604	0.044961095	0.9063	0.00295	0.47698
N612 - 40.d	3.470174	0.0451579	0.9069	0.0029	0.64797
N612 - 41.d	3.520755	0.045864145	0.9083	0.00285	0.44117
N612 - 42.d	3.51358	0.045677405	0.9082	0.0028	0.38754
N612 - 43.d	3.624502	0.046636395	0.9078	0.0027	0.1859
N612 - 44.d	3.42818	0.0452468	0.909	0.00315	0.43166
N612 - 45.d	3.535193	0.0456162	0.9052	0.00285	0.39256
N612 - 46.d	3.548616	0.045963265	0.9058	0.0029	0.5263
N612 - 47.d	3.649635	0.047285415	0.9099	0.0029	0.40791
N612 - 48.d	3.71761	0.048372195	0.9059	0.0028	0.41138
N614 - 1.d	1.137656	0.01747254	0.881	0.009	0.55372
N614 - 2.d	1.248751	0.017153175	0.8701	0.00465	0.77474
N614 - 3.d	1.233806	0.01674506	0.8681	0.0042	0.47403
N614 - 4.d	1.253447	0.017282425	0.8733	0.00475	0.49656
N614 - 5.d	1.220554	0.01713215	0.8754	0.005	0.32085
N614 - 6.d	1.234263	0.01675746	0.8626	0.0047	0.59315
N614 - 7.d	1.235178	0.01678231	0.8679	0.005	0.66829
N614 - 8.d	1.236552	0.016819685	0.8704	0.0042	0.54092
N614 - 9.d	1.234873	0.01677402	0.8728	0.0045	0.64936
N614 - 10.d	1.247038	0.01710615	0.8716	0.00405	0.33412
N614 - 11.d	1.235941	0.016803055	0.8617	0.0044	0.45669
N614 - 12.d	1.214329	0.016220545	0.871	0.00435	0.60165
N614 - 13.d	1.230012	0.016642235	0.8662	0.00425	0.46295
N614 - 14.d	1.241311	0.01694938	0.8787	0.00445	0.33995
N614 - 15.d	1.237317	0.0168405	0.8785	0.00475	0.56869
N614 - 16.d	1.238543	0.01687389	0.8763	0.005	0.57133
N614 - 17.d	1.230769	0.01666272	0.873	0.00455	0.61847
N614 - 18.d	1.242236	0.016974655	0.8674	0.00425	0.51123
N614 - 19.d	1.230164	0.01664633	0.8718	0.00485	0.61539
N614 - 20.d	1.230921	0.016666825	0.8711	0.005	0.64023

N614 - 21.d	1.248907	0.01715746	0.8669	0.005	0.52817
N614 - 22.d	1.239465	0.016898995	0.8723	0.005	0.52292
N614 - 23.d	1.216249	0.01627188	0.8754	0.00495	0.51749
N614 - 24.d	1.234263	0.01675746	0.8774	0.00475	0.51985
N614 - 25.d	1.230921	0.016666825	0.873	0.00465	0.57596
N614 - 26.d	1.234263	0.01675746	0.8702	0.0045	0.79988
N614 - 27.d	1.227747	0.01658099	0.8707	0.00475	0.52143
N614 - 28.d	1.242699	0.016987315	0.8694	0.0047	0.41132
N614 - 29.d	1.24471	0.01704233	0.8735	0.0044	0.51753
N614 - 30.d	1.235178	0.01678231	0.874	0.005	0.54182
N614 - 31.d	1.230921	0.016666825	0.866	0.00475	0.42847
N614 - 32.d	1.247349	0.017114685	0.8755	0.00485	0.46521
N614 - 33.d	1.263903	0.01677323	0.8721	0.0055	0.58696
N614 - 34.d	1.205836	0.01599445	0.8695	0.0048	0.60779
N614 - 35.d	1.226242	0.01654035	0.8716	0.0046	0.62332
N614 - 36.d	1.22459	0.01649582	0.8638	0.00475	0.44671
N614 - 37.d	1.222046	0.01717405	0.8803	0.00495	0.5831
N614 - 38.d	1.243626	0.017012675	0.8714	0.00465	0.58069
N614 - 39.d	1.241003	0.016940965	0.8715	0.00485	0.44495
N614 - 40.d	1.238697	0.01687807	0.8665	0.00445	0.33186
N614 - 41.d	1.222494	0.016439405	0.8704	0.00495	0.49324
N614 - 42.d	1.245175	0.017055065	0.881	0.0047	0.44852
N614 - 43.d	1.251251	0.017221925	0.8679	0.0044	0.28389
N614 - 44.d	1.247505	0.017118955	0.8743	0.00495	0.52419
N614 - 45.d	1.217137	0.016295655	0.8726	0.0045	0.58756
N614 - 46.d	1.208313	0.01606023	0.8639	0.00435	0.47013
N614 - 47.d	1.241619	0.016957795	0.8764	0.0055	0.51811
N614 - 48.d	1.245485	0.017063565	0.862	0.0046	0.53395
prague - 1.d	13.08901	0.21415255	0.1503	0.0045	-0.052152
prague - 2.d	14.0056	0.20596475	0.0921	0.00195	-0.25829
prague - 3.d	9.881423	0.21481355	0.284	0.01	0.32158
prague - 4.d	5.988024	0.3227079	0.318	0.013	-0.88682
prague - 5.d	6.587615	0.10632185	0.2963	0.0043	-0.051005
prague - 6.d	13.33333	0.32	0.092	0.0075	0.032901
prague - 7.d	12.37624	0.2220983	0.125	0.0048	-0.9789
prague - 8.d	12.75998	0.17909895	0.0966	0.0016	-0.020456
prague - 9.d	3.10559	0.1591374	0.631	0.0105	-0.83398
prague - 10.d	10.75269	0.2601457	0.159	0.0095	-0.86438

prague - 11.d	13.21004	0.2006809	0.0645	0.00175	-0.38042
prague - 12.d	4.710316	0.09873245	0.568	0.0065	-0.65267
prague - 13.d	0.7633588	0.0553581	0.787	0.009	-0.50088
prague - 14.d	12.77139	0.2854398	0.152	0.006	0.073831
prague - 15.d	8.920607	0.1949642	0.212	0.006	-0.82902
prague - 16.d	10.08065	0.19307685	0.146	0.0055	-0.084031
prague - 17.d	8.264463	0.1229424	0.2481	0.00265	0.23035
prague - 18.d	12.9199	0.1919623	0.0622	0.0018	0.17349
prague - 19.d	9.13242	0.16263215	0.211	0.0045	-0.16976
prague - 20.d	11.72333	0.1786674	0.1022	0.00245	-0.65679
prague - 21.d	12.07729	0.2114985	0.0985	0.0042	0.1682
prague - 22.d	10.81081	0.1577794	0.1368	0.00245	0.021881
prague - 23.d	9.29368	0.1770636	0.226	0.0055	-0.82159
prague - 24.d	9.606148	0.15225885	0.2776	0.00465	-0.62596
WC1 - 1.d	21.37666	0.29702495	0.1149	0.00195	0.37836
WC1 - 2.d	21.39953	0.2976609	0.1068	0.00225	0.20263
WC1 - 3.d	20.83333	0.30381945	0.1259	0.0022	0.31791
WC1 - 4.d	21.23593	0.2931271	0.1173	0.00185	0.17222
WC1 - 5.d	20.6441	0.27701615	0.1184	0.00225	0.39814
WC1 - 6.d	20.4499	0.2927388	0.1237	0.0022	0.13892
WC1 - 7.d	20.90738	0.28412705	0.1286	0.0018	0.22032
WC1 - 8.d	20.5719	0.2962421	0.1423	0.0021	0.28054
WC1 - 9.d	21.68257	0.3055869	0.1178	0.0021	0.15023
WC1 - 10.d	20.69108	0.2996846	0.1117	0.00205	0.37891
WC1 - 11.d	20.70822	0.3001813	0.1119	0.00215	0.32548
WC1 - 12.d	20.47502	0.2934585	0.1302	0.00215	0.27999
WC1 - 13.d	20.60581	0.2972196	0.114	0.00215	0.13862
WC1 - 14.d	20.54232	0.29539075	0.1192	0.00185	0.056197
WC1 - 15.d	19.97603	0.2992813	0.1075	0.00215	0.037816
WC1 - 16.d	19.48178	0.28465495	0.1343	0.00215	0.42295
WC1 - 17.d	20.12882	0.3038772	0.1239	0.0025	0.44333
WC1 - 18.d	19.72776	0.2724291	0.1161	0.0021	0.23104
WC1 - 19.d	19.04762	0.29024945	0.1415	0.00195	-0.084762
WC1 - 20.d	19.97603	0.2793292	0.1242	0.0019	0.33838
WC1 - 21.d	20.21019	0.28591615	0.1142	0.00175	0.21755

WC1 - 22.d	20.63558	0.2980789	0.1132	0.00215	0.38094
WC1 - 23.d	20.45827	0.29297845	0.1231	0.00205	0.35326
WC1 - 24.d	20.28398	0.28800775	0.1162	0.00195	0.31147
WC1 - 25.d	19.64637	0.28948475	0.1254	0.00255	0.18911
WC1 - 26.d	20.39984	0.29130735	0.1013	0.00215	0.28097
WC1 - 27.d	20.21836	0.2861474	0.1163	0.00185	0.12555
WC1 - 28.d	19.4742	0.26547105	0.1251	0.0019	0.29022
WC1 - 29.d	19.48558	0.2657815	0.1261	0.0021	0.34755
WC1 - 30.d	20.04008	0.28112335	0.128	0.0022	0.38918
WC1 - 31.d	20.46245	0.29309835	0.1221	0.0018	0.2092
WC1 - 32.d	19.75114	0.2925805	0.1207	0.0021	0.29509
WC1 - 33.d	20.16536	0.2846491	0.1193	0.0023	0.1863
WC1 - 34.d	20.15723	0.28441965	0.1295	0.00195	0.42241
WC1 - 35.d	20.69965	0.27850905	0.1256	0.00185	0.096656
WC1 - 36.d	19.88072	0.29643215	0.1275	0.00245	0.3697
WC1 - 37.d	20.44572	0.29261915	0.1151	0.0018	0.11617
WC1 - 38.d	20.62706	0.2765592	0.1288	0.00185	0.17162
WC1 - 39.d	21.21341	0.31500605	0.095	0.00195	0.031739
WC1 - 40.d	20.17349	0.28487885	0.1081	0.0021	0.39629
WC1 - 41.d	18.77934	0.2644978	0.1499	0.00225	0.19237
WC1 - 42.d	19.76285	0.29292755	0.1312	0.0021	0.047324
WC1 - 43.d	19.88862	0.27689015	0.128	0.00185	0.15914
WC1 - 44.d	19.94416	0.29832705	0.1178	0.00245	0.20079
WC1 - 45.d	21.45462	0.29919555	0.1184	0.0021	0.31355
WC1 - 46.d	21.58895	0.3029537	0.1041	0.00215	0.098868
WC1 - 47.d	20.98636	0.2862777	0.1208	0.00195	0.23986
WC1 - 48.d	20.76412	0.30180405	0.1229	0.00205	0.29813
10b - 1.d	14.14427	0.32009665	0.403	0.015	0.56798
10b - 2.d	12.31527	0.2729986	0.43	0.014	0.33449
10b - 3.d	17.76199	0.457458	0.289	0.0155	0.41168
10b - 4.d	16.63894	0.41528125	0.376	0.015	0.52187
10b - 5.d	12.39157	0.29942465	0.452	0.0145	0.16932
10b - 6.d	12.7551	0.2847121	0.401	0.014	0.54887
10b - 7.d	16.83502	0.35427225	0.332	0.011	0.34368
10b - 8.d	14.14427	0.31009365	0.35	0.0115	0.43605
10b - 9.d	9.861933	0.213967	0.469	0.0115	0.44929
10b - 10.d	9.65251	0.24224445	0.498	0.018	0.52345
10b - 11.d	10.39501	0.29715465	0.471	0.014	0.20431
10b - 12.d	13.44086	0.2800179	0.42	0.012	0.18743
10b - 13.d	15.77287	0.4104927	0.346	0.014	0.49698
10b - 14.d	10.27749	0.2587858	0.448	0.017	0.36668
10b - 15.d	16.36661	0.4419789	0.331	0.014	0.36138
10b - 16.d	12.46883	0.34203765	0.417	0.0155	0.28962
10b - 17.d	13.35113	0.34759295	0.434	0.015	0.36598
10b - 18.d	10.70664	0.28084865	0.455	0.015	0.42895
10b - 19.d	13.73626	0.3585014	0.39	0.013	0.13504

10b - 20.d	11.21076	0.28906675	0.431	0.0155	0.26313
10b - 21.d	11.94743	0.3068934	0.466	0.012	0.09431
		0			
10aY - 1.d	8.333333	0.5208335	0.94	0.06	0.51529
10aY - 2.d	20.70393	1.2216605	0.62	0.075	0.51104
10aY - 3.d	3.773585	0.2278391	1.04	0.095	0.62408
10aY - 4.d	33.11258	2.6314635	0.312	0.041	0.56502
10aY - 5.d	8.264463	0.4781094	0.9	0.06	0.35154
10aY - 6.d	19.45525	1.438326	0.74	0.08	0.81514
10aY - 7.d	9.67118	0.406863	0.722	0.043	0.70816
10aY - 8.d	13.1406	0.6302655	0.552	0.044	0.52038
10aY - 9.d	13.21004	0.5933175	0.585	0.0335	0.62929
10aY - 10.d	10.86957	0.7679585	0.85	0.065	0.68625
10aY - 11.d	8.62069	0.44589775	0.98	0.08	0.71956
10aY - 12.d	9.345794	0.4803913	0.82	0.07	0.60263
10aY - 13.d	9.07441	0.3664349	0.683	0.039	0.33268
10aY - 14.d	10.84599	0.44701465	0.629	0.0405	0.76484
10aY - 15.d	7.874016	0.46500095	0.78	0.055	0.76551
10aY - 16.d	5.780347	0.23388685	0.836	0.048	0.76244
10aY - 17.d	25.83979	1.468929	0.487	0.043	0.91839
10aY - 18.d	8.62069	0.520214	0.71	0.055	0.60345
10aY - 19.d	34.96503	2.750746	0.52	0.055	0.24715
10aY - 20.d	29.15452	1.3599775	0.393	0.0405	0.17741
10aY - 21.d	14.66276	0.9352345	0.76	0.1	0.73455
10aY - 22.d	36.23188	1.969124	0.579	0.049	0.77611
10aY - 23.d	25.5102	1.1388485	0.291	0.028	0.44234
10aY - 24.d	19.60784	2.1145715	0.73	0.155	0.67157
10aY - 25.d	23.69668	1.4319085	0.432	0.031	0.86487
10aY - 26.d	9.345794	0.698751	0.74	0.085	0.68763
10aY - 27.d	19.30502	0.670831	0.395	0.024	0.48368
10aY - 28.d	40.32258	2.764048	0.54	0.065	0.51054
10aY - 29.d	13.47709	0.899078	0.55	0.065	0.38703
10aY - 30.d	2.293578	0.2262015	1.04	0.135	0.67473
10aY - 31.d	18.76173	1.337609	0.317	0.0295	0.38116
10aY - 32.d	13.85042	0.700194	0.53	0.05	0.44316
10aY - 33.d	16.55629	0.6441605	0.349	0.0335	0.32839
10aY - 34.d	11.23596	0.8206035	0.51	0.06	0.37372
10aY - 35.d	10.6383	0.6224535	0.431	0.036	0.45671
10aY - 36.d	11.76471	0.7612455	0.528	0.049	0.58699
10aY - 37.d	13.49528	0.746702	0.545	0.0485	0.59024
10aY - 38.d	9.90099	0.5881775	0.7	0.095	0.79486
10aY - 39.d	15.625	0.744629	0.411	0.027	0.61227
10aY - 40.d	8.474576	0.790003	0.48	0.16	0.44363
10aY - 41.d	27.85515	1.62941	0.4	0.05	0.69241
10aY - 42.d	60.97561	4.0898275	0.53	0.055	0.6444
10aY - 43.d	13.88889	0.80054	0.636	0.0495	0.56112
10aY - 44.d	18.24818	0.649342	0.364	0.03	0.47851

10aY - 45.d	21.23142	1.893248	0.56	0.08	0.45791
10aY - 46.d	10.86957	0.649811	0.87	0.08	0.35223
10aY - 47.d	4.504505	0.3043584	0.629	0.025	0.32162
10aY - 48.d	26.38522	1.322742	0.516	0.039	0.3832
10aY - 49.d	22.22222	2.962963	0.87	0.095	0.82377
10aY - 50.d	318.4713	12.678	0.468	0.0185	0.27027
10aY - 51.d	6.535948	0.46990475	0.616	0.0335	0.24682
10aY - 52.d	48.78049	2.7364665	0.352	0.0425	-0.068193
10aY - 53.d	26.88172	1.8426985	0.77	0.07	0.7528
10aY - 54.d	19.12046	0.8043025	0.484	0.029	0.64208
10aY - 55.d	30.58104	2.24448	0.29	0.09	0.43454
10aY - 56.d	63.29114	3.2046145	0.66	0.07	0.80961
10aY - 57.d	20.04008	1.184734	0.488	0.0265	0.34514
10aY - 58.d	12.04819	0.7257945	0.692	0.036	0.42407
10aY - 59.d	20.87683	1.0242285	0.676	0.041	0.49218
10aY - 60.d	34.36426	2.5389405	0.552	0.045	0.23297
10aY - 61.d	10.30928	0.6376875	0.99	0.09	0.73977
10aY - 62.d	5.025126	0.4040302	0.81	0.085	0.44946
10aY - 63.d	29.67359	3.2579315	0.98	0.15	0.58297
10aY - 64.d	17.24138	2.2294885	1.32	0.26	0.79341
10aY - 65.d	5.747126	0.46241245	0.985	0.0465	0.45163
10aY - 66.d	5.714286	0.35918365	0.76	0.07	0.3755
10aY - 67.d	3.30033	0.16882875	0.819	0.045	0.56482
10aY - 68.d	7.246377	0.34131485	0.674	0.0455	0.4382
10aY - 69.d	5.464481	0.34339635	0.641	0.0475	0.56611
10aY - 70.d	7.27802	0.2648479	0.546	0.026	0.65111
10aY - 71.d	5.291005	0.23795525	0.78	0.065	0.30937
10aY - 72.d	19.37984	0.938946	0.385	0.028	0.72784
10aY - 73.d	11.29944	0.35749625	0.523	0.0285	0.42179
10aY - 74.d	151.5152	16.06979	1.12	0.15	0.91553
10aY - 75.d	15.625	1.3427735	0.65	0.075	0.47753
10aY - 76.d	4.444444	0.2271605	0.542	0.0325	0.41566
10aY - 77.d	11.79245	0.507576	0.378	0.031	0.40036
10aY - 78.d	26.73797	1.215362	0.619	0.0345	0.44269
10aY - 79.d	281.6901	12.299145	0.521	0.028	0.38107
10aY - 80.d	315.4574	15.92214	0.468	0.0345	0.41543
10aY - 81.d	369.0037	15.65883	0.322	0.0155	-0.58376
8a - 1.d	2.457002	0.0875345	0.736	0.0225	0.59234
8a - 2.d	4.016064	0.1209658	0.721	0.014	0.26337
8a - 3.d	1.440922	0.029067595	0.726	0.014	0.60961
8a - 4.d	1.102536	0.03707535	0.699	0.02	0.12821
8a - 5.d	1.168224	0.02865971	0.707	0.0115	0.33054
8a - 6.d	1.083424	0.04049633	0.731	0.0145	0.37506
8a - 7.d	1.079914	0.036152615	0.7	0.0165	0.32194
8a - 8.d	3.401361	0.1041233	0.707	0.017	0.43908
8a - 9.d	2.28833	0.049746295	0.69	0.013	0.49828

8a - 10.d	1.992032	0.045634195	0.701	0.0145	0.49231
8a - 11.d	1.692047	0.03435629	0.727	0.01	0.26356
8a - 12.d	1.373626	0.029246165	0.704	0.0115	0.079139
8a - 13.d	1.582278	0.035050475	0.707	0.0135	0.50552
8a - 14.d	0.8984726	0.02058495	0.717	0.0115	0.37005
8a - 15.d	1.589825	0.03285807	0.723	0.015	0.34421
8a - 16.d	1.564945	0.033062225	0.694	0.011	0.53114
8a - 17.d	1.497006	0.02913335	0.737	0.0125	0.42297
8a - 18.d	1.893939	0.037663565	0.706	0.0135	0.52464
8a - 19.d	2.604167	0.0712077	0.757	0.018	0.51609
8a - 20.d	1.106195	0.022026	0.735	0.01	0.40985
8a - 21.d	2.016129	0.038615375	0.715	0.015	0.45232
8a - 22.d	2.55102	0.0553155	0.738	0.017	0.37264
8a - 23.d	1.094092	0.026933335	0.717	0.017	0.28748
8b - 1.d	11.90476	1.346372	0.72	0.075	0.24998
8b - 2.d	6.756757	0.570672	0.81	0.115	0.76573
8b - 3.d	3.597122	0.3623001	0.39	0.18	0.61427
8b - 4.d	45.6621	3.2317925	0.92	0.105	0.74312
8b - 5.d	27.3224	2.874078	1.15	0.165	0.43505
8b - 6.d	23.47418	1.9286295	0.64	0.07	0.5427
8b - 7.d	222.7171	7.93647	0.289	0.023	0.71722
8b - 8.d	314.8615	4.907318	0.1174	0.0033	0.22728
8b - 9.d	84.74576	4.3091065	0.513	0.039	0.47063
8b - 10.d	80	4.48	0.363	0.0345	-0.057057
8b - 11.d	187.6173	5.63204	0.301	0.0085	0.49942
8b - 12.d	187.9699	13.24976	0.445	0.0325	0.1397
8b - 13.d	44.05286	3.784277	0.8	0.115	0.73305
8b - 14.d	271.0027	7.71146	0.285	0.008	0.21734
8b - 15.d	29.06977	1.2253245	0.325	0.0345	0.64686
8b - 16.d	28.98551	0.5881115	0.137	0.00495	0.24099
8b - 17.d	21.50538	0.832466	0.311	0.027	0.43558
8b - 18.d	118.7648	5.359935	0.33	0.0285	0.43855
8b - 19.d	100	7.5	0.423	0.0495	0.18738
8b - 20.d	7.8125	0.6713865	0.89	0.17	0.69001
8b - 21.d	21.36752	0.8903135	0.221	0.02	0.28199
8b - 22.d	23.20186	0.5921585	0.164	0.0095	0.23654
8b - 23.d	26.24672	0.620001	0.134	0.0075	0.23872
8b - 24.d	24.5098	0.961169	0.148	0.0125	0.17072
8b - 25.d	24.57002	0.6640545	0.154	0.0115	0.35726
8b - 26.d	21.69197	0.7293395	0.186	0.0145	0.38191
8b - 27.d	24.44988	1.374932	0.47	0.055	0.50375
8b - 28.d	15.36098	0.8730515	0.57	0.06	0.37551
8b - 29.d	55.55556	5.709875	0.37	0.07	0.9184
8b - 30.d	21.2766	1.109099	0.54	0.05	0.57002
8b - 31.d	26.59574	1.096367	0.232	0.0245	0.59855
8b - 32.d	9.345794	0.8734385	0.31	0.155	0.73231

8b - 33.d	34.60208	1.257169	0.193	0.014	0.36773
8b - 34.d	34.36426	2.5389405	0.3	0.075	0.48259
8b - 35.d	25.64103	0.7232085	0.163	0.012	0.5037
8b - 36.d	13.69863	1.219741	0.62	0.17	0.68262
8b - 37.d	26.66667	1.991111	0.417	0.049	0.82339
7b - 1.d	14.88095	0.27680345	0.345	0.0075	0.39027
7b - 2.d	5.025126	0.39140425	0.392	0.01	0.4345
7b - 3.d	17.82531	0.365403	0.237	0.008	0.32186
7b - 4.d	10.1833	0.25924895	0.416	0.012	0.33932
7b - 5.d	9.532888	0.1953833	0.423	0.0105	0.48929
7b - 6.d	10.57082	0.2067233	0.406	0.0105	0.3596
7b - 7.d	10.31992	0.3354772	0.417	0.022	0.69374
7b - 8.d	6.963788	0.19155265	0.525	0.019	0.61114
7b - 9.d	16.75042	0.29460535	0.249	0.005	0.3955
7b - 10.d	8.183306	0.27456265	0.443	0.011	0.36537
7b - 11.d	13.1406	0.267647	0.311	0.0095	0.28863
7b - 12.d	10.98901	0.2717063	0.41	0.014	0.38086
7b - 13.d	9.541985	0.23672865	0.369	0.013	0.43453
7b - 14.d	7.716049	0.1547973	0.434	0.0115	0.41209
7b - 15.d	11.18568	0.33156665	0.412	0.0175	0.32445
7b - 16.d	17.03578	0.49337	0.274	0.016	0.29837
7b - 17.d	12.36094	0.32850455	0.392	0.0145	0.54605
7b - 18.d	15.31394	0.2931458	0.294	0.01	0.32825
7b - 19.d	14.28571	0.31632655	0.332	0.0125	0.15673
7b - 20.d	9.960159	0.3174553	0.375	0.0105	0.41938
7b - 21.d	8.196721	0.3695243	0.433	0.0095	0.28065
7b - 22.d	9.960159	0.26289265	0.408	0.013	0.5004
7b - 23.d	6.896552	0.47562425	0.463	0.0245	0.51436
7b - 24.d	9.98004	0.18924225	0.377	0.0085	0.37682
7b - 25.d	9.174312	0.505008	0.32	0.0145	0.064522
7b - 26.d	8.960573	0.29306535	0.393	0.0165	0.49644
7b - 27.d	17.3913	0.30245745	0.254	0.0065	0.21141
7b - 28.d	19.23077	0.33284025	0.222	0.006	0.31981
7b - 29.d	17.09402	0.42369785	0.266	0.0115	0.50204
7b - 30.d	16.72241	0.32158475	0.237	0.0075	0.35281
7b - 31.d	18.72659	0.4558908	0.212	0.0085	0.16647
7b - 32.d	16.75042	0.3086342	0.26	0.0085	0.19769
7b - 33.d	15.31394	0.36350075	0.323	0.0135	0.42996
12aSlick(2) - 1.d	3.484321	0.09105365	0.6443	0.0032	0.090834
12aSlick(2) - 2.d	7.89266	0.1526205	0.5896	0.0036	0.17656
12aSlick(2) - 3.d	2.695418	0.1525708	0.635	0.00415	-0.7513
12aSlick(2) - 4.d	3.292723	0.05421015	0.6507	0.0031	0.1386

12aSlick(2) - 5.d	7.369197	0.18735245	0.605	0.0055	-0.0041048
12aSlick(2) - 6.d	6.476684	0.20973715	0.625	0.0055	-0.096215
12aSlick(2) - 7.d	3.36587	0.06230995	0.6737	0.0032	0.12108
12aSlick(2) - 8.d	3.589375	0.0708599	0.6711	0.00325	0.092073
12aSlick(2) - 9.d	6.738544	0.11124955	0.6194	0.00395	0.11261
12aSlick(2) - 10.d	6.369427	0.2434176	0.6265	0.00405	-0.70551
12aSlick(2) - 11.d	5.51572	0.0988753	0.6038	0.004	0.067554
12aSlick(2) - 12.d	3.159558	0.05989685	0.6747	0.00275	0.092777
12aSlick(2) - 13.d	3.450656	0.0595351	0.6415	0.00375	0.39956
12aSlick(2) - 14.d	3.846154	0.0887574	0.6635	0.00275	-0.089088
12aSlick(2) - 15.d	3.450656	0.0535816	0.6808	0.0031	0.094789
12aSlick(2) - 16.d	2.267574	0.041135125	0.715	0.00275	0.1627
12aSlick(2) - 17.d	0.2513194	0.004421302	0.6413	0.00195	0.26106
12aSlick(2) - 18.d	0.5347594	0.02001773	0.8244	0.0028	-0.4515
12aSlick(2) - 19.d	0.6993007	0.034231505	0.8252	0.00275	-0.50289
12aSlick(2) - 20.d	2.666667	0.0711111	0.7265	0.0044	-0.61984
12aSlick(2) - 21.d	4.819277	0.0975468	0.62	0.00275	0.0080478
12aSlick(2) - 22.d	4.418913	0.09763395	0.6039	0.0032	-0.0081682
12aSlick(2) - 23.d	19.72387	0.46683705	0.541	0.0065	0.18947
12aSlick(2) - 24.d	17.92115	0.43357615	0.518	0.0055	-0.2031
12aSlick(2) - 25.d	19.12046	0.5118285	0.499	0.005	-0.1071
12aSlick(2) - 26.d	21.36752	0.3652568	0.5131	0.0044	-0.048109
12aSlick(2) - 27.d	9.52381	0.2222222	0.567	0.007	-0.012862
12aSlick(2) - 28.d	12.57862	0.3164432	0.5562	0.0049	0.03161
12aSlick(2) - 29.d	3.28084	0.05381955	0.6305	0.00315	0.0049553
12aSlick(2) - 30.d	3.311258	0.08223325	0.6257	0.0027	-0.32241
12aSlick(2) - 31.d	3.938558	0.06049775	0.6302	0.0032	0.070453

12aSlick(2) - 32.d	4.928536	0.0825876	0.6137	0.00285	0.021175
12aSlick(2) - 33.d	0.929368	0.01943381	0.6519	0.0024	0.39108
12aSlick(2) - 34.d	1.16144	0.022257565	0.6656	0.0024	-0.049706
12aSlick(2) - 35.d	1.109878	0.02032518	0.6688	0.00285	0.053474
12aSlick(2) - 36.d	0.9823183	0.01688661	0.6717	0.0024	0.041402
12aSlick(2) - 37.d	2.12585	0.0338943	0.654	0.00325	0.12897
12aSlick(2) - 38.d	2.583979	0.06009255	0.6408	0.0038	0.16151
12aSlick(2) - 39.d	2.640613	0.04183701	0.6375	0.0031	0.10728
12aSlick(2) - 40.d	3.071253	0.047162975	0.6411	0.00425	0.2842
12aSlick(2) - 41.d	1.805054	0.040727755	0.6467	0.0031	-0.16239
12aSlick(2) - 42.d	3.387534	0.0688523	0.6191	0.0031	0.078007
12aSlick(2) - 43.d	2.935995	0.05603045	0.6261	0.00245	0.17155
12aSlick(2) - 44.d	4.697041	0.11031095	0.6132	0.0031	0.059433
12aSlick(2) - 45.d	4.145937	0.064458	0.6252	0.00335	0.15588
12aSlick(2) - 46.d	4.239084	0.0862552	0.6163	0.00395	0.26091
12aSlick(2) - 47.d	0.066313	0.002000823	0.8624	0.00315	0.27513
12aSlick(2) - 48.d	0.1149425	0.00726648	0.8364	0.00375	-0.79919
12aSlick(2) - 49.d	0.3745318	0.018937005	0.835	0.0295	0.0079586
12aSlick(2) - 50.d	0.02169197	0.001388098	0.8567	0.00275	0.20661
12aSlick(2) - 51.d	3.410641	0.06979485	0.6636	0.00305	0.0666
12aSlick(2) - 52.d	4.748338	0.0890595	0.6849	0.0036	0.0001869
12aSlick(2) - 53.d	8.375209	0.1648387	0.606	0.006	-0.13211
12aSlick(2) - 54.d	6.455778	0.1250312	0.6221	0.00405	0.0096643
12aSlick(2) - 55.d	1.398601	0.025429115	0.6528	0.00315	-0.14877
12aSlick(2) - 56.d	2.369668	0.04492262	0.6931	0.00355	-0.047953
12aSlick(2) - 57.d	4.024145	0.0890656	0.72	0.00305	-0.069179
12aSlick(2) - 58.d	4.458315	0.09640135	0.6916	0.0047	-0.29885

12aSlick(2) - 59.d	1.612903	0.06113425	0.6299	0.00245	-0.0935
12aSlick(2) - 60.d	3.225806	0.08844955	0.6346	0.0026	-0.2404
12aSlick(2) - 61.d	4.578755	0.06813625	0.6493	0.00375	0.11251
12aSlick(2) - 62.d	2.057613	0.033870175	0.7787	0.00275	-0.12341
12aSlick(2) - 63.d	10.36269	0.31141775	0.5859	0.005	-0.59361
12aSlick(2) - 64.d	1.865672	0.05743205	0.6546	0.0023	0.21749
12aSlick(2) - 65.d	4.716981	0.0945621	0.6199	0.00345	0.084896
12aSlick(2) - 66.d	12.40695	0.31556135	0.5916	0.00375	-0.13322
12aSlick(2) - 67.d	8.826125	0.24928155	0.5994	0.0032	-0.34398
12aSlick(2) - 68.d	8.510638	0.2390222	0.6245	0.00285	-0.21169
12aSlick(2) - 69.d	14.32665	0.28735395	0.54	0.005	0.22216
12aSlick(2) - 70.d	2.932551	0.09889835	0.6255	0.00235	0.18731
12aSlick(2) - 71.d	2.325581	0.0838291	0.6357	0.00295	-0.43793
12aSlick(2) - 72.d	7.581501	0.25578225	0.5933	0.0037	-0.57223
12aSlick(2) - 73.d	6.954103	0.1474966	0.5998	0.0031	0.24498
12aSlick(2) - 74.d	2.994012	0.07171285	0.6343	0.00385	-0.28471
12aSlick(2) - 75.d	1.838235	0.028722425	0.644	0.0028	-0.02744
7a - 1.d	4.830918	0.16336435	0.331	0.0075	0.14266
7a - 2.d	4.424779	0.234944	0.437	0.027	0.19078
7a - 3.d	4.807692	0.16179735	0.428	0.0205	0.53469
7a - 4.d	2.785515	0.0814705	0.37	0.0145	0.32236
7a - 5.d	10.2459	0.3306823	0.395	0.0185	0.30238
7a - 6.d	5.555556	0.2314815	0.38	0.0255	0.20089
7a - 7.d	6.35324	0.2018183	0.517	0.029	0.52977
7a - 8.d	4.672897	0.1310158	0.4	0.017	0.45132
7a - 9.d	5.681818	0.19369835	0.386	0.0145	0.1096
7a - 10.d	13.55014	0.4314745	0.382	0.017	0.66679
7a - 11.d	12.01923	0.3394855	0.402	0.0095	0.1523
7a - 12.d	5.724098	0.16055	0.341	0.0105	0.21876
7a - 13.d	7.874016	0.37200075	0.355	0.0195	0.63405
7a - 14.d	4.56621	0.1355268	0.371	0.015	0.35381
7a - 15.d	12.36094	0.4430992	0.366	0.0155	0.39493
7a - 16.d	80.64516	3.902185	0.342	0.0245	0.37564

7a - 17.d	16.18123	1.008054	0.368	0.0255	0.2946
7a - 18.d	4.329004	0.1874028	0.362	0.0255	0.38869
7a - 19.d	55.24862	2.441928	0.319	0.024	0.37319
10a(O) - 1.d	7.518797	0.537057	0.7	0.085	0.68866
10a(O) - 2.d	80.64516	8.129555	0.54	0.145	0.43738
10a(O) - 3.d	48.54369	2.945612	0.6	0.07	0.77664
10a(O) - 4.d	34.72222	1.627604	0.581	0.0435	0.56744
10a(O) - 5.d	26.04167	2.000597	0.56	0.105	0.59301
10a(O) - 6.d	25.7732	2.9891595	0.94	0.18	0.80451
10a(O) - 7.d	49.26108	7.15863	0.5	0.305	0.61311
10a(O) - 8.d	6.896552	0.546968	0.69	0.095	0.69188
10a(O) - 9.d	11.23596	0.75748	0.42	0.05	0.83866
10a(O) - 10.d	20	1.54	0.51	0.055	0.40644
10a(O) - 11.d	80.64516	5.202915	0.44	0.08	0.28941
10a(O) - 12.d	120.4819	11.612715	0.18	0.085	0.52217
10a(O) - 13.d	17.09402	0.9496675	0.787	0.0455	0.54973
10a(O) - 14.d	36.63004	2.951871	0.56	0.08	0.52766
10a(O) - 15.d	13.88889	0.8777005	0.737	0.0485	0.46369
10a(O) - 16.d	29.85075	2.4504345	0.702	0.037	0.027502
10a(O) - 17.d	38.91051	2.876652	0.56	0.09	0.48284
10a(O) - 18.d	72.46377	4.200798	0.58	0.055	0.96051
10a(O) - 19.d	19.41748	1.2630785	0.41	0.0355	0.46155
10a(O) - 20.d	11.23596	1.073097	0.62	0.1	0.60554
10a(O) - 21.d	16.44737	1.0414865	0.4	0.065	0.47804
10a(O) - 22.d	17.85714	1.7538265	0.74	0.095	0.55077
10a(O) - 23.d	130.719	7.518475	0.33	0.0375	0.53887
10a(O) - 24.d	24.5098	1.3516435	0.444	0.036	0.4574

10a(O) - 25.d	9.708738	0.9897255	0.36	0.1	0.24897
10a(O) - 26.d	12.04819	1.0161125	0.59	0.125	0.48094
10a(O) - 27.d	7.407407	0.6035665	0.613	0.0425	0.73455
10a(O) - 28.d	2.770083	0.10359035	0.503	0.008	0.084147
10a(O) - 29.d	28.6533	1.313618	0.422	0.038	0.62688
12a(2) - 1.d	0.1751313	0.003833874	0.654	0.0075	0.32137
12a(2) - 2.d	1.715266	0.0750245	0.6583	0.00325	0.20456
12a(2) - 3.d	1.176471	0.044290655	0.6563	0.0034	0.14797
12a(2) - 4.d	4.739336	0.1459985	0.6589	0.0035	0.34387
12a(2) - 5.d	0.1083424	0.002171543	0.6489	0.00405	-0.1149
12a(2) - 6.d	5.681818	0.137203	0.647	0.006	0.14036
12a(2) - 7.d	2.070393	0.0793008	0.6484	0.0026	0.17482
12a(2) - 8.d	1.012146	0.03380649	0.6533	0.00295	0.18097
12a(2) - 9.d	0.01712329	0.000571754	0.6483	0.0027	0.076765
12a(2) - 10.d	0.03891051	0.001892535	0.6513	0.0033	0.095271
12a(2) - 11.d	6.493506	0.2951594	0.652	0.0115	0.13482
12a(2) - 12.d	6.038647	0.20055895	0.667	0.0165	0.23026
12a(2) - 13.d	0.06944444	0.003134645	0.6518	0.0037	-0.083975
12a(2) - 14.d	1.745201	0.042640155	0.6538	0.00305	0.35554
12a(2) - 15.d	1.053741	0.02775924	0.66	0.0105	0.22706
12a(2) - 16.d	2.04499	0.0690027	0.629	0.015	0.65615
12a(2) - 17.d	6.451613	0.2289282	0.653	0.0115	0.42225
12a(2) - 18.d	4.347826	0.13232515	0.675	0.0245	0.6478
12a(2) - 19.d	24.03846	0.4622781	0.641	0.0065	0.22246
12a(2) - 20.d	35.84229	1.28467	0.662	0.0105	0.10865
12a(2) - 21.d	14.68429	0.3557867	0.628	0.009	0.17518
12a(2) - 22.d	5.714286	0.19591835	0.702	0.0355	0.55371
12a(2) - 23.d	31.15265	1.843926	0.562	0.0395	-0.11976
12a(2) - 24.d	11.94743	0.32830455	0.608	0.01	0.13773
12a(2) - 25.d	20.57613	0.4233772	0.643	0.013	0.45196

12a(2) - 26.d	118.0638	3.4847625	0.62	0.011	0.25602
12a(2) - 27.d	65.87615	1.106615	0.627	0.0065	0.49283
12a(2) - 28.d	20.83333	0.889757	0.639	0.006	0.051543
12a(2) - 29.d	75.98784	1.90547	0.607	0.011	0.24274
12a(2) - 30.d	216.4502	10.307155	0.531	0.018	0.43287
12a(2) - 31.d	6.756757	0.6619795	0.634	0.0095	-0.14687
12a(2) - 32.d	134.2282	2.882753	0.626	0.012	0.4831
12a(2) - 33.d	37.03704	1.0288065	0.608	0.006	-0.21595
12a(2) - 34.d	230.4147	9.02546	0.667	0.0355	0.49173
12a(2) - 35.d	6.253909	0.1936013	0.65	0.0165	0.34678
12a(2) - 36.d	1.285347	0.07682345	0.634	0.0075	0.046951
12a(2) - 37.d	6.40615	0.1621031	0.625	0.011	0.032484
12a(2) - 38.d	6.802721	0.3008006	0.621	0.0075	-0.033195
12a(2) - 39.d	8.347245	0.18812655	0.633	0.014	0.72411
12a(2) - 40.d	9.469697	0.4483758	0.598	0.012	0.074335
12a(2) - 41.d	7.961783	0.3011025	0.649	0.0305	0.28202
12a(2) - 42.d	7.042254	0.22317	0.579	0.015	0.39462
12a(2) - 43.d	19.49318	1.3679425	0.522	0.011	0.085959
12a(2) - 44.d	10.03009	0.28671775	0.587	0.024	0.71447
12a(2) - 45.d	3.739716	0.08391285	0.592	0.013	0.37511
12a(2) - 46.d	5.208333	0.23057725	0.61	0.01	-0.12165
12a(2) - 47.d	3.690037	0.21786195	0.629	0.014	0.043286
12a(2) - 48.d	4.950495	0.3185962	0.57	0.025	0.21291
12a(2) - 49.d	2.409639	0.07548265	0.62	0.0215	0.44368
12a(2) - 50.d	3.623188	0.1115837	0.605	0.0115	0.39825
12a(2) - 51.d	3.584229	0.25051065	0.63	0.0215	0.30452
12a(2) - 52.d	7.092199	0.4275439	0.624	0.026	0.13985

12a(2) - 53.d	9.13242	0.3711349	0.608	0.0215	0.39601
12a(2) - 54.d	6.024096	0.2903179	0.628	0.012	0.20316
12bSlick - 1.d	12.21001	0.2310808	0.5085	0.0042	-0.16945
12bSlick - 2.d	11.0011	0.2238948	0.545	0.006	0.22637
12bSlick - 3.d	7.173601	0.1286514	0.5854	0.0045	0.21648
12bSlick - 4.d	10.66098	0.34096955	0.575	0.006	0.046585
12bSlick - 5.d	11.13586	0.4526267	0.53	0.008	-0.22667
12bSlick - 6.d	9.532888	0.2226461	0.585	0.0095	-0.11498
12bSlick - 7.d	12.56281	0.24462765	0.547	0.0075	0.29942
12bSlick - 8.d	13.29787	0.3359835	0.53	0.008	-0.10072
12bSlick - 9.d	11.16071	0.20552655	0.5981	0.0041	0.047762
12bSlick - 10.d	9.174312	0.2188368	0.567	0.00415	-0.073395
12bSlick - 11.d	8.764242	0.19971105	0.576	0.007	0.018432
12bSlick - 12.d	10.91703	0.33966745	0.579	0.0085	0.17662
12bSlick - 13.d	6.939625	0.21430485	0.607	0.006	0.086575
12bSlick - 14.d	8.920607	0.32228775	0.637	0.007	0.074
12bSlick - 15.d	4.933399	0.12169215	0.6253	0.005	0.049355
12bSlick - 16.d	5.434783	0.16245275	0.659	0.0065	0.01043
12bSlick - 17.d	6.666667	0.24444445	0.646	0.0065	-0.091505
12bSlick - 18.d	2.136752	0.1620827	0.776	0.0075	-0.71377
12bSlick - 19.d	0.3968254	0.01259763	0.844	0.00315	-0.14049
12bSlick - 20.d	7.429421	0.27598145	0.643	0.0055	-0.073199
12bSlick - 21.d	4.568296	0.08869465	0.6431	0.005	0.17025
12bSlick - 22.d	3.937008	0.12400025	0.6645	0.00465	-0.087613
12bSlick - 23.d	0.2439024	0.01011303	0.842	0.008	0.22136
12bSlick - 24.d	0.3921569	0.013071895	0.8332	0.00305	-0.36135

12bSlick - 25.d	2.95858	0.07002555	0.726	0.012	0.35855
12bSlick - 26.d	2.824859	0.0598487	0.751	0.0085	0.028844
12bSlick - 27.d	2.857143	0.18367345	0.723	0.009	-0.57424
12bSlick - 28.d	4.079967	0.08323065	0.599	0.009	0.3572
12bSlick - 29.d	2.570694	0.04956351	0.742	0.0055	0.05389
12bSlick - 30.d	2.352941	0.08581315	0.739	0.0065	-0.11151
12bSlick - 31.d	4.793864	0.11490565	0.6307	0.00465	0.20395
12bSlick - 32.d	6.60502	0.17232385	0.651	0.0075	0.231
12bSlick - 33.d	4.894763	0.0826575	0.647	0.0065	0.43263
12bSlick - 34.d	0.78125	0.088501	0.781	0.007	-0.84838
12bSlick - 35.d	9.276438	0.167802	0.59	0.0065	-0.11795
12bSlick - 36.d	4.587156	0.126252	0.6319	0.00485	-0.28746
12bSlick - 37.d	9.624639	0.18989905	0.53	0.0055	0.041383
12bSlick - 38.d	8.045052	0.26536375	0.5577	0.00465	-0.096986
12bSlick - 39.d	8.53971	0.2844139	0.5769	0.0048	-0.010226
12bSlick - 40.d	6.666667	0.26666665	0.58	0.0065	0.005947
12bSlick - 41.d	5.178664	0.1045924	0.583	0.006	0.040321
12bSlick - 42.d	5.402485	0.14593425	0.596	0.0055	0.21756
12bSlick - 43.d	5.913661	0.13289125	0.5931	0.005	0.081816
12bSlick - 44.d	12.18027	0.34122555	0.535	0.0055	-0.30566
12bSlick - 45.d	12.42236	0.27776705	0.5078	0.0044	0.088187
12bSlick - 46.d	9.017133	0.2642532	0.5567	0.0042	-0.27353
12a - 1.d	9.930487	0.42404265	0.644	0.033	0.4226
12a - 2.d	13.03781	0.47595655	0.63	0.0365	0.69639
12a - 3.d	50.76142	3.4785745	0.494	0.037	0.83477
12a - 4.d	21.88184	1.556148	0.65	0.08	0.55002
12a - 5.d	27.54821	0.6830135	0.46	0.018	0.46563
12a - 6.d	23.92344	1.058813	0.529	0.032	0.53735
12a - 7.d	77.57952	2.7384545	0.459	0.0235	0.3097

12a - 8.d	12.34568	1.44795	0.87	0.17	0.95869
12a - 9.d	12.21001	0.46961585	0.546	0.018	0.43219
12a - 10.d	13.22751	0.7523585	0.618	0.025	0.23377
12a - 11.d	48.30918	3.1505985	0.534	0.0255	-0.099126
12a - 12.d	17.66784	0.686736	0.593	0.0275	0.49904
12a - 13.d	34.24658	0.879621	0.498	0.015	0.43865
12a - 14.d	34.24658	0.9382625	0.485	0.011	0.062833
12a - 15.d	128.866	3.5703845	0.352	0.0155	0.342
12a - 16.d	40.81633	1.6659725	0.593	0.021	0.14783
12a - 17.d	5.181347	0.59062	0.605	0.0055	-0.63873
12a - 18.d	0.4948046	0.012241575	0.641	0.008	0.61951
12a - 19.d	8.474576	0.610457	0.7	0.055	0.396
12a - 20.d		0	no value	#VALUE!	NaN
12a - 21.d	20.66116	1.8142545	1.03	0.205	0.95627
12a - 22.d	37.31343	1.3226775	0.512	0.0235	0.19424
12a - 23.d	21.59827	1.0029435	0.612	0.037	0.35898
12a - 24.d	24.8139	1.169886	0.615	0.0325	0.42854
12a - 25.d	28.90173	1.461793	0.77	0.065	0.79673
12a - 26.d	10.17294	0.4708736	0.66	0.05	0.52793
12a - 27.d	30.58104	1.21576	0.78	0.055	0.44889
12a - 28.d	23.80952	0.878685	0.547	0.029	0.34922
12a - 29.d	41.66667	1.4756945	0.403	0.025	0.46546
12a - 30.d	57.80347	4.6777375	0.5	0.065	0.53526
12a - 31.d	31.15265	1.1160605	0.525	0.0295	0.50808
12a - 32.d	74.62687	3.063043	0.361	0.0225	0.49397
12a - 33.d	35.84229	1.027736	0.46	0.021	0.28185
12a - 34.d	168.6341	4.834366	0.415	0.022	0.22356
12a - 35.d	9.416196	0.430024	0.681	0.046	0.71791
12a - 36.d	44.44444	2.1728395	0.627	0.0425	0.43012
12a - 37.d	145.7726	8.818605	0.323	0.027	-0.25004
12a - 38.d	12.15067	0.716048	0.692	0.0305	0.35256
12a - 39.d	0.8	0.0384	0.637	0.0055	-0.092235

Calcite elemental Maps:

8b:

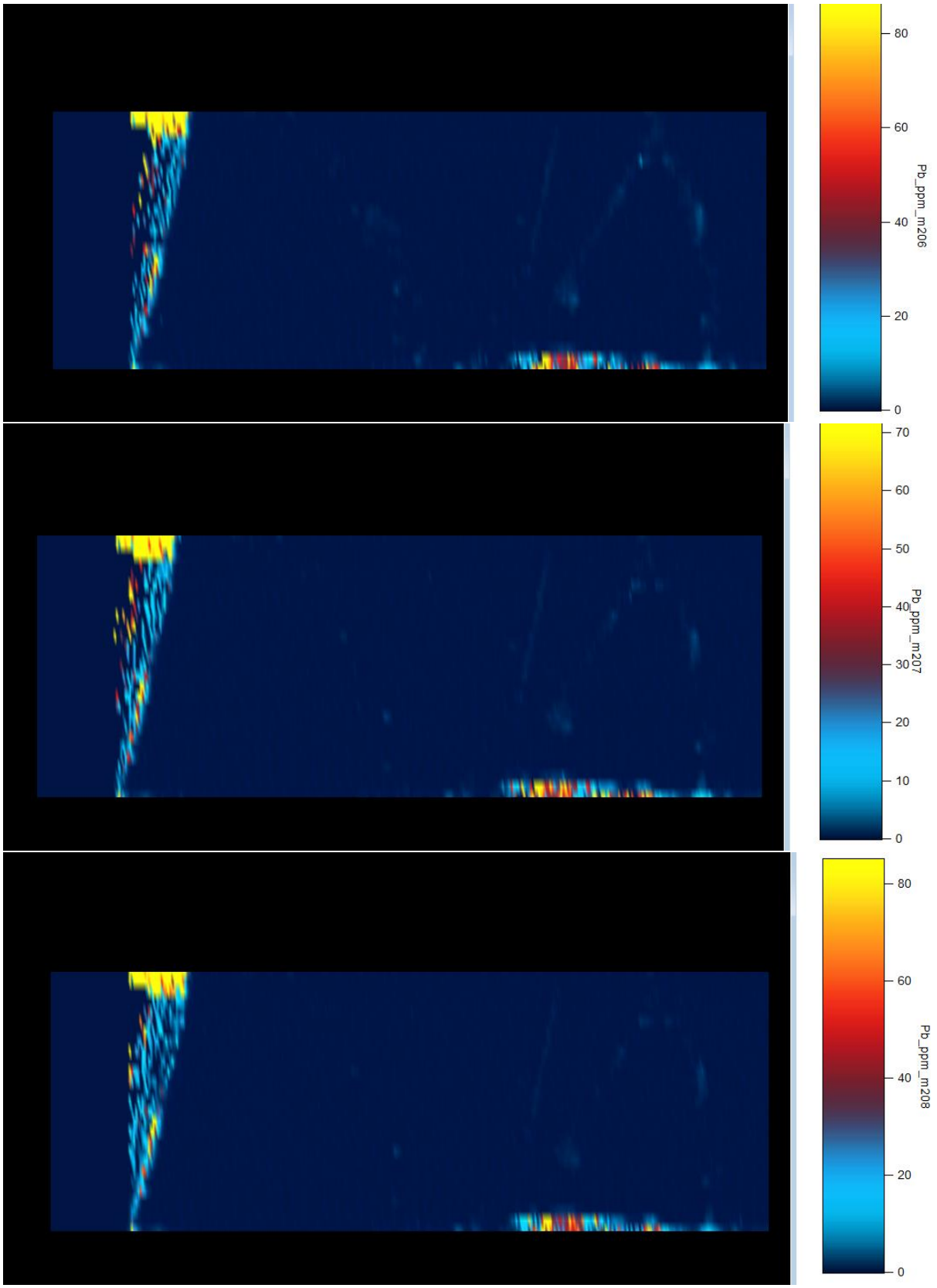

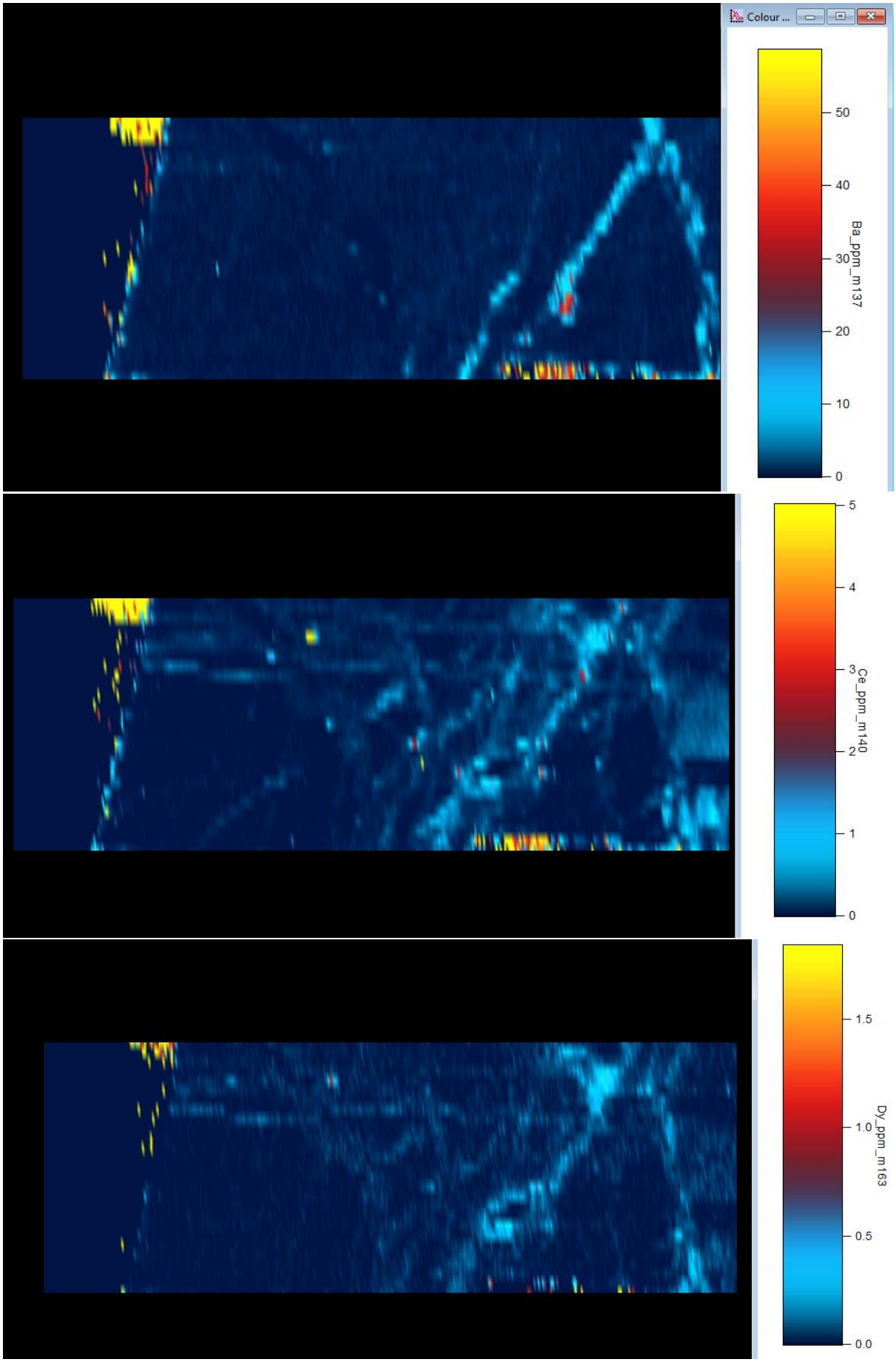
Colour ...
50
40
30
20
10
0
Ba_ppm_m137
5
4
3
2
1
0
Ce_ppm_m140
1.5
1.0
0.5
0.0
Dy_ppm_m163

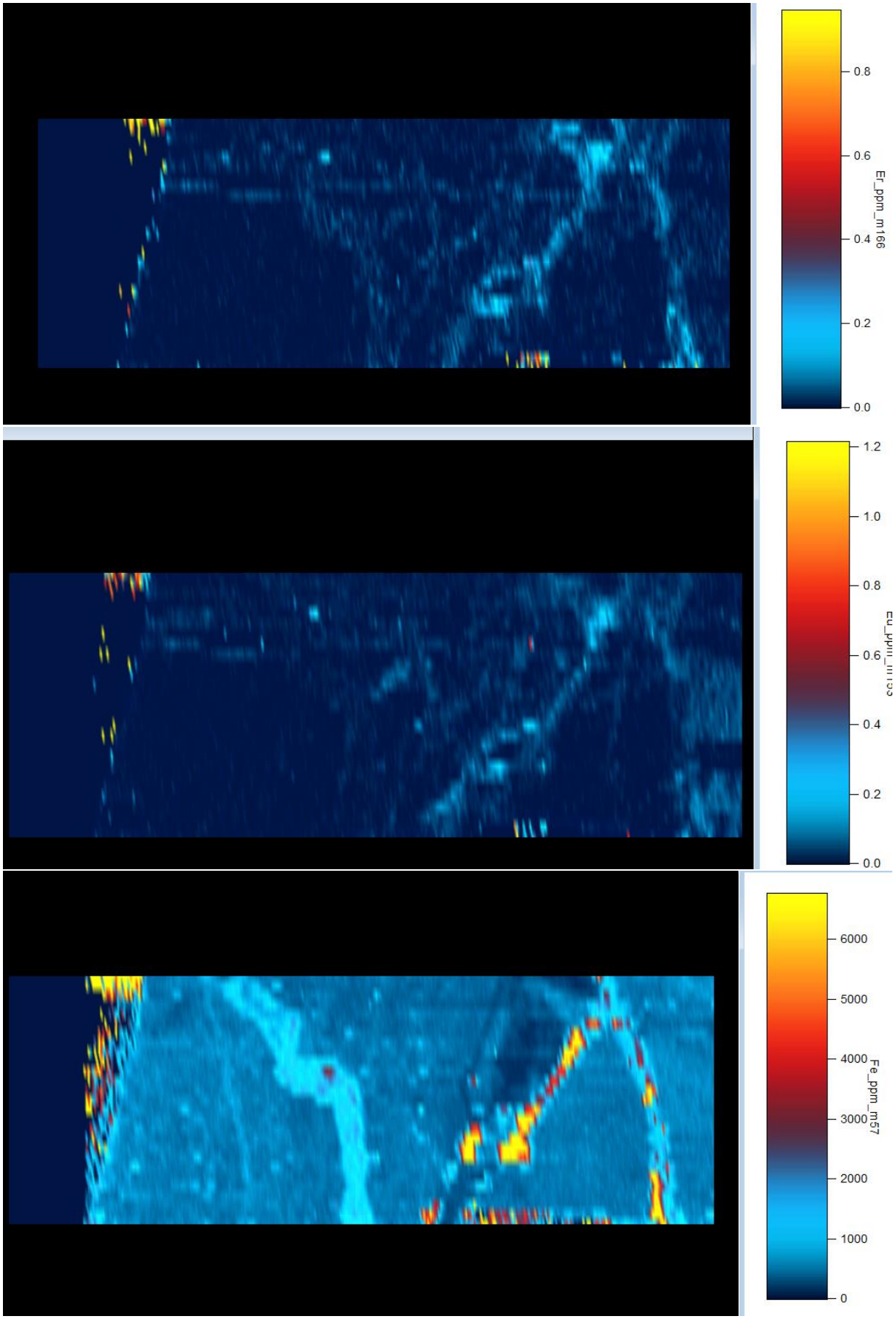
0.8
0.6
Er_ppm_m166
0.4
0.2
0.0
1.2
1.0
0.8
0.6
0.4
0.2
0.0
6000
5000
4000
Fe_ppm_m57
3000
2000
1000
0

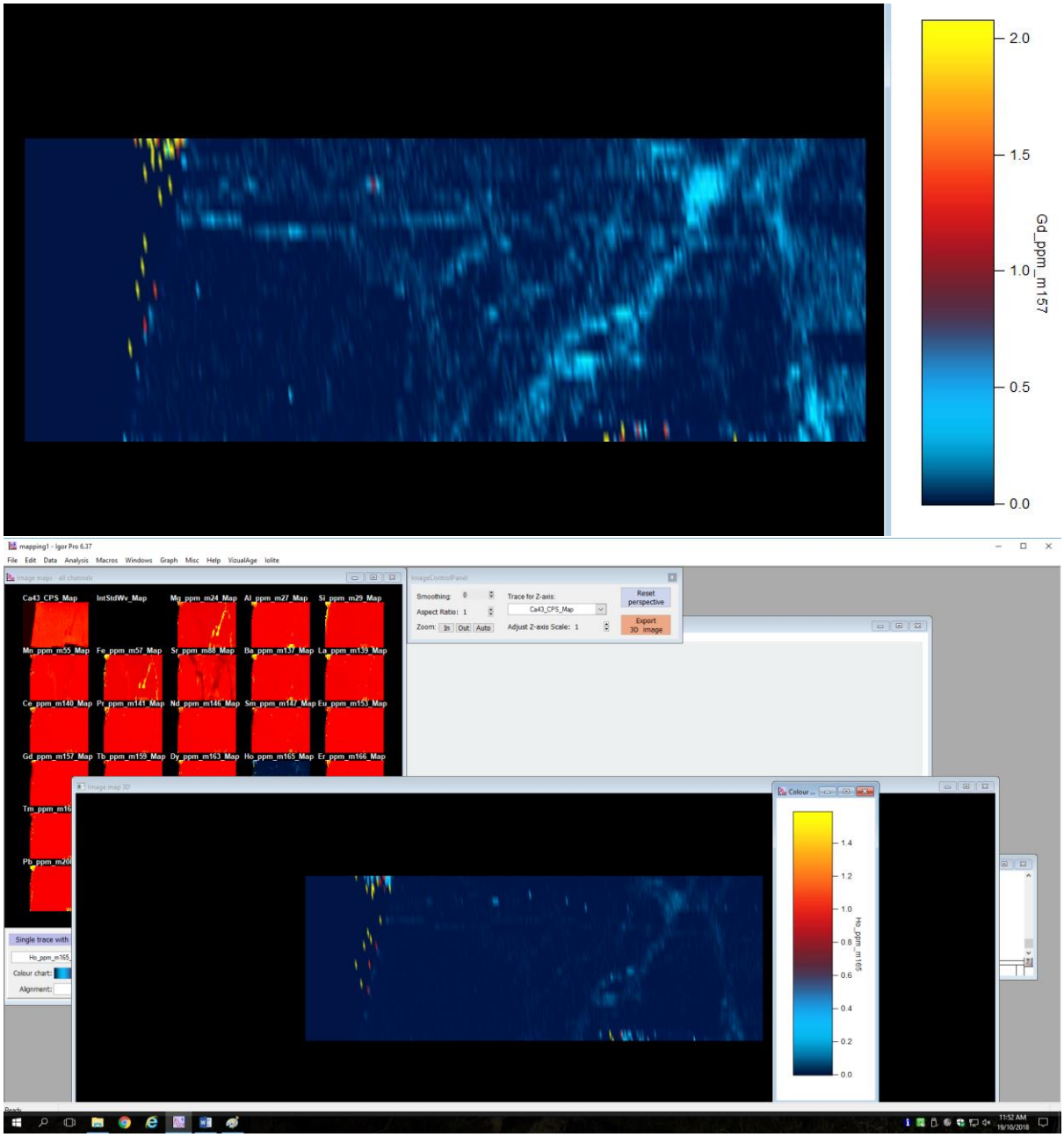
2.0
1.5
1.0
0.5
0.0
Gd_ppm_m157
mapping1 - Igor Pro 6.37
File Edit Data Analysis Macros Windows Graph Misc Help VizualAge Iolite
Ca43_CPS_Map
IntStdWv_Map
Mg_ppm_m24_Map
Al_ppm_m27_Map
Si_ppm_m29_Map
Mn_ppm_m55_Map
Fe_ppm_m57_Map
Sr_ppm_m88_Map
Ba_ppm_m137_Map
La_ppm_m139_Map
Ce_ppm_m140_Map
Pr_ppm_m141_Map
Nd_ppm_m146_Map
Sm_ppm_m147_Map
Eu_ppm_m153_Map
Gd_ppm_m157_Map
Tb_ppm_m159_Map
Dy_ppm_m163_Map
Ho_ppm_m165_Map
Er_ppm_m166_Map
Tm_ppm_m16
Pb_ppm_m20
Single trace with
Ho_ppm_m165_
Colour chart:
Alignment:
Smoothing:
Aspect Ratio: 1
Zoom: In Out Auto
Trace for Z-axis:
Ca43_CPS_Map
Adjust Z-axis Scale: 1
Reset perspective
Export 3D image
Colour ...
1.4
1.2
1.0
0.8
0.6
0.4
0.2
0.0
Ho_ppm_m165
11:52 AM
19/10/2018

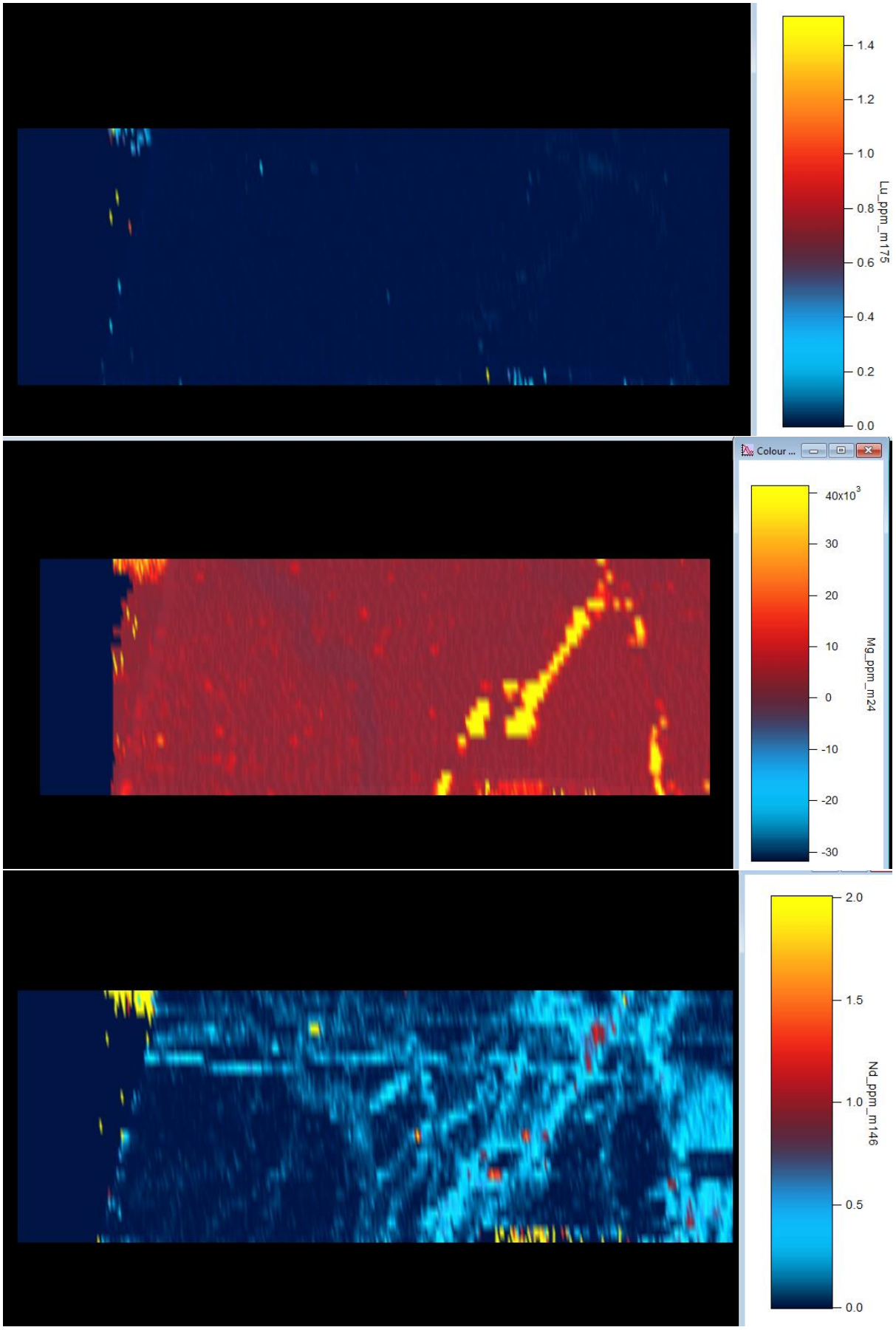
1.4
1.2
1.0
0.8
0.6
0.4
0.2
0.0
Lu_ppm_m175
Colour ...
40x10^3
30
20
10
0
-10
-20
-30
Mg_ppm_m24
2.0
1.5
1.0
0.5
0.0
Nd_ppm_m146

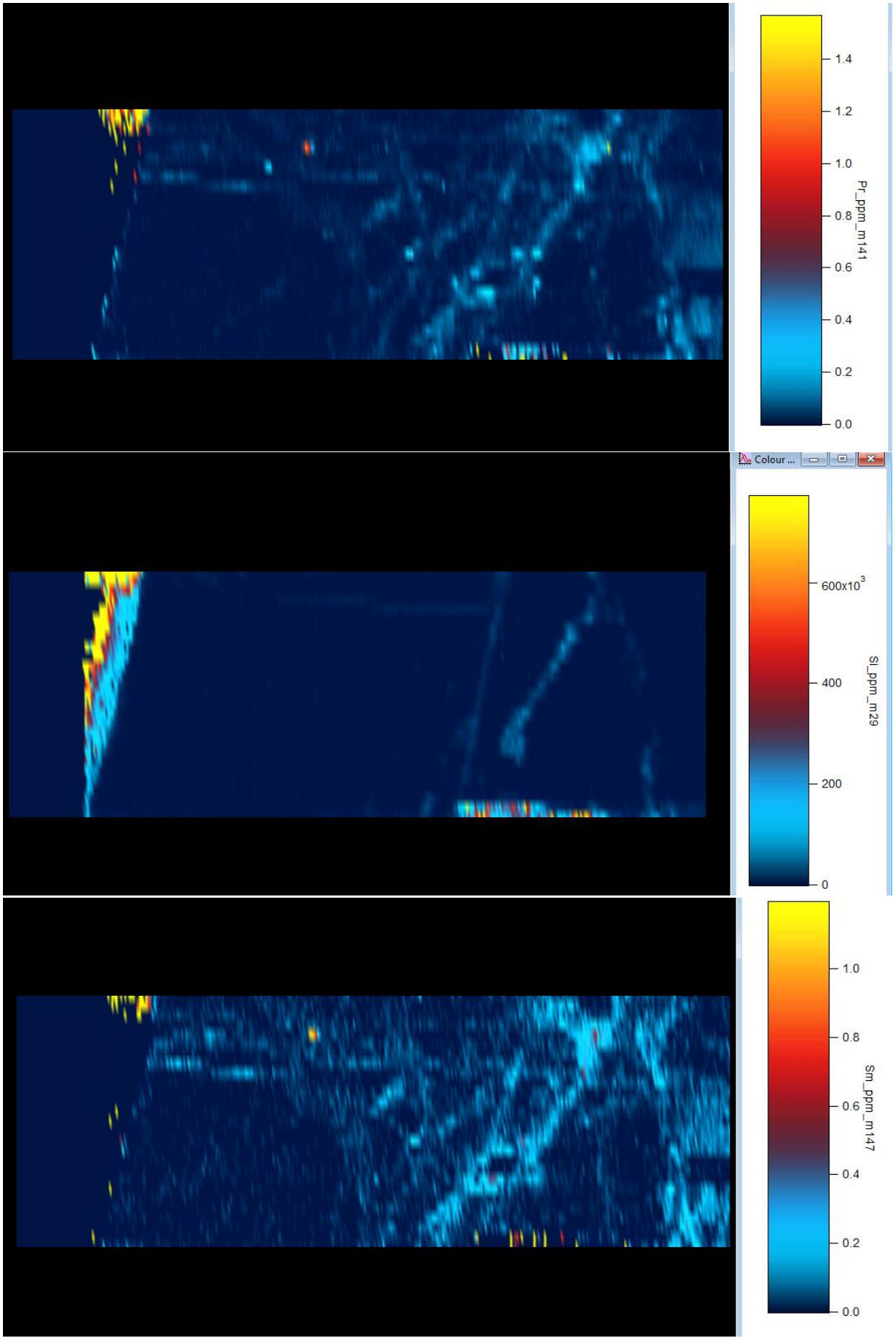
1.4
1.2
1.0
0.8
0.6
0.4
0.2
0.0
Pr_ppm_m141
Colour ...
600x10^3
400
200
0
Sl_ppm_m29
1.0
0.8
0.6
0.4
0.2
0.0
Sm_ppm_m147

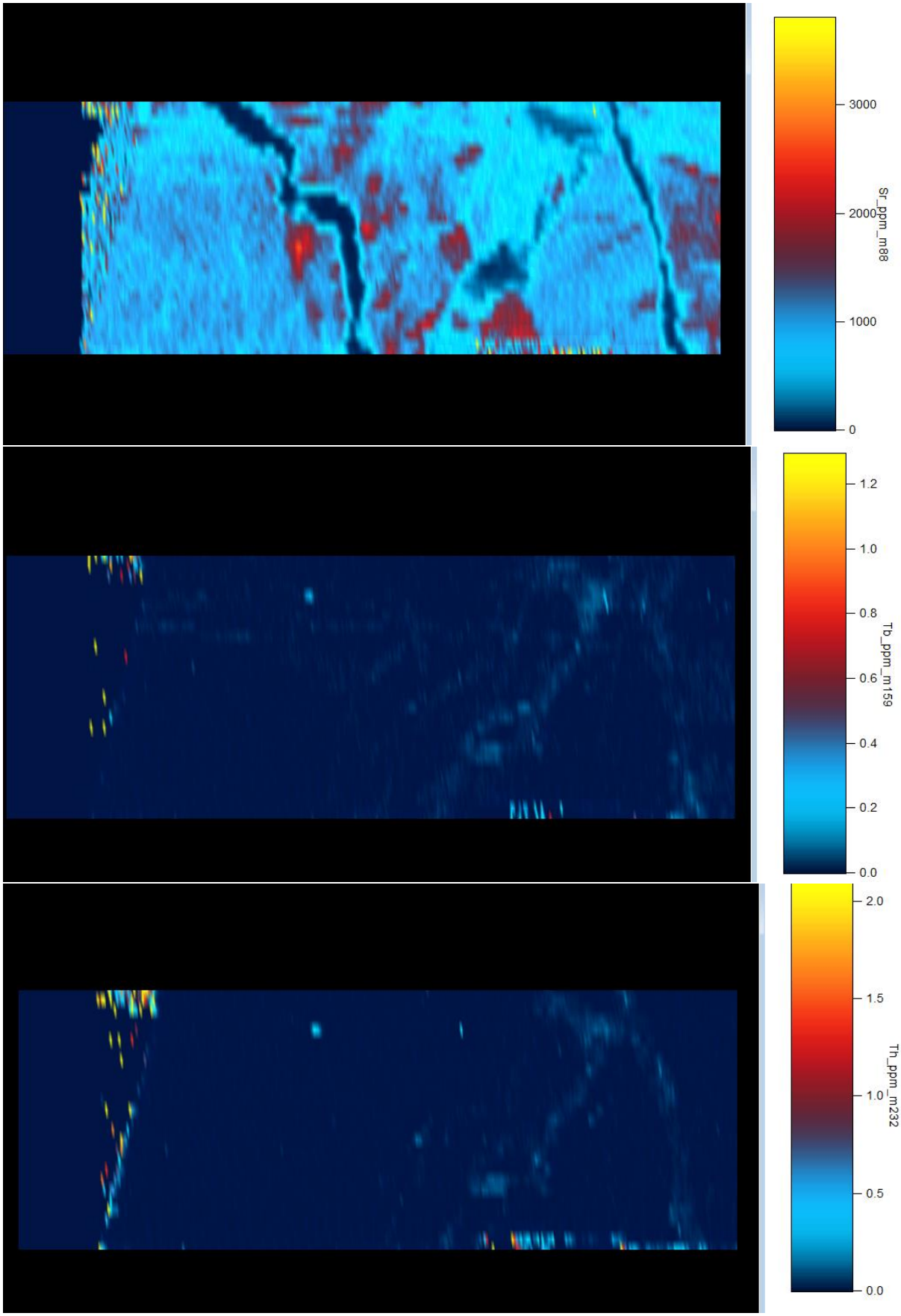
3000
2000
1000
0
Sr_ppm_m88
1.2
1.0
0.8
0.6
0.4
0.2
0.0
Tb_ppm_m159
2.0
1.5
1.0
0.5
0.0
Th_ppm_m232

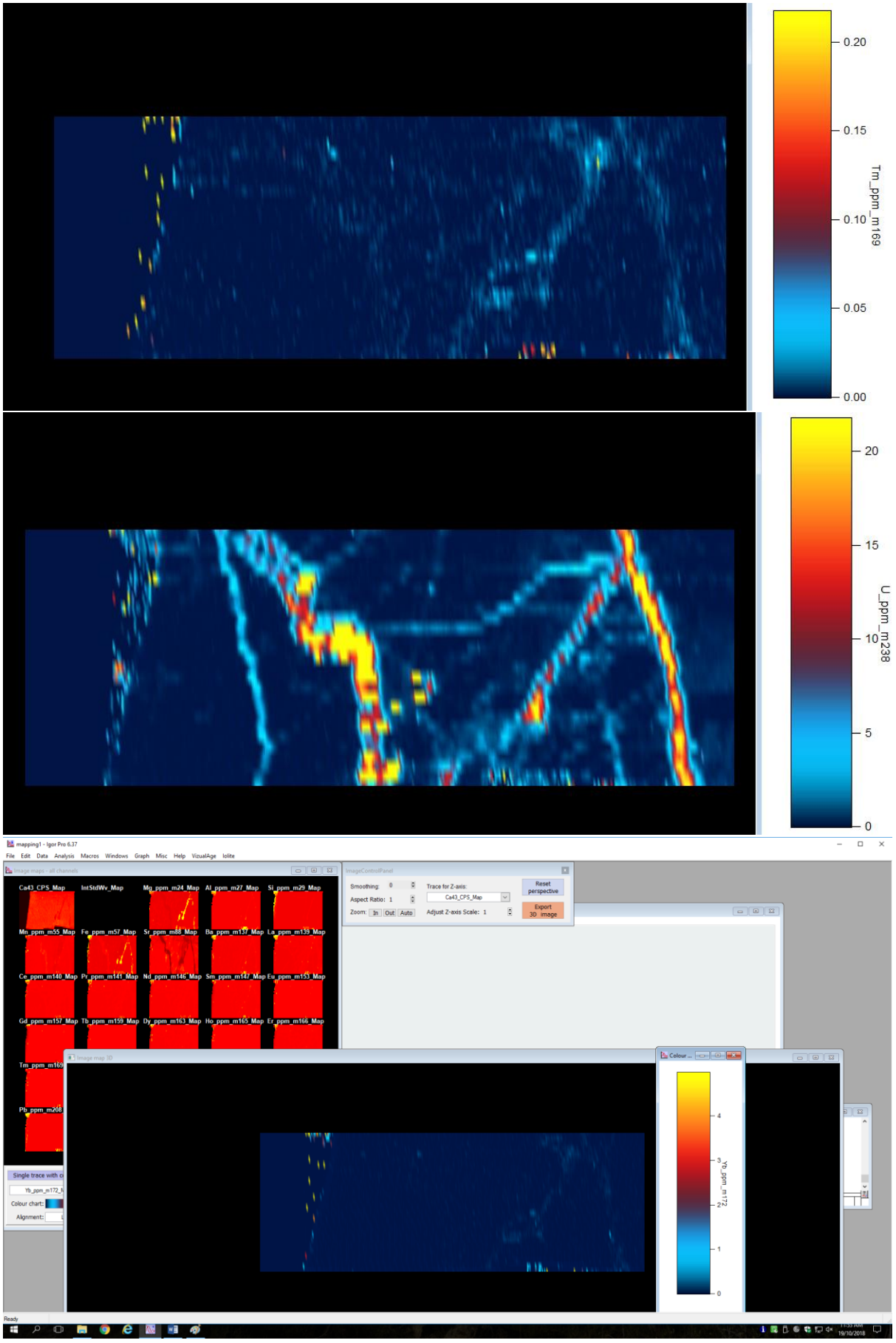
0.20
0.15
0.10
0.05
0.00
Tm_ppm_m169
20
15
10
5
0
U_ppm_m238
mapping1 - Igor Pro 6.37
File Edit Data Analysis Macros Windows Graph Misc Help VizualAge Iolite
Ca43_CPS_Map
IntStdWv_Map
Mg_ppm_m24_Map
Al_ppm_m27_Map
Si_ppm_m29_Map
Mn_ppm_m55_Map
Fe_ppm_m57_Map
Sr_ppm_m88_Map
Ba_ppm_m137_Map
La_ppm_m139_Map
Ce_ppm_m140_Map
Pr_ppm_m141_Map
Nd_ppm_m146_Map
Sm_ppm_m147_Map
Eu_ppm_m153_Map
Gd_ppm_m157_Map
Tb_ppm_m159_Map
Dy_ppm_m163_Map
Ho_ppm_m165_Map
Er_ppm_m166_Map
Tm_ppm_m169
Pb_ppm_m208
Smoothing:
Aspect Ratio:
Zoom:
Trace for Z-axis:
Adjust Z-axis Scale:
Reset perspective
Export 3D image
Yb_ppm_m172
Ready

12a

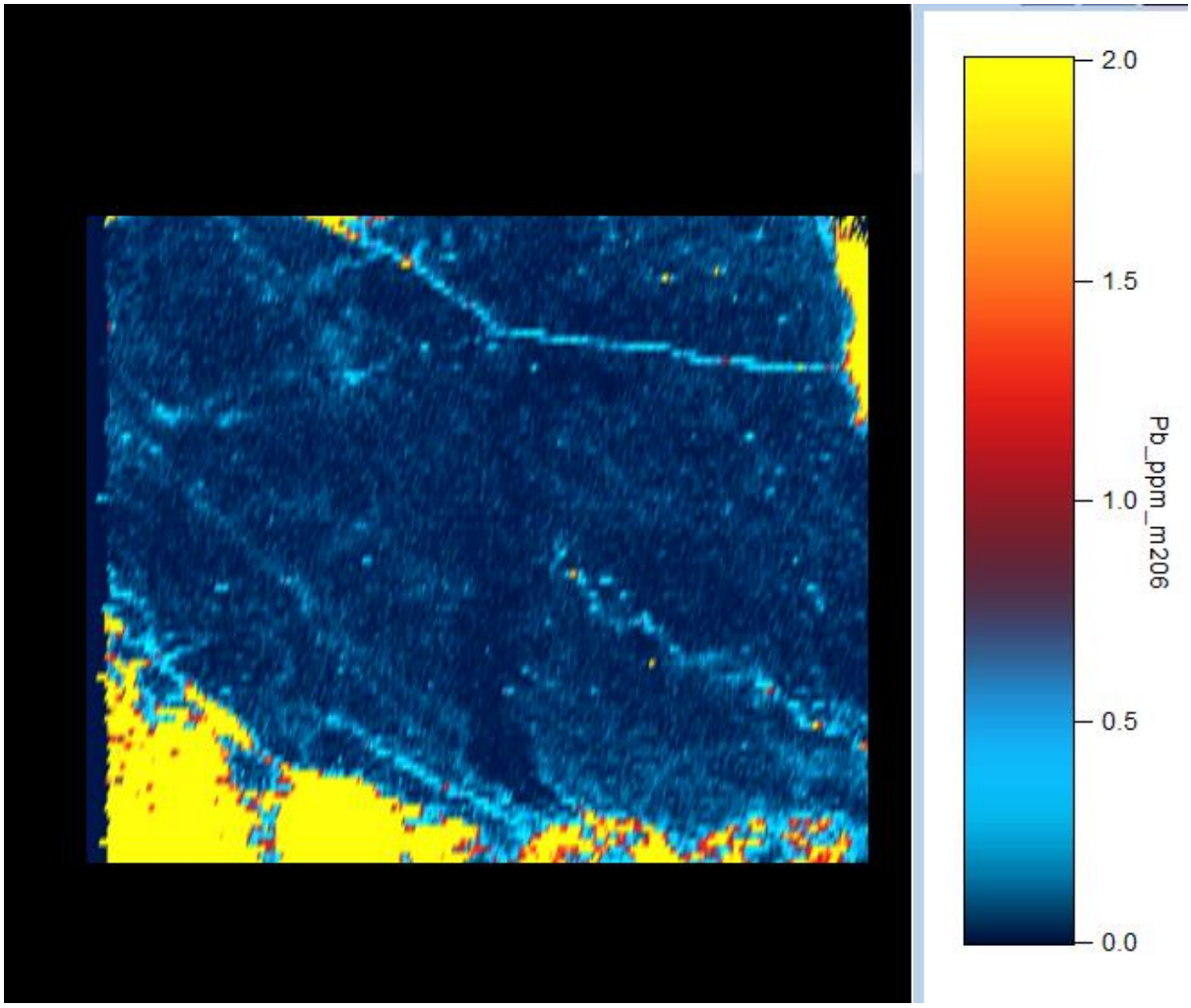
2.0
1.5
1.0
0.5
0.0
Pb_ppm_m206

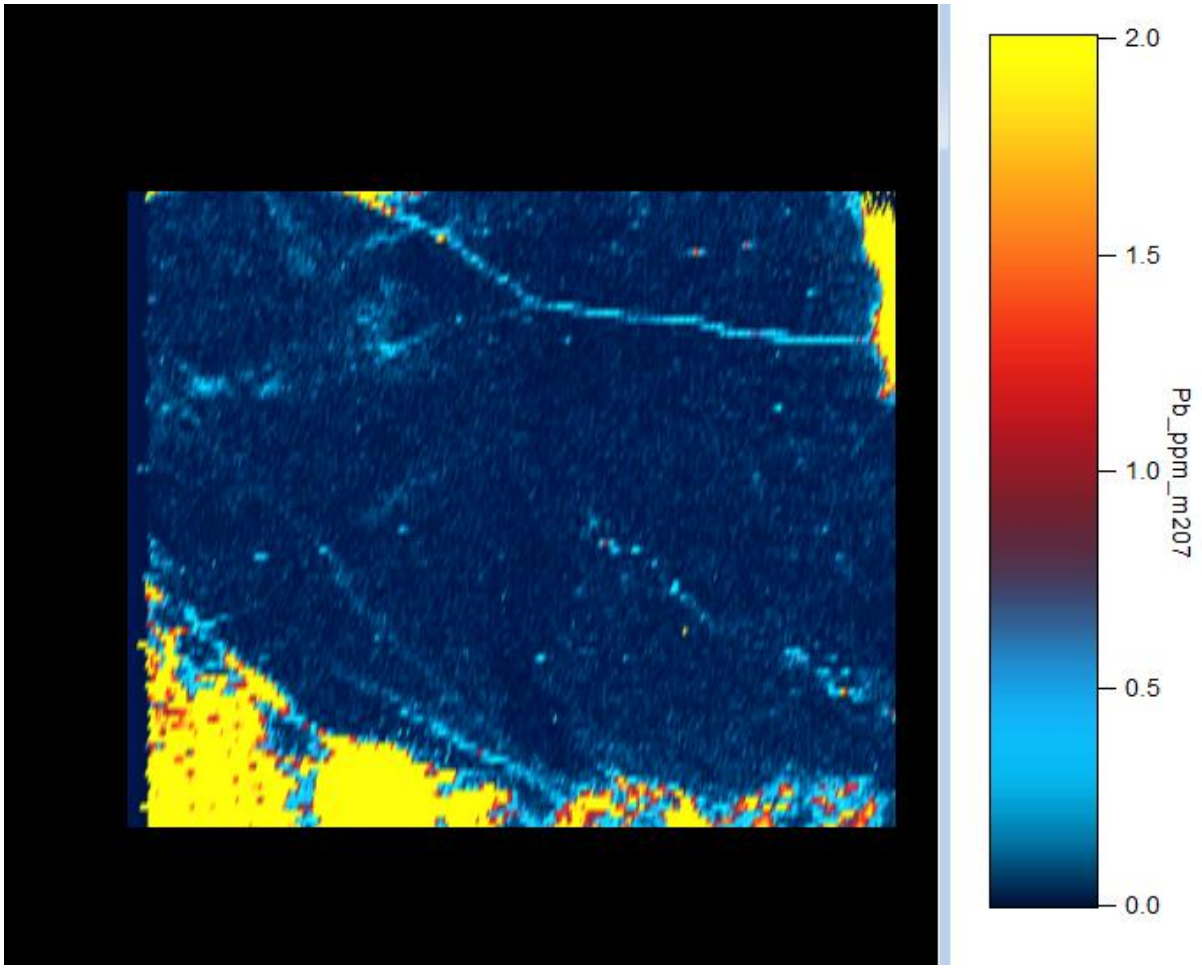
2.0
1.5
1.0
0.5
0.0
Pb_ppm_m207

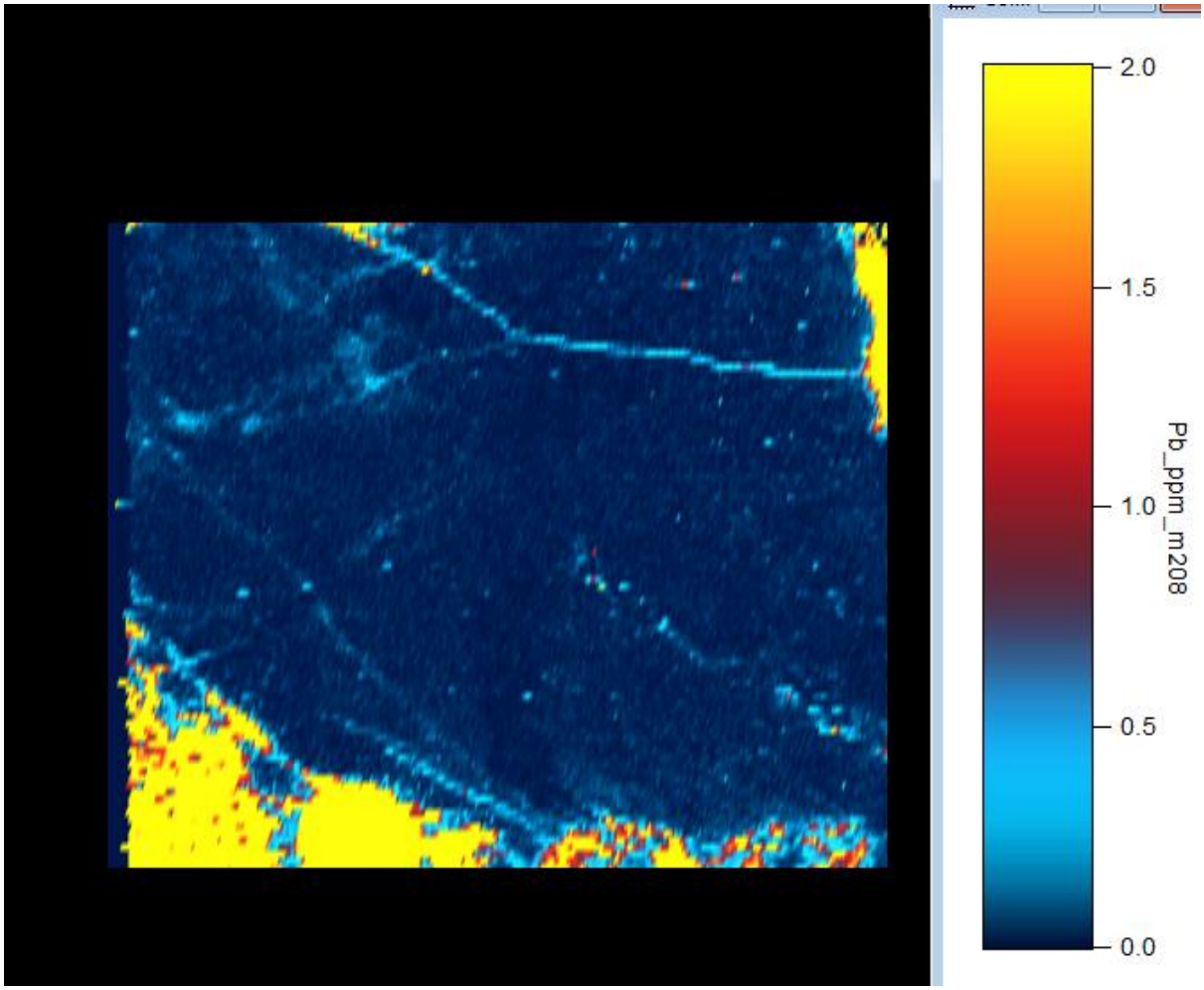
2.0
1.5
1.0
0.5
0.0
Pb_ppm_m208

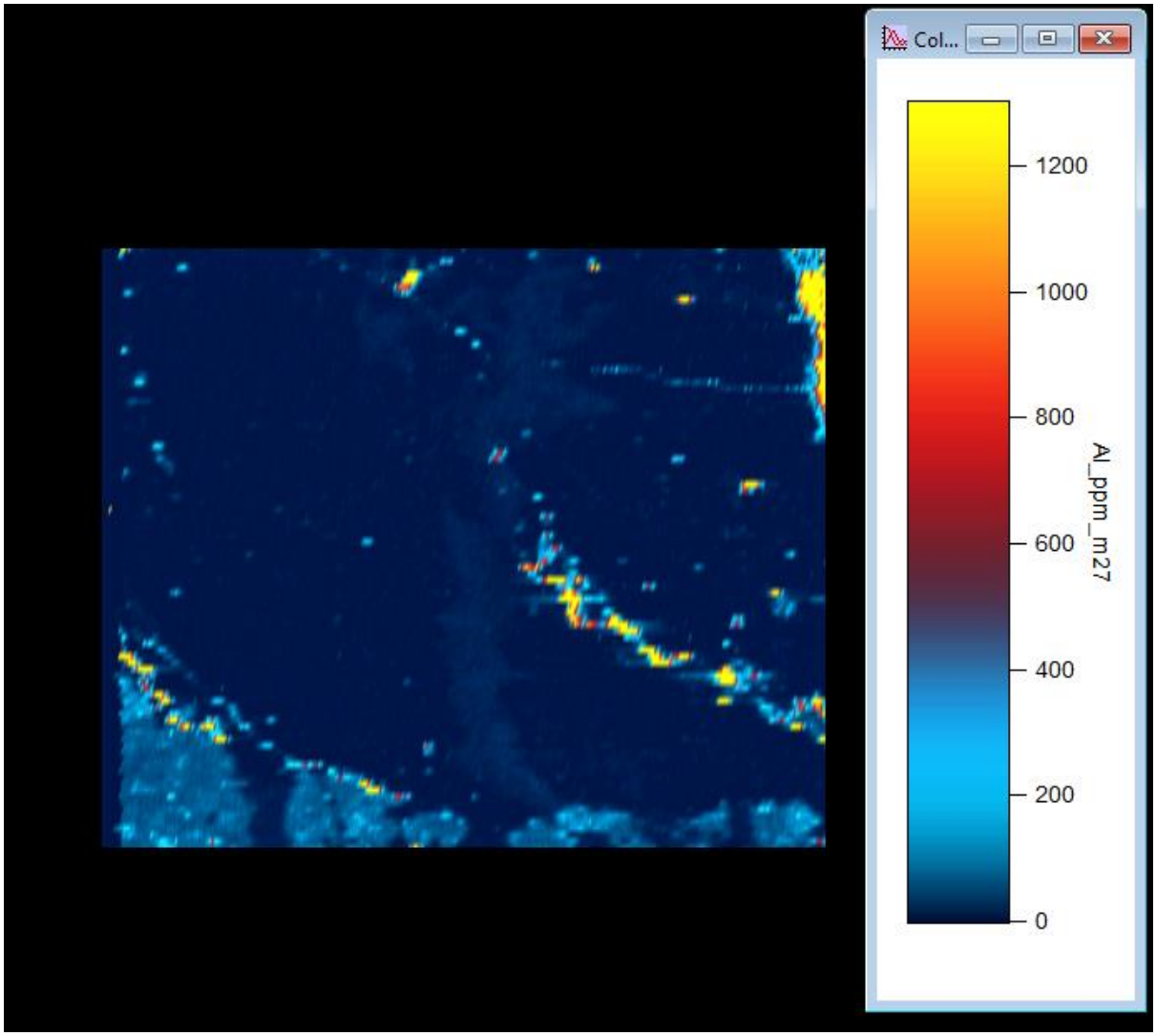
Col...
1200
1000
800
600
400
200
0
Al_ppm_m27

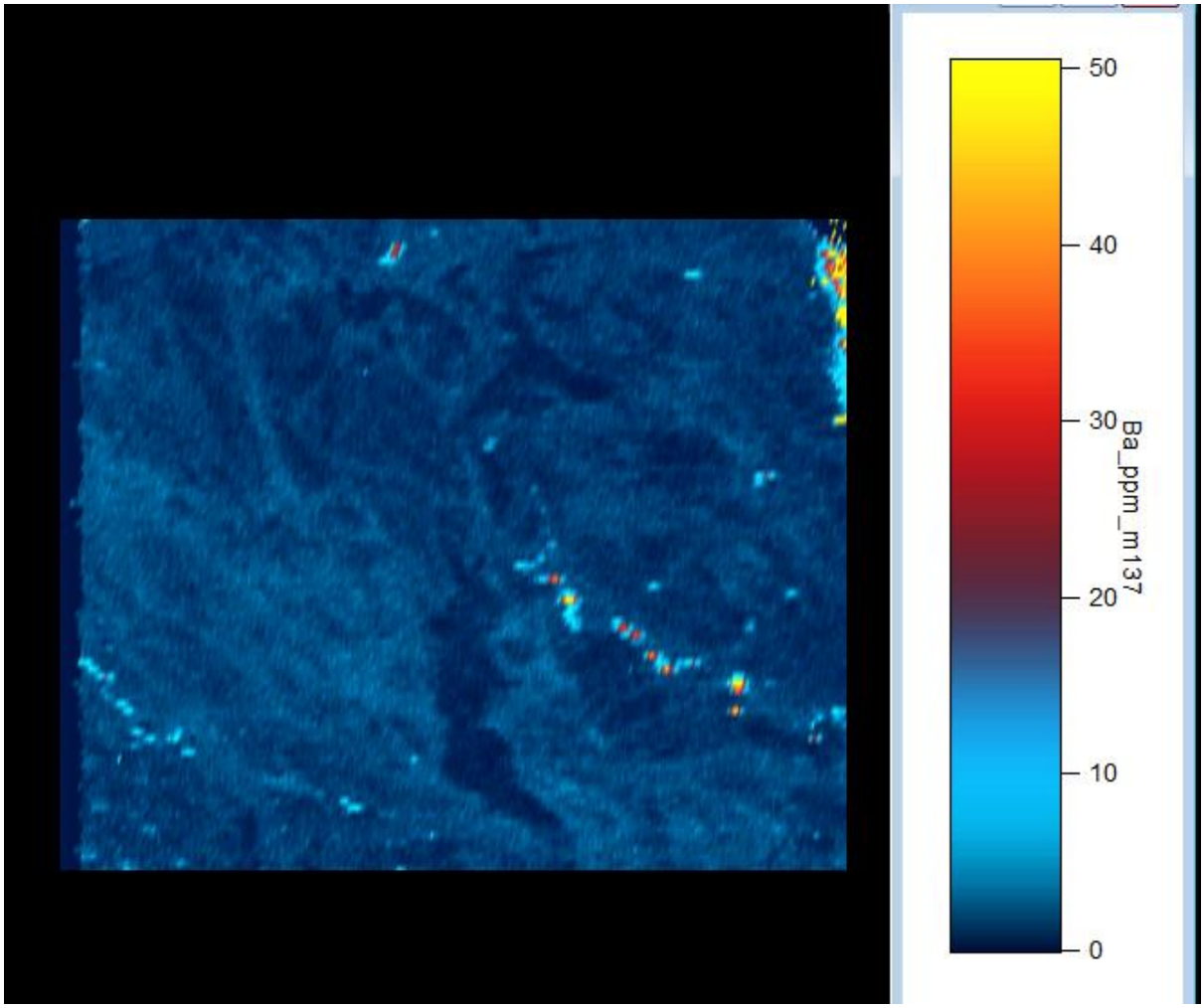
50
40
30
20
10
0
Ba_ppm_m137

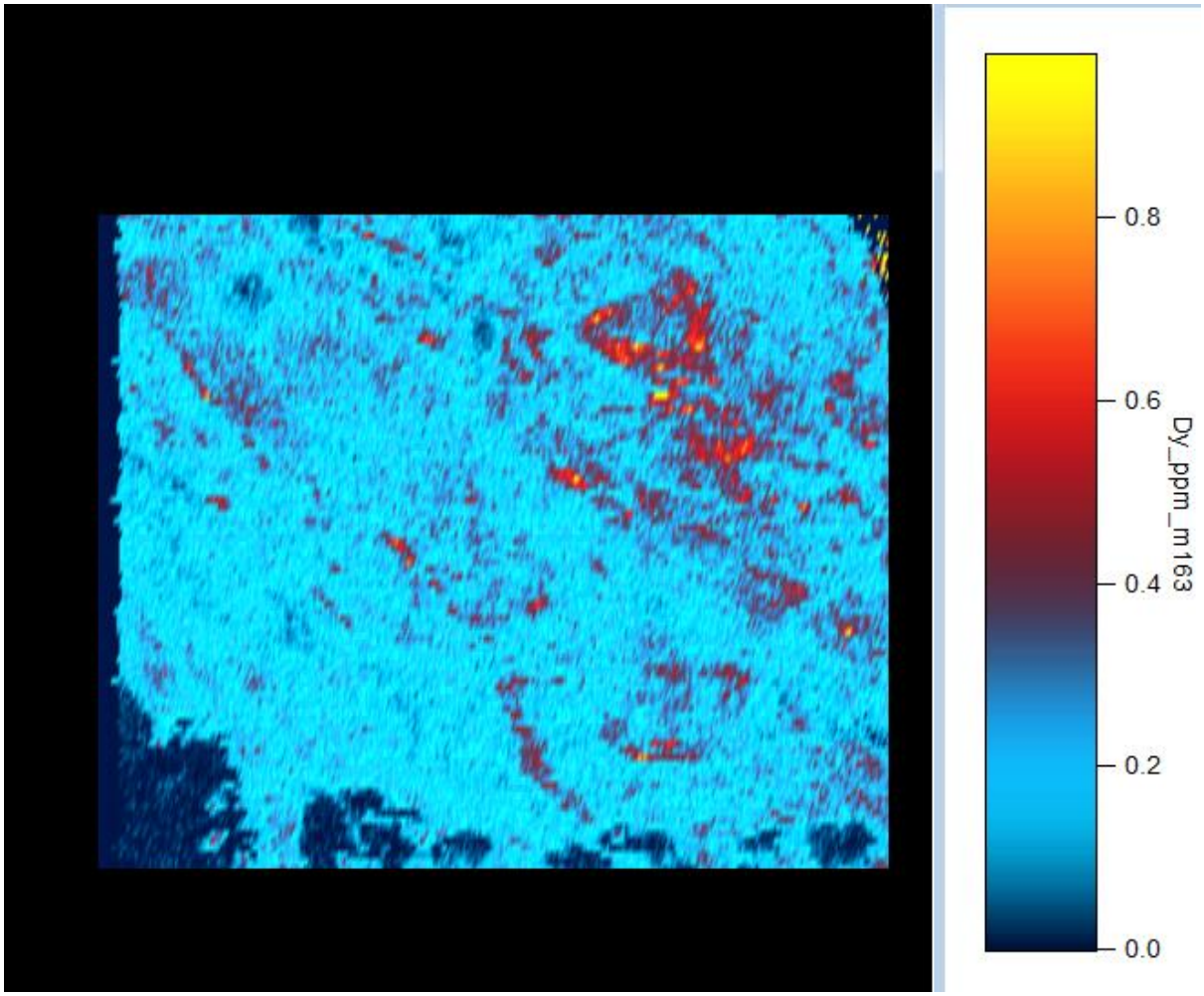
0.8
0.6
0.4
0.2
0.0
Dy_ppm_m163

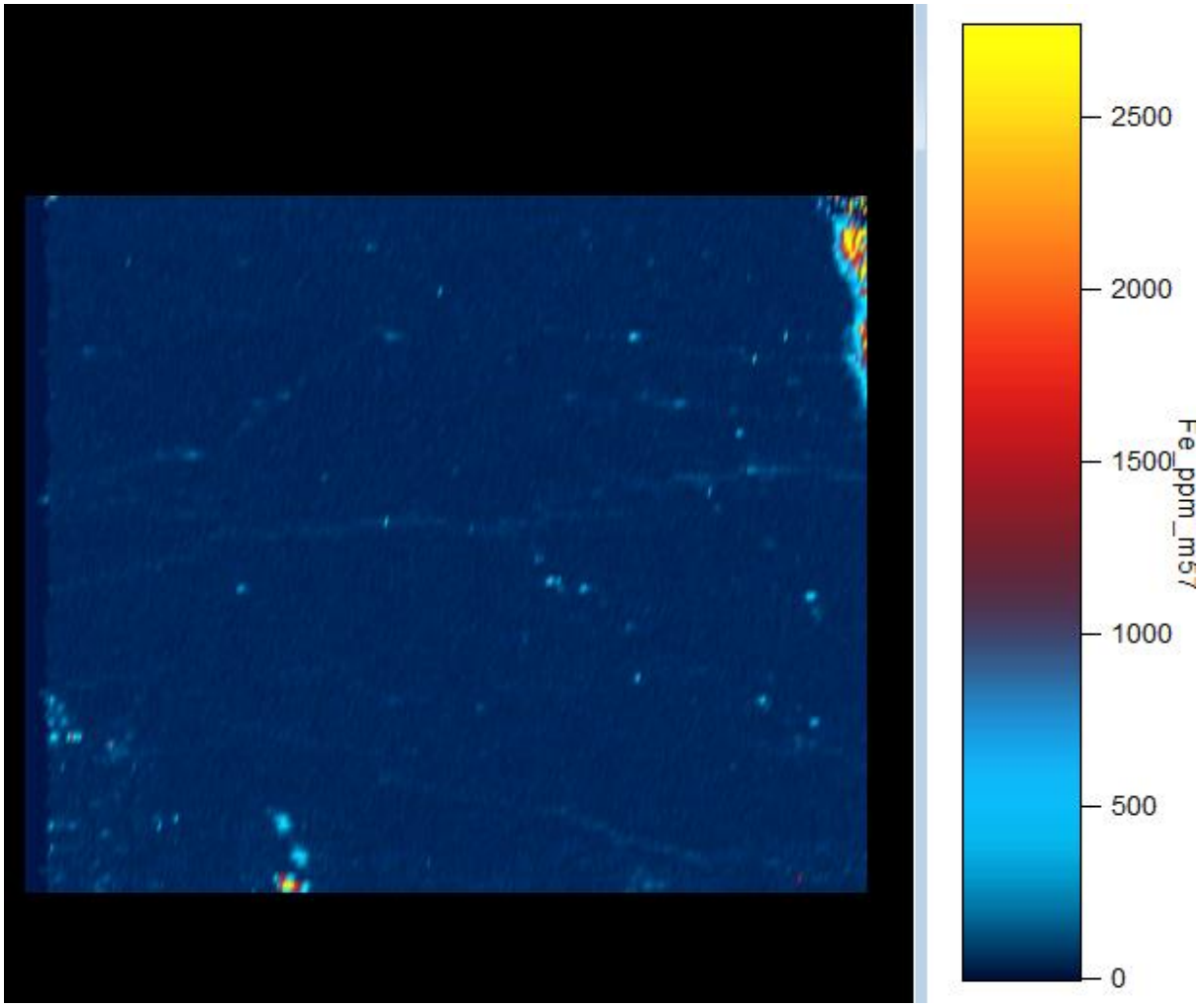
2500
2000
1500
1000
500
0
Fe_ppm_m57

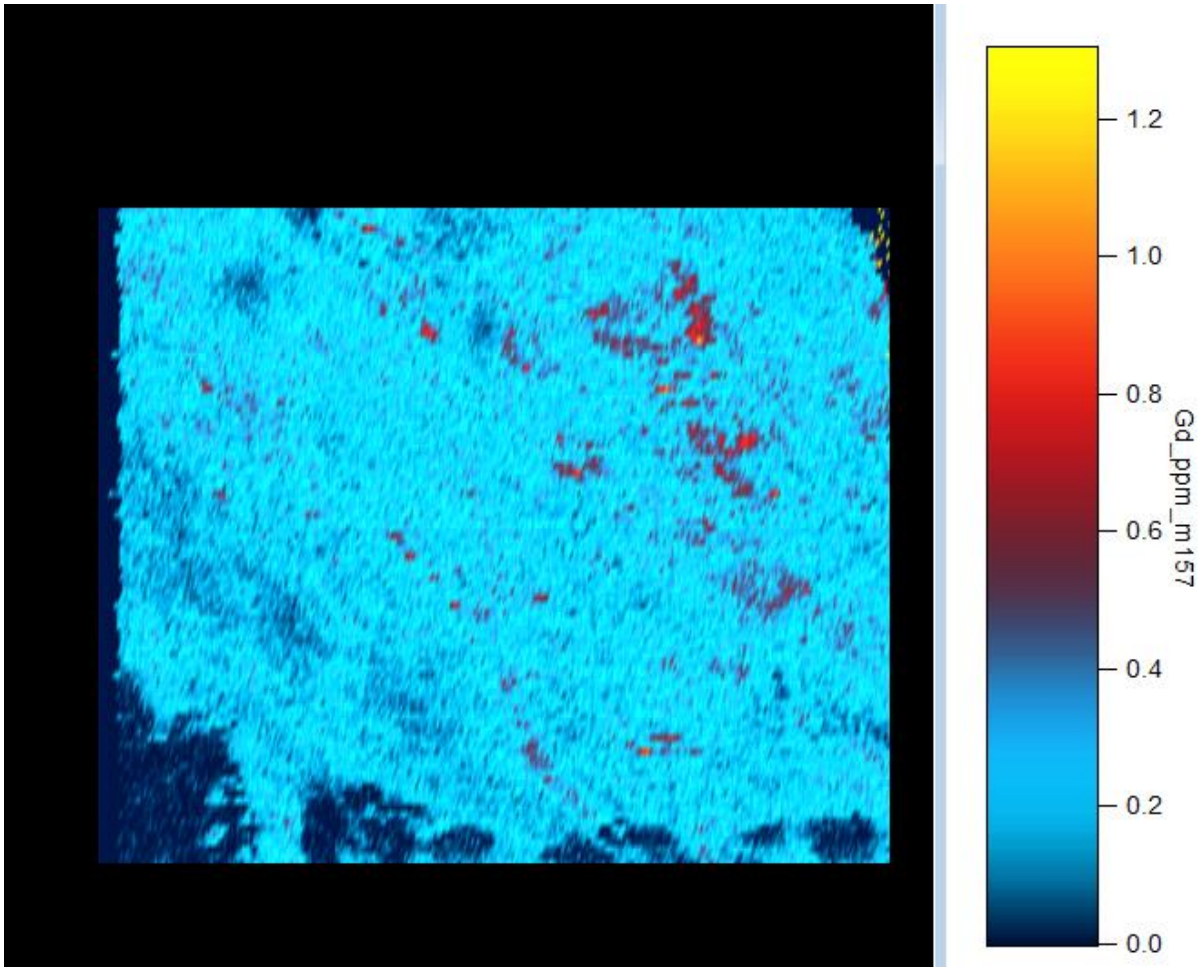
1.2
1.0
0.8
0.6
0.4
0.2
0.0
Gd_ppm_m157

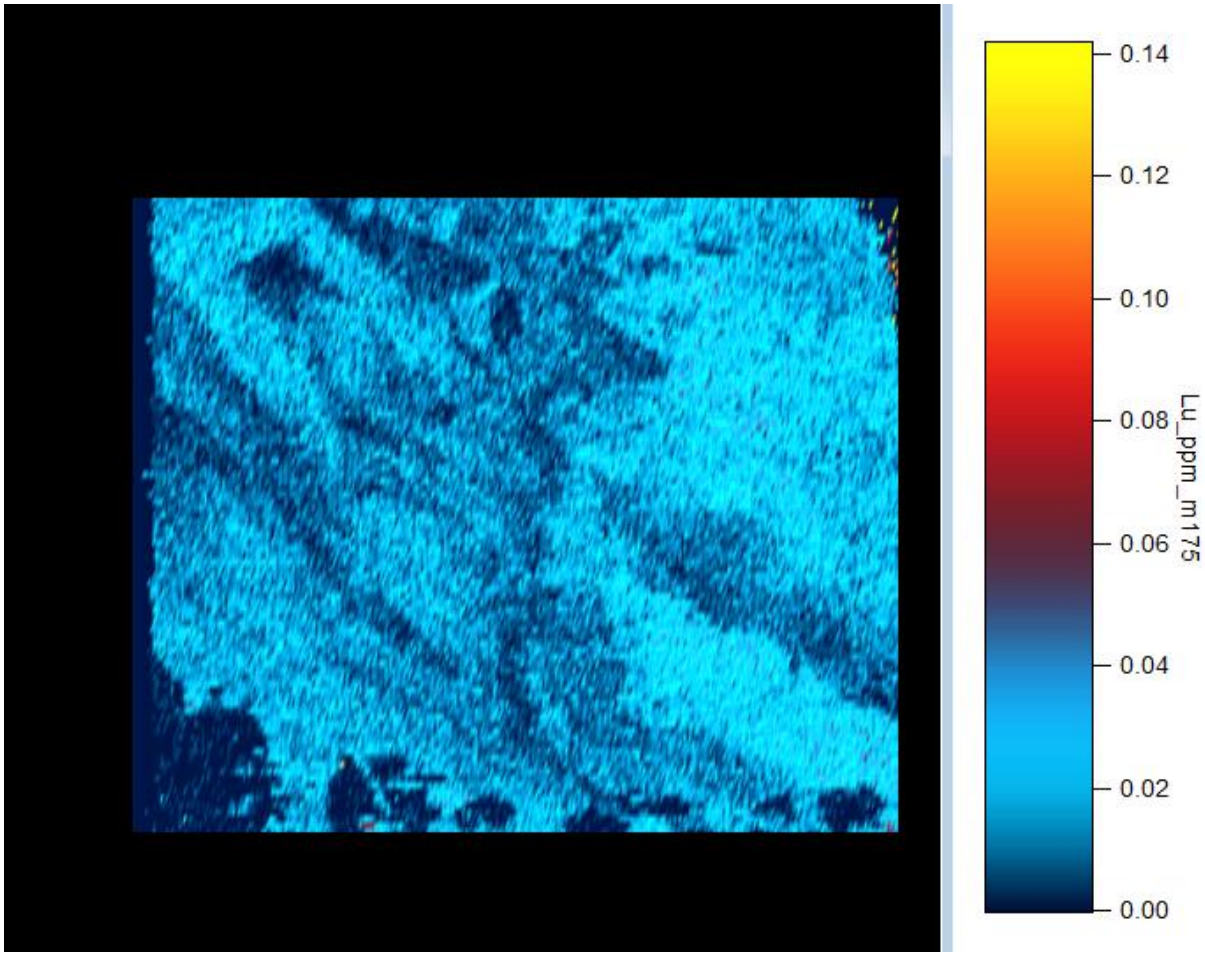
0.14
0.12
0.10
0.08
0.06
0.04
0.02
0.00
Lu_ppm_m175

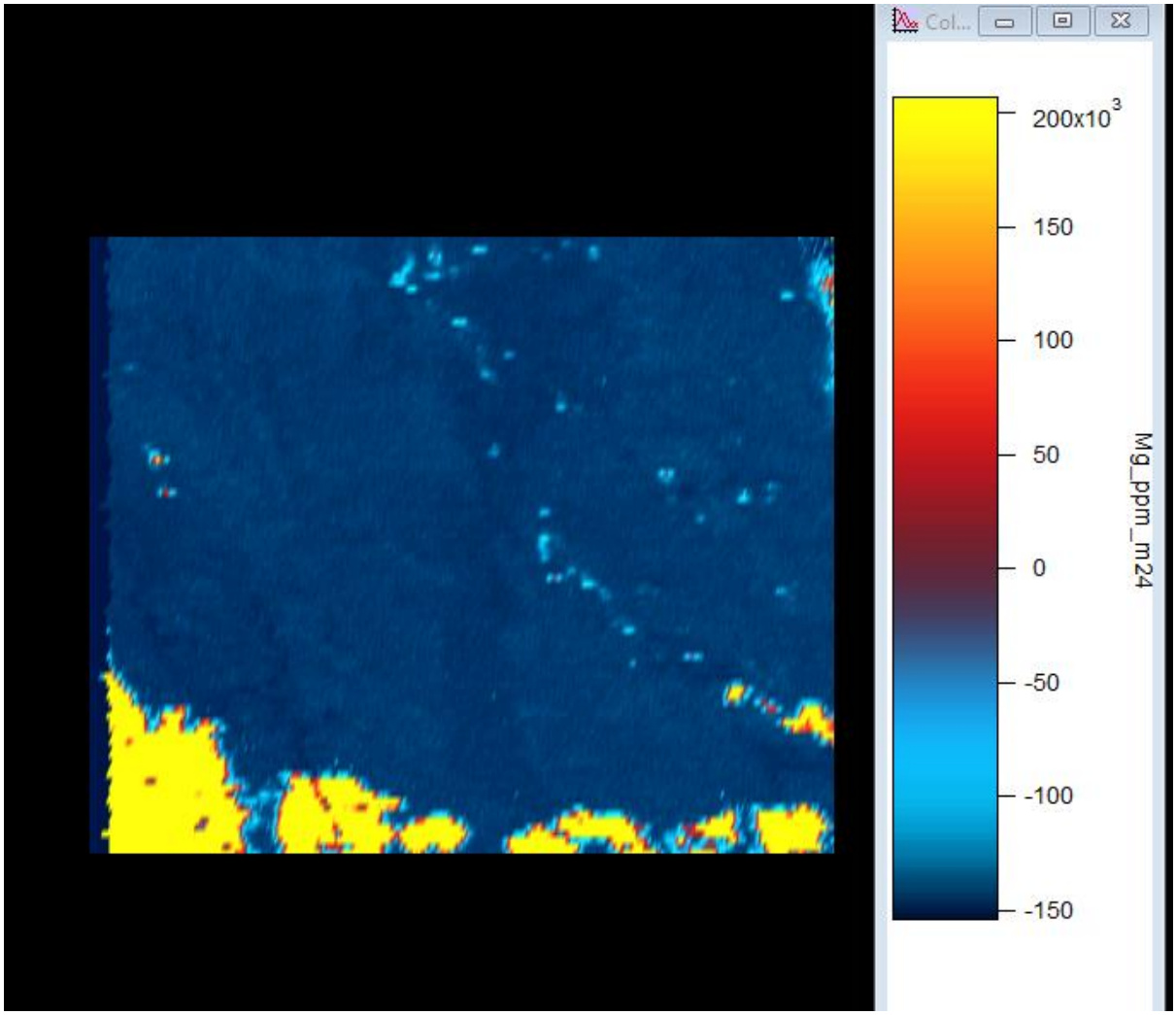
Col...
200x10^3
150
100
50
0
-50
-100
-150
Mg_ppm_m24

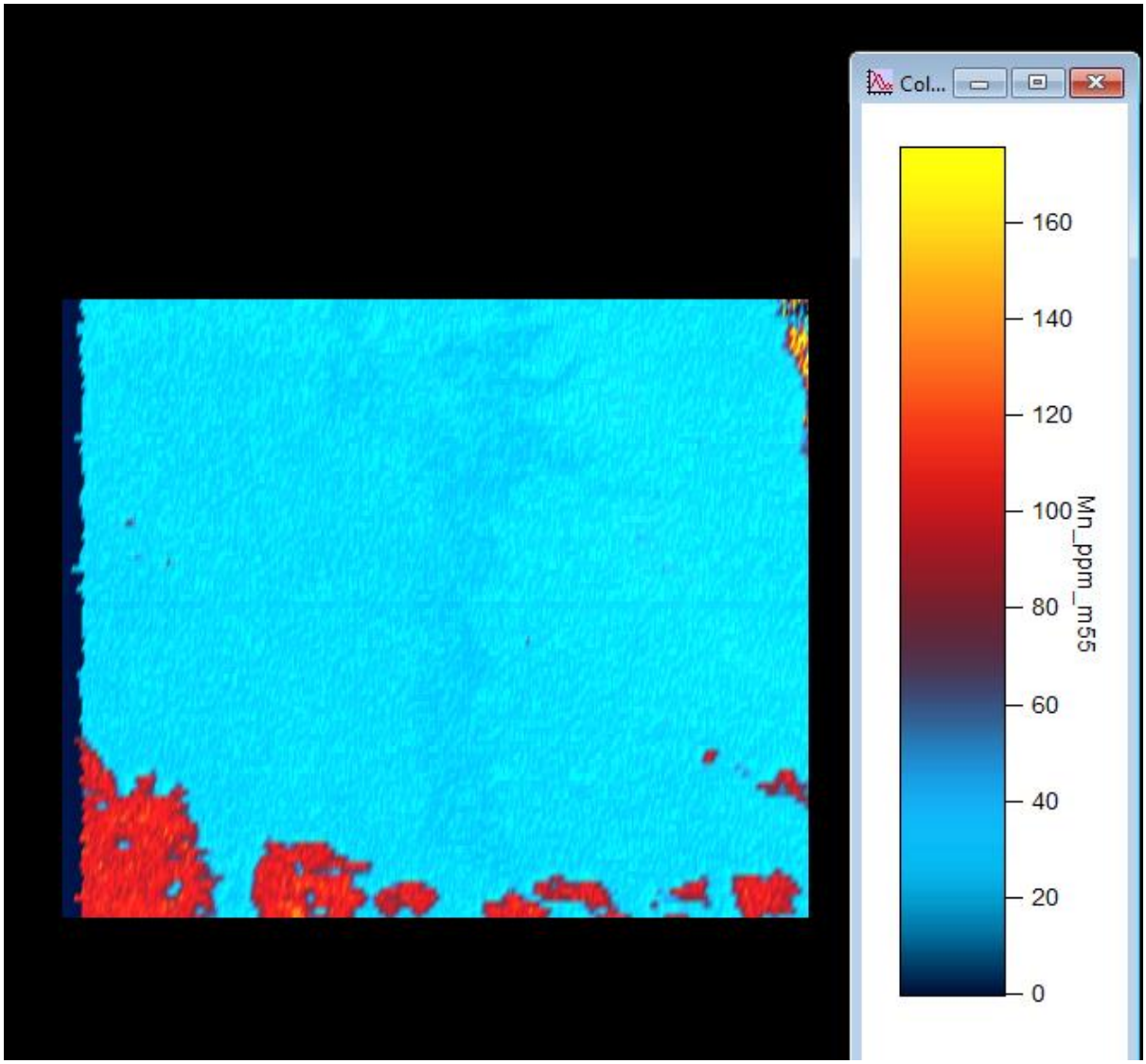
Col...
160
140
120
100
80
60
40
20
0
Mn_ppm_m55

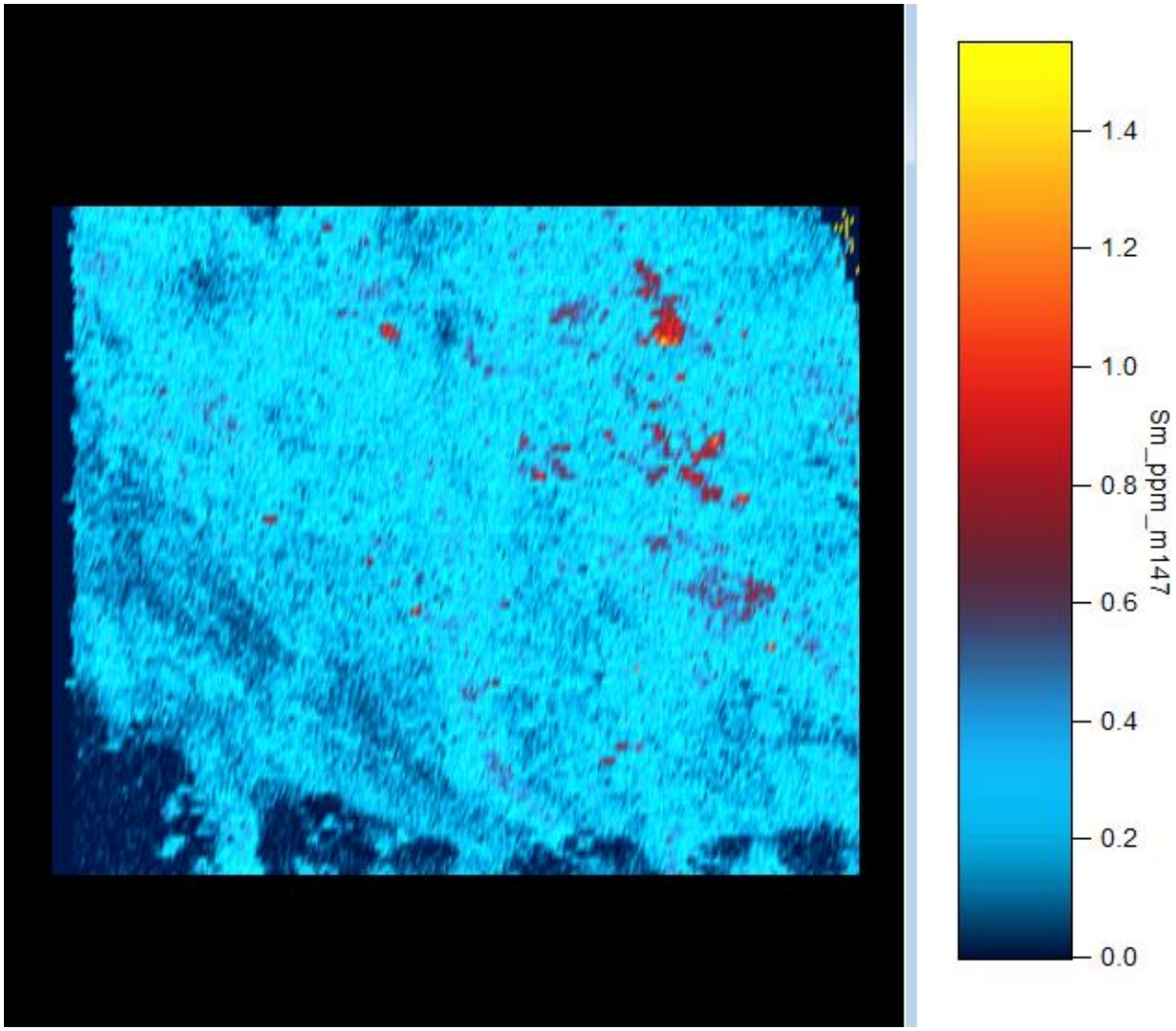
1.4
1.2
1.0
0.8
0.6
0.4
0.2
0.0
Sm_ppm_m147

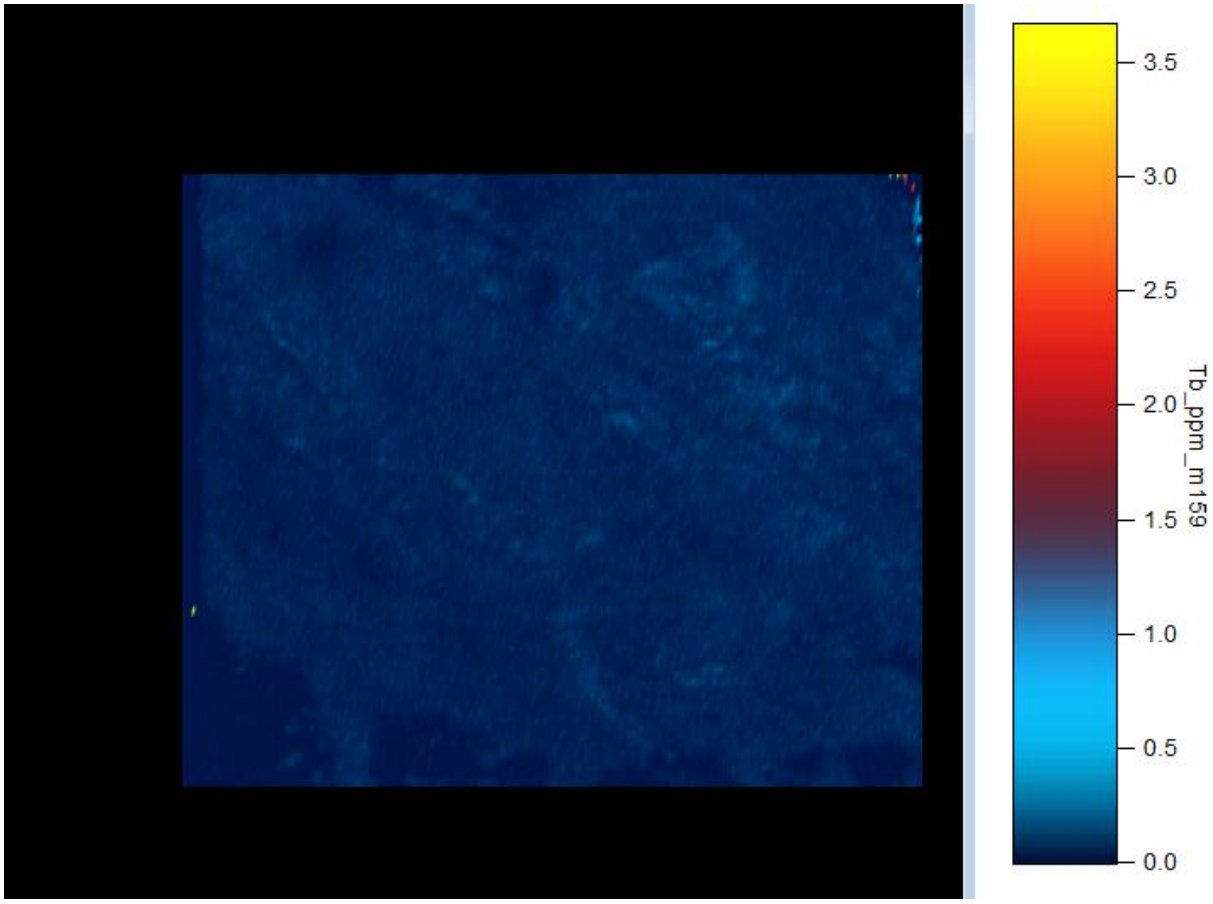
3.5
3.0
2.5
2.0
1.5
1.0
0.5
0.0
Tb_ppm_m159

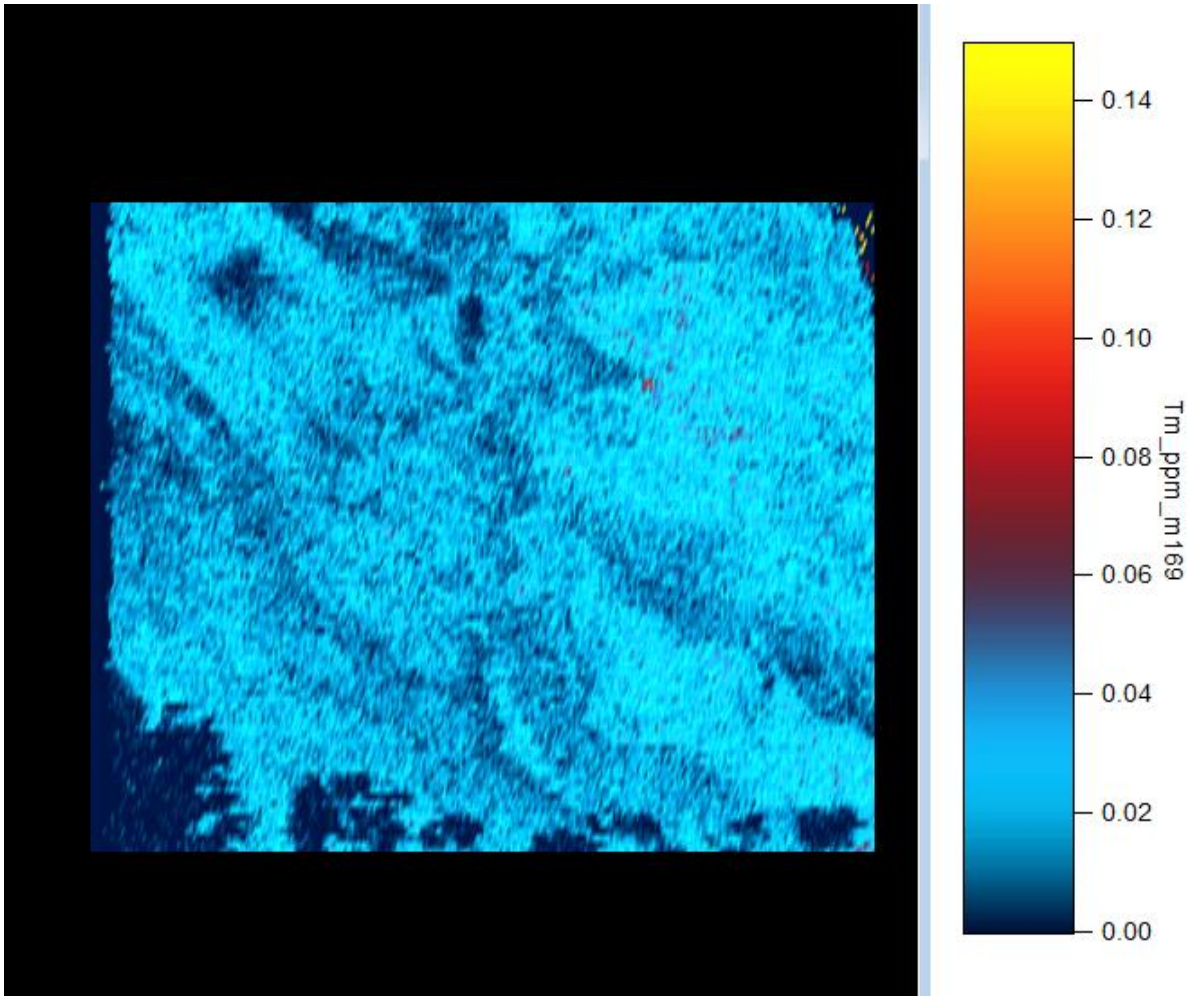
0.14
0.12
0.10
0.08
0.06
0.04
0.02
0.00
Tm_ppm_m169

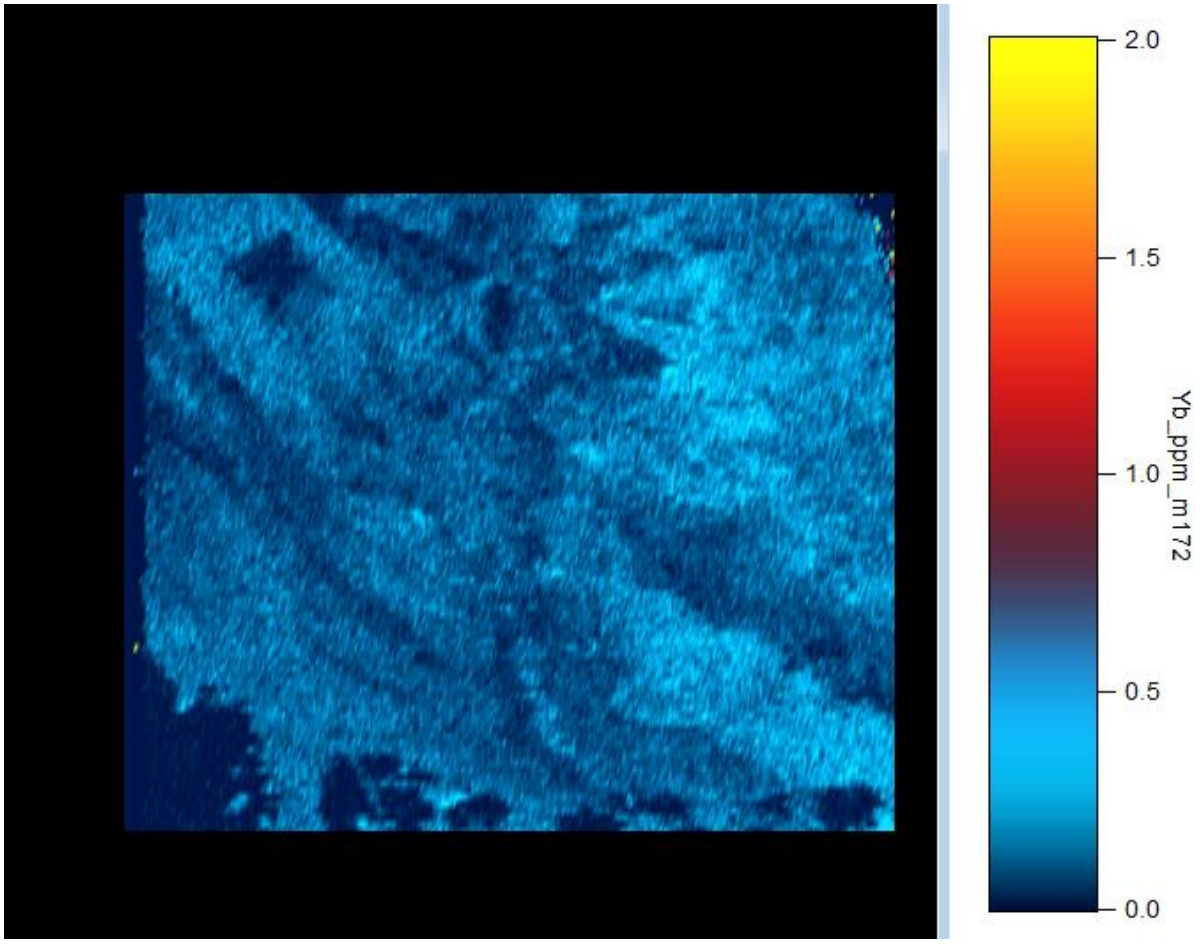
2.0
1.5
1.0
0.5
0.0
Yb_ppm_m172

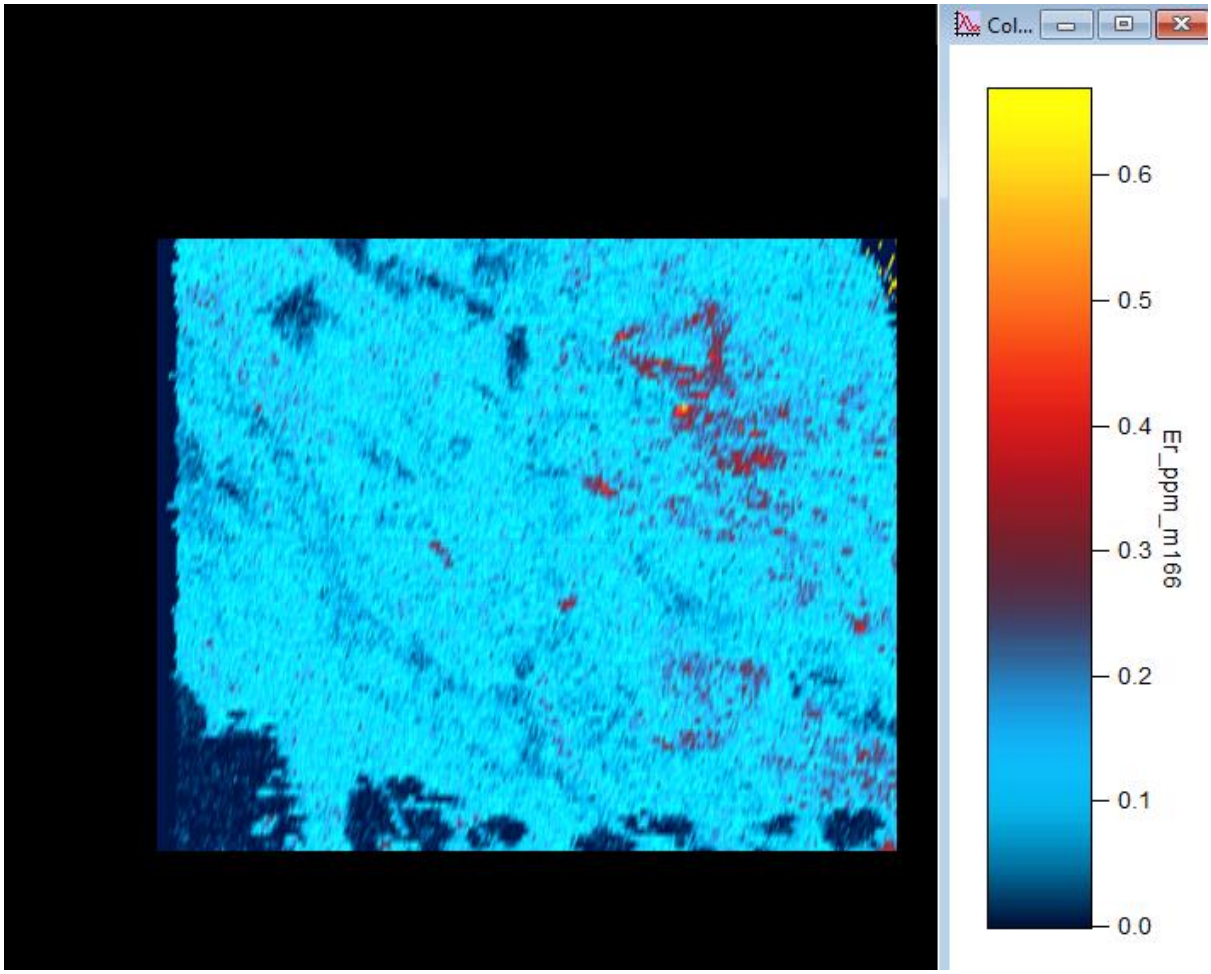
Col...
0.6
0.5
0.4
0.3
0.2
0.1
0.0
Er_ppm_m166

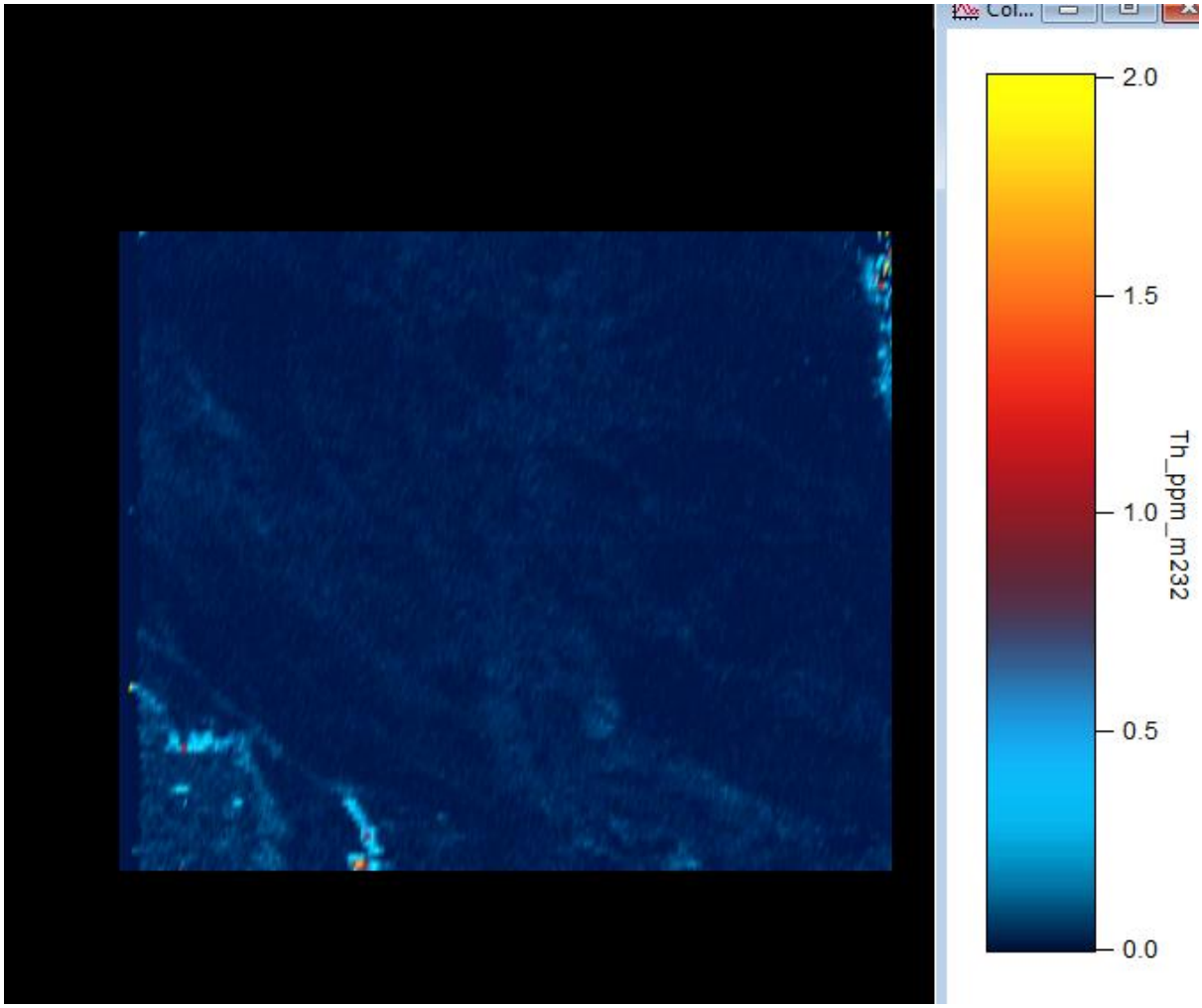
Col...
2.0
1.5
1.0
0.5
0.0
Th_ppm_m232

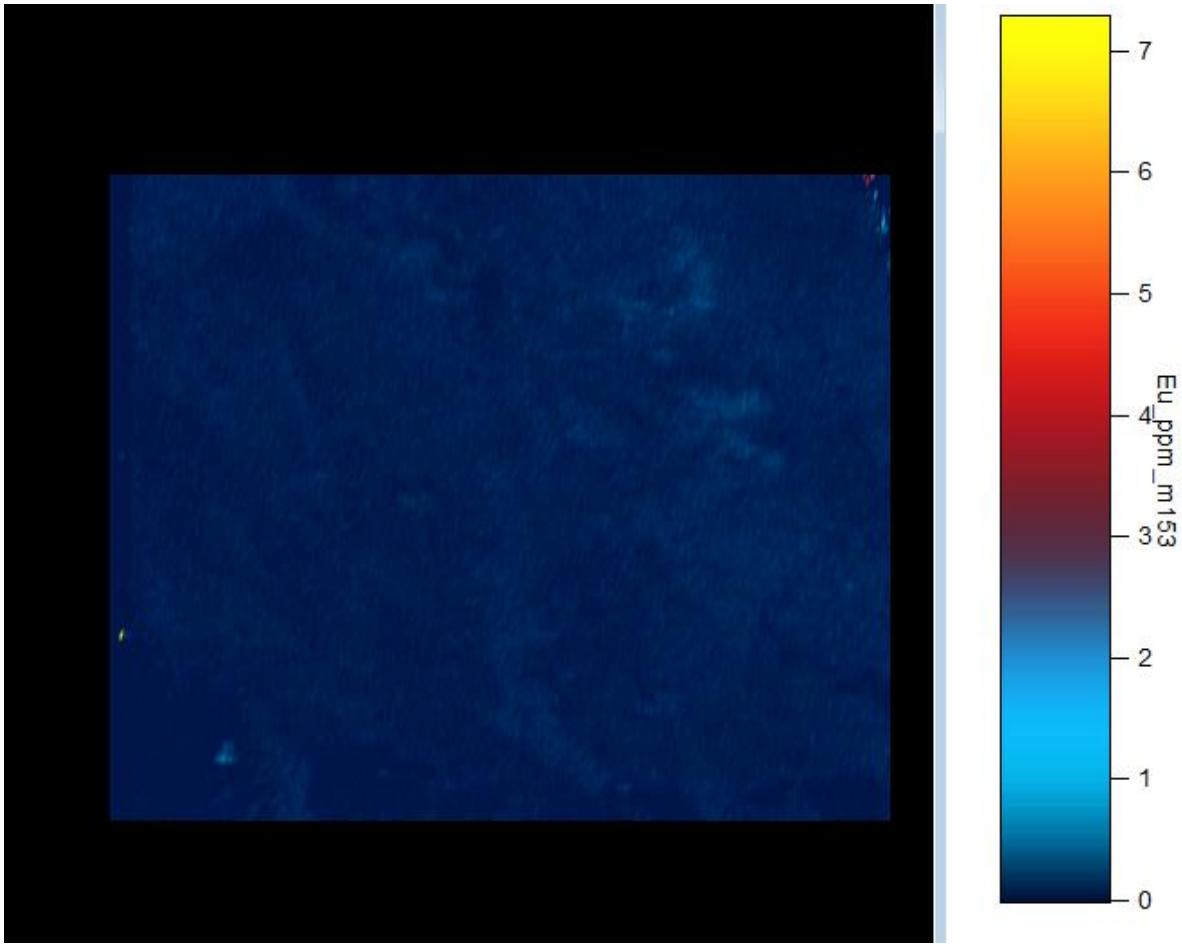
7
6
5
4
3
2
1
0
Eu_ppm_m153

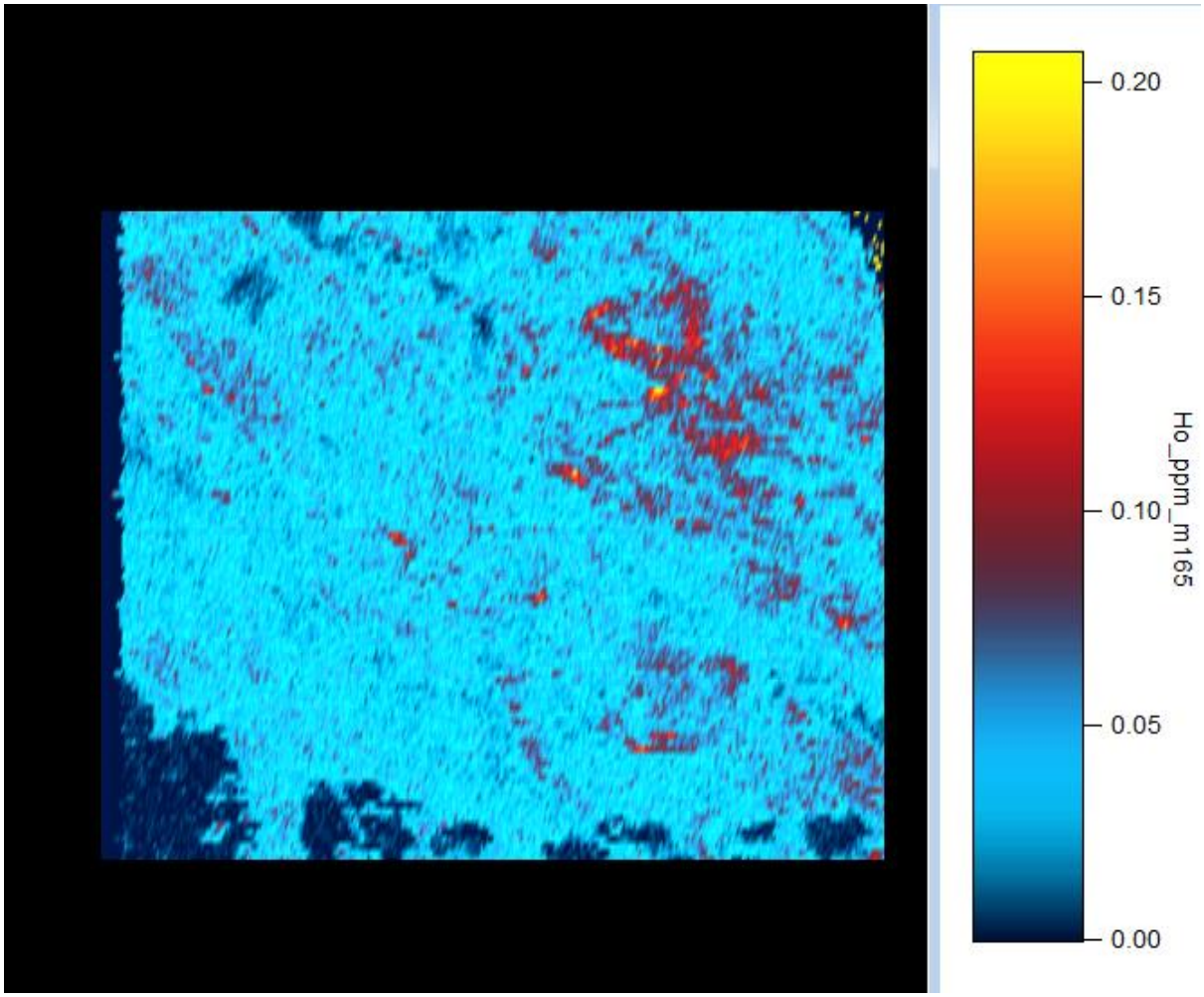
0.20
0.15
0.10
0.05
0.00
Ho_ppm_m165

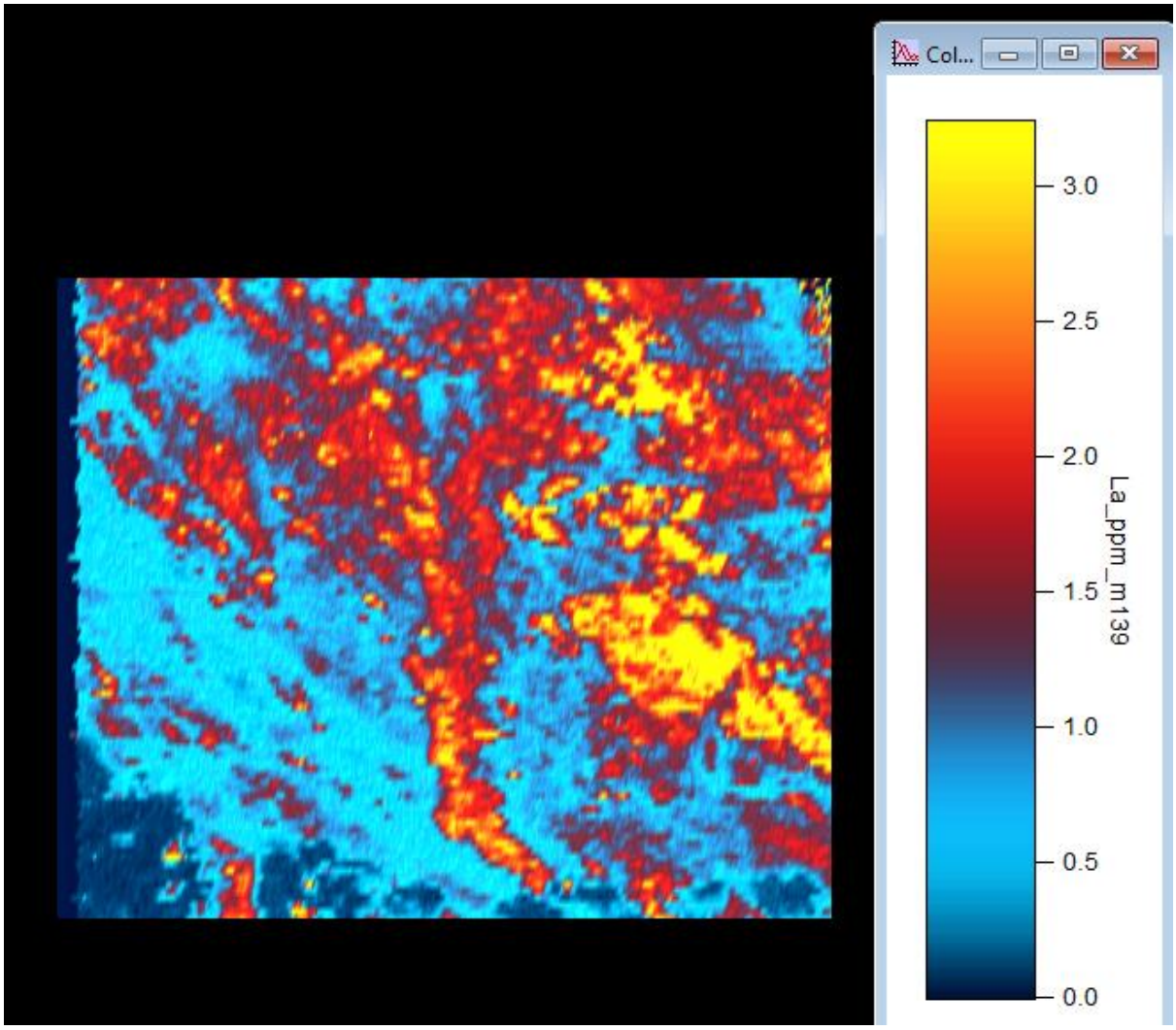
Col...
3.0
2.5
2.0
1.5
1.0
0.5
0.0
La_ppm_m139

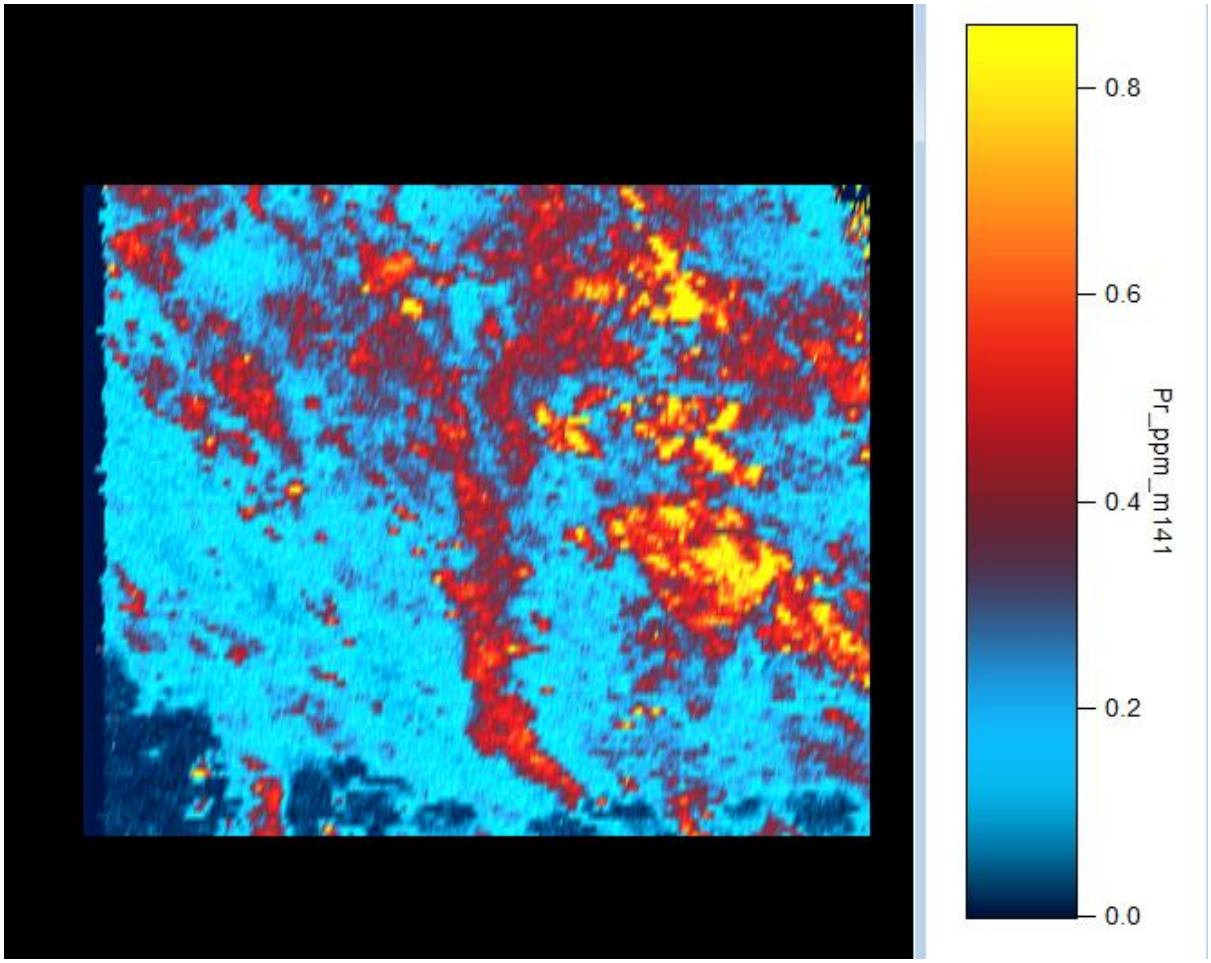
0.8
0.6
0.4
0.2
0.0
Pr_ppm_m141

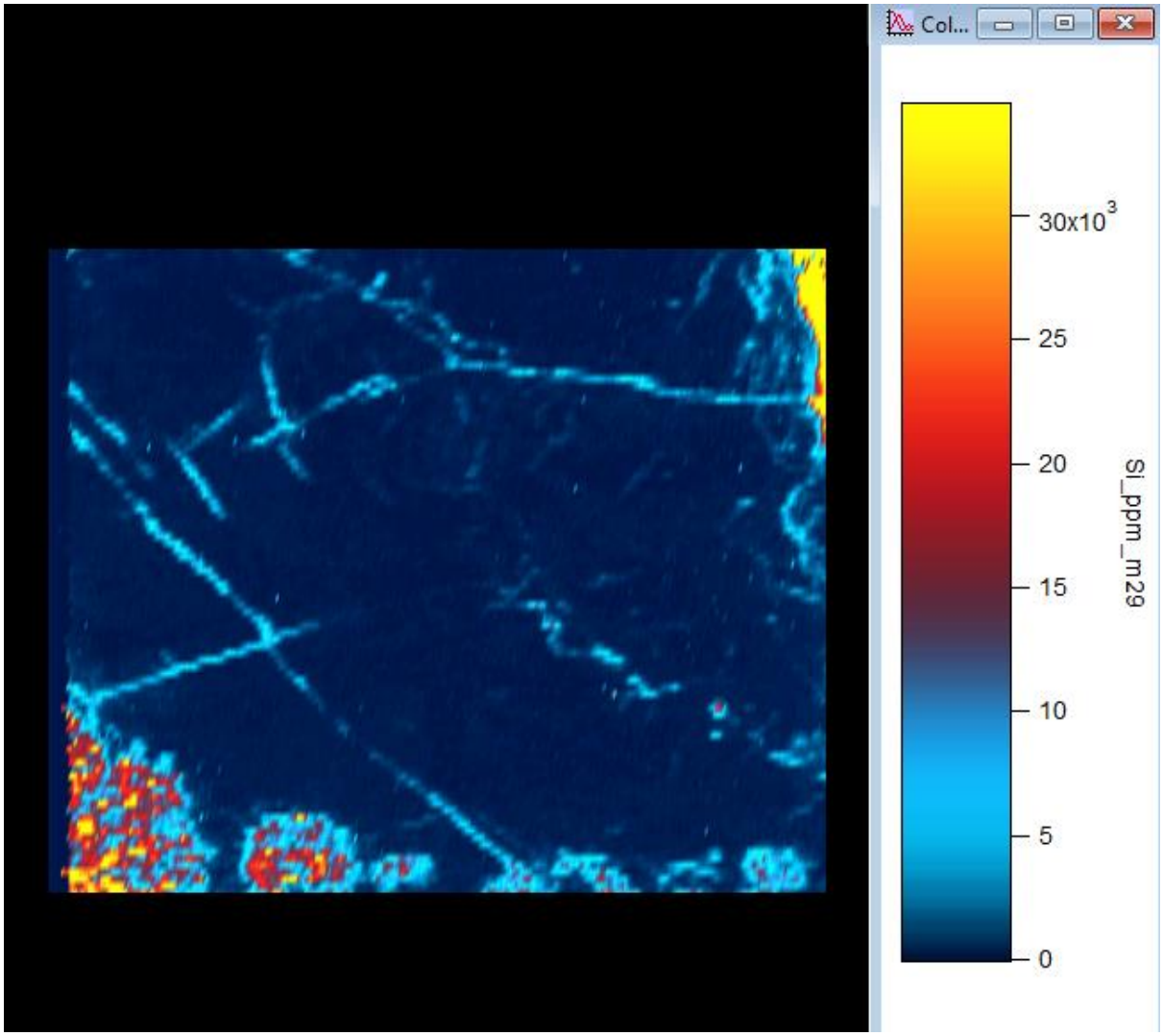
Col...
30x10^3
25
20
15
10
5
0
SI_ppm_m29

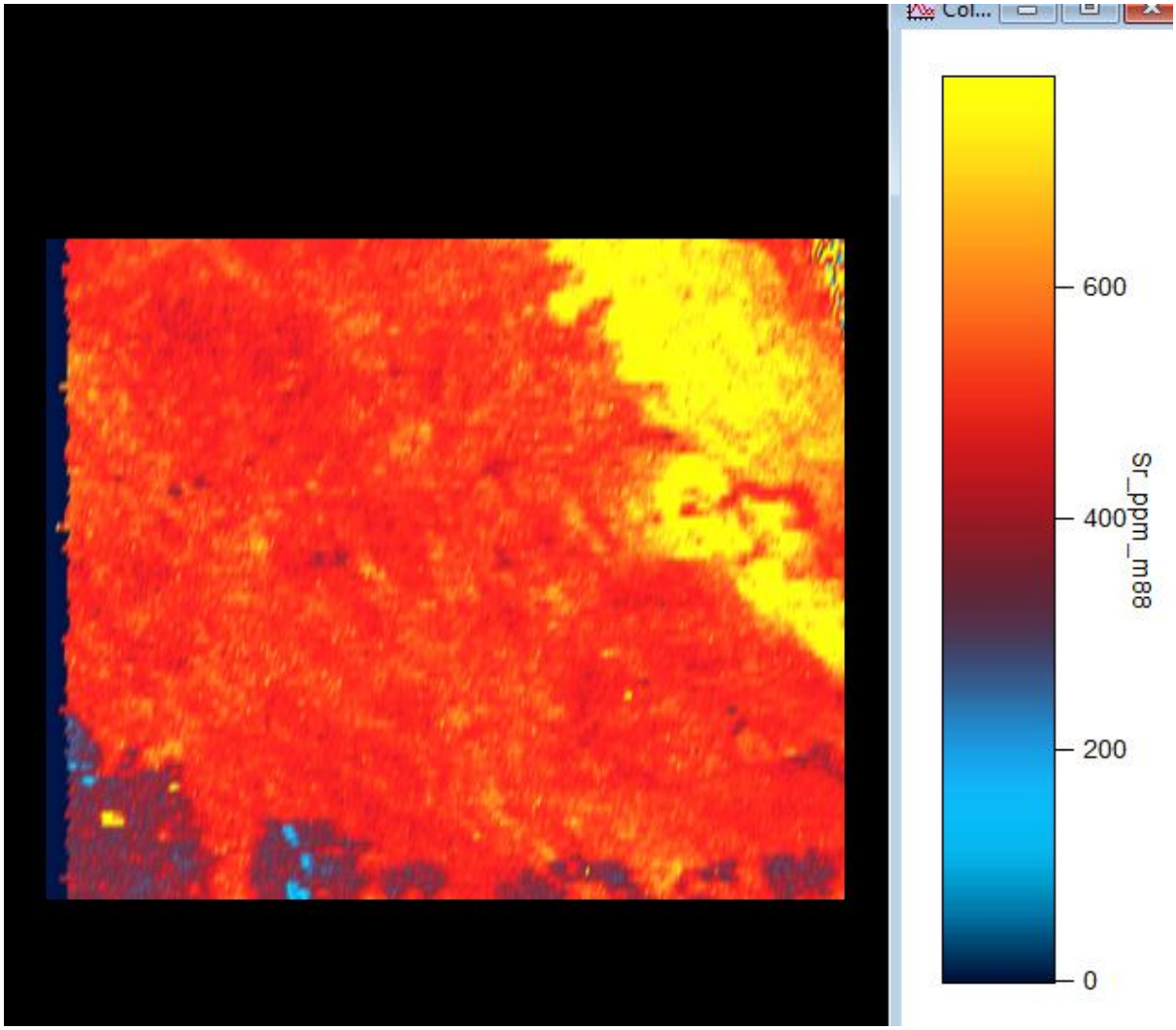
Col...
600
400
200
0
Sr_ppm_m88

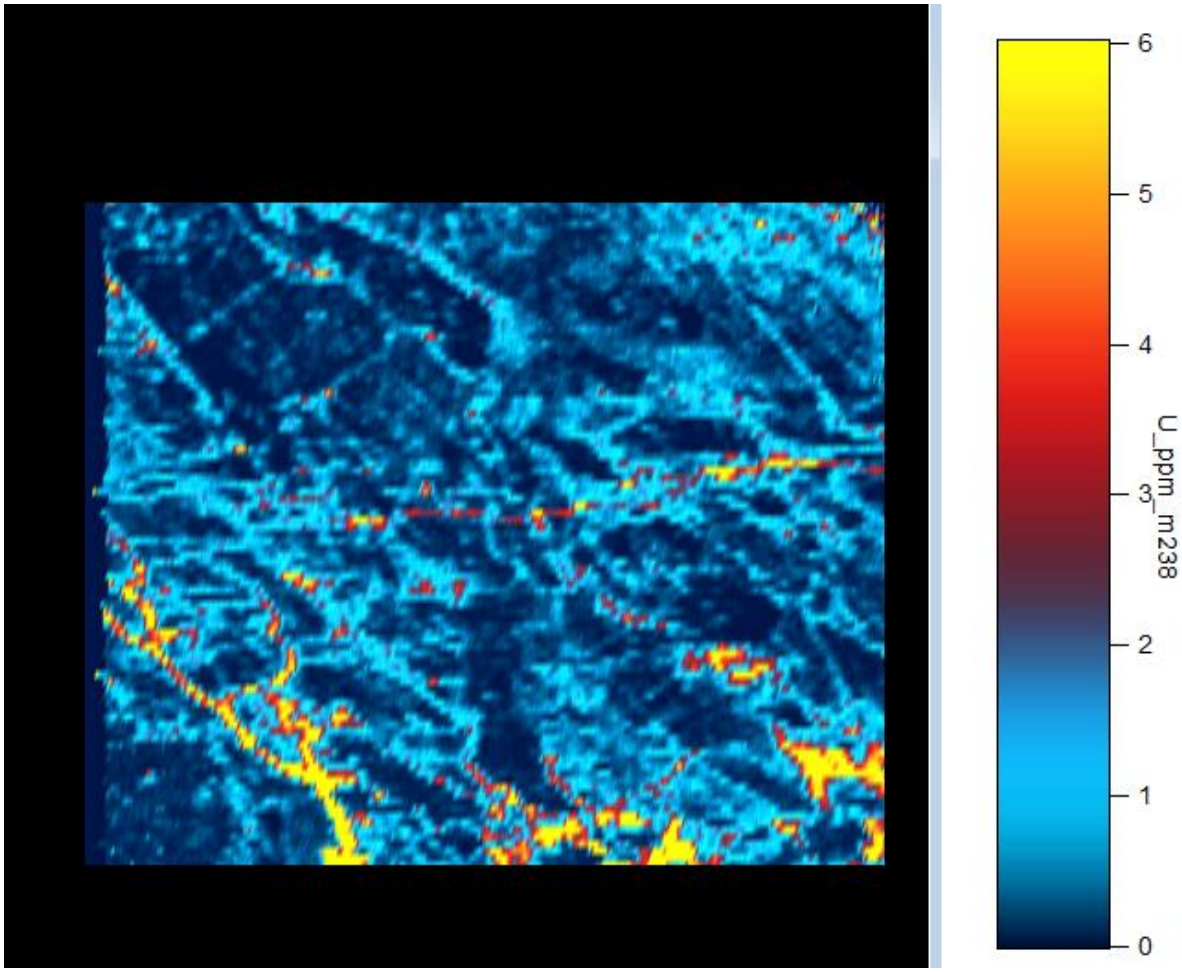
6
5
4
3
2
1
0
U_ppm_m238

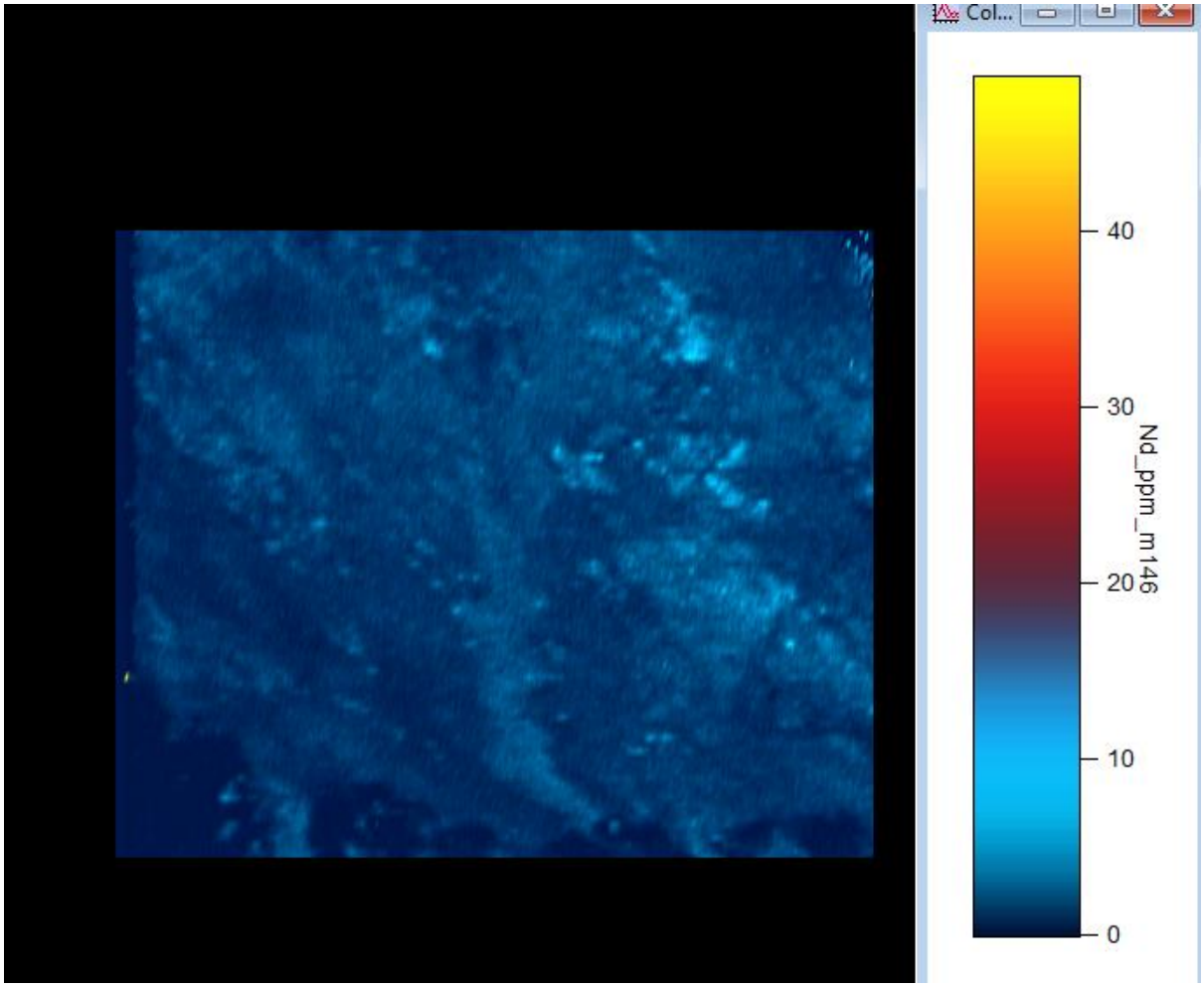

Apatite U-Pb data tables:

	Final238_206	Final238_206_Prop2SE	Final207_206	Final207_206_Prop2SE	ErrorCorrelation_38_6vs7_6
Durango - 1.d	157.7287	9.95134	0.268	0.0365	0.9456
Durango - 2.d	137.3626	7.358715	0.183	0.022	0.081313
Durango - 3.d	150.8296	7.16611	0.263	0.0335	0.22861
Durango - 4.d	148.5884	8.389835	0.308	0.0355	0.037562
Durango - 5.d	157.2327	9.64163	0.34	0.05	0.94505
Durango - 6.d	133.3333	7.02222	0.324	0.039	0.80087
Durango - 7.d	161.0306	9.98338	0.3	0.05	0.57457

Durango - 8.d	129.5337	5.788745	0.302	0.04	0.80981
Durango - 9.d	140.8451	7.73656	0.153	0.026	0.45562
Durango - 10.d	139.8601	8.01995	0.217	0.027	0.22354
Durango - 11.d	145.3488	6.86604	0.19	0.0295	0.43456
Durango - 12.d	153.8462	7.218935	0.213	0.0285	0.20776
Durango - 13.d	101.0101	5.61167	0.402	0.04	0.13642
Durango - 14.d	148.1481	7.572015	0.232	0.0275	0.22875
Durango - 15.d	142.6534	6.817245	0.265	0.03	0.49286
Durango - 16.d	149.925	8.42907	0.268	0.025	0.69719
Durango - 17.d	144.3001	7.287885	0.334	0.037	0.15366
Durango - 18.d	153.3742	6.82186	0.216	0.025	0.30768
Durango - 19.d	150.8296	9.441065	0.323	0.038	0.31202
Durango - 20.d	177.9359	11.55634	0.265	0.037	0.96308
Durango - 21.d	166.3894	8.720905	0.33	0.038	0.29749
Madagascar - 1.d	13.03781	0.22098	0.0582	0.0041	0.26631
Madagascar - 2.d	13.10616	0.223303	0.058	0.00415	0.40542
Madagascar - 3.d	12.97017	0.218693	0.0578	0.004	0.12775
Madagascar - 4.d	13.05483	0.204514	0.058	0.00365	0.3894
Madagascar - 5.d	13.0039	0.219832	0.0573	0.004	0.09206
Madagascar - 6.d	12.9199	0.250386	0.0582	0.0047	0.15951
Madagascar - 7.d	13.36898	0.214476	0.0574	0.0035	0.24555
Madagascar - 8.d	12.85347	0.223036	0.0579	0.00375	0.32987
Madagascar - 9.d	12.9199	0.217001	0.0579	0.00435	0.097566
Madagascar - 10.d	13.17523	0.234342	0.0547	0.00385	0.090701

Madagascar - 11.d	13.17523	0.225663	0.0582	0.00455	0.26797
Madagascar - 12.d	13.1406	0.224478	0.0556	0.00345	0.32955
Madagascar - 13.d	13.1406	0.259013	0.0565	0.00355	0.29851
Madagascar - 14.d	13.45895	0.226429	0.058	0.00395	0.26404
Madagascar - 15.d	13.1406	0.250379	0.0568	0.0045	0.28541
Madagascar - 16.d	13.24503	0.210517	0.0581	0.0044	0.25506
Madagascar - 17.d	13.10616	0.223303	0.0544	0.00445	0.17762
Madagascar - 18.d	13.44086	0.225821	0.0552	0.0033	0.093835
Madagascar - 19.d	13.0039	0.228287	0.0562	0.0037	0.11303
Madagascar - 20.d	13.05483	0.221557	0.057	0.00315	0.093154
Madagascar - 21.d	13.0039	0.228287	0.0585	0.00375	0.23868
Madagascar - 22.d	13.08901	0.214153	0.058	0.00435	0.33738
Madagascar - 23.d	13.29787	0.221042	0.0577	0.0046	0.32227
Madagascar - 24.d	13.1406	0.224478	0.0573	0.00405	0.095669
Madagascar - 25.d	13.51351	0.24653	0.0574	0.0039	0.039963
Madagascar - 26.d	12.82051	0.230112	0.0576	0.0047	0.45001
Madagascar - 27.d	13.42282	0.243232	0.0579	0.0045	0.45425
Madagascar - 28.d	12.8866	0.207581	0.0569	0.00355	0.23546
Madagascar - 29.d	13.55014	0.220327	0.0571	0.00375	0.020635
Madagascar - 30.d	12.72265	0.202332	0.0572	0.00405	0.40993
Madagascar - 31.d	12.93661	0.22593	0.0573	0.00395	0.19416
Madagascar - 32.d	13.31558	0.239361	0.0582	0.00425	0.27439
Madagascar - 33.d	13.21004	0.218131	0.0571	0.0046	0.10146
Madagascar - 34.d	13.0039	0.202922	0.0572	0.00455	0.23357
Madagascar - 35.d	13.17523	0.234342	0.057	0.0039	0.14002

Madagascar - 36.d	13.02083	0.220405	0.0567	0.00445	0.11522
Madagascar - 37.d	12.7551	0.22777	0.0571	0.00395	0.2438
Madagascar - 38.d	13.35113	0.222816	0.0573	0.00425	0.11037
Madagascar - 39.d	13.2626	0.219871	0.0565	0.00435	0.11999
Madagascar - 40.d	13.15789	0.251039	0.0581	0.0045	0.38707
Madagascar - 41.d	12.69036	0.225463	0.0578	0.00435	0.435
Madagascar - 42.d	13.15789	0.242382	0.0581	0.0043	0.29027
McClure - 1.d	7.861635	0.154513	0.37	0.0105	0.3751
McClure - 2.d	7.24113	0.133707	0.417	0.011	0.34159
McClure - 3.d	7.220217	0.164214	0.403	0.012	0.44002
McClure - 4.d	8.340284	0.163467	0.317	0.008	0.47383
McClure - 5.d	8.130081	0.152026	0.331	0.01	0.27507
McClure - 6.d	7.930214	0.160365	0.315	0.01	0.29668
McClure - 7.d	8.257638	0.153424	0.326	0.0115	0.14662
McClure - 8.d	8.006405	0.173077	0.295	0.009	0.08491
McClure - 9.d	9.615385	0.157175	0.205	0.005	-0.03284
McClure - 10.d	10.1833	0.155549	0.1689	0.0038	-0.00029
McClure - 11.d	9.099181	0.16559	0.208	0.005	-0.15132
McClure - 12.d	9.285051	0.163803	0.239	0.0065	0.31941
McClure - 13.d	8.216927	0.175547	0.286	0.009	0.49016
McClure - 14.d	8.598452	0.17744	0.285	0.01	0.56954
McClure - 15.d	4.098361	0.251948	0.517	0.0245	-0.87051
McClure - 16.d	8.319468	0.15227	0.31	0.008	0.44411
McClure - 17.d	9.606148	0.221467	0.218	0.0065	0.19739

McClure - 18.d	9.389671	0.20719	0.222	0.0065	0.46696
McClure - 19.d	9.0009	0.194439	0.229	0.0075	0.425
McClure - 20.d	8.481764	0.208627	0.255	0.01	0.40131
McClure - 21.d	9.225092	0.234031	0.241	0.01	0.46818
McC - 1.d	11.19821	0.15675	0.1258	0.00205	-0.11685
McC - 2.d	11.02536	0.151948	0.142	0.00285	0.086428
McC - 3.d	11.01322	0.157678	0.1538	0.00345	0.085167
McC - 4.d	8.375209	0.143795	0.281	0.0055	0.36098
McC - 5.d	9.07441	0.148221	0.268	0.006	0.47
McC - 6.d	8.643042	0.145669	0.293	0.005	0.41597
McC - 7.d	8.583691	0.139992	0.283	0.006	0.32164
McC - 8.d	8.984726	0.149342	0.264	0.006	0.35784
NIST610 - 1.d	3.985652	0.052422	0.9329	0.0026	0.1492
NIST610 - 2.d	3.935458	0.051884	0.9269	0.0026	0.065625
NIST610 - 3.d	3.961965	0.05337	0.9354	0.00275	0.2548
NIST610 - 4.d	3.974563	0.052131	0.9293	0.0025	0.33262
NIST610 - 5.d	3.992016	0.05498	0.9295	0.00245	0.30093
NIST610 - 6.d	4.003203	0.054487	0.9336	0.00265	0.25471
NIST610 - 7.d	3.971406	0.053625	0.9299	0.00255	0.2352
NIST610 - 8.d	3.977725	0.053005	0.9266	0.00225	0.10982
NIST610 - 9.d	3.961965	0.052586	0.9293	0.0028	0.12892
NIST610 - 10.d	3.977725	0.052214	0.9296	0.0025	-0.01139
NIST610 - 11.d	3.957262	0.054027	0.9249	0.0027	0.20784
NIST610 - 12.d	3.972984	0.052089	0.9302	0.0025	0.063534
NIST610 - 13.d	3.976143	0.053753	0.9262	0.0023	0.17551
NIST610 - 14.d	3.982477	0.053131	0.9316	0.0025	0.19715
NIST610 - 15.d	3.965107	0.053455	0.929	0.002	0.14021
NIST610 - 16.d	3.937008	0.0527	0.9269	0.00195	0.040093

NIST610 - 17.d	3.958828	0.052502	0.9298	0.00255	0.036862
NIST610 - 18.d	3.947888	0.052992	0.9288	0.00235	0.30853
NIST610 - 19.d	3.963535	0.053413	0.926	0.0023	0.1539
NIST610 - 20.d	3.955696	0.052419	0.9242	0.0025	0.25136
NIST610 - 21.d	3.903201	0.051037	0.9234	0.00195	0.095153
NIST610 - 22.d	3.92773	0.051681	0.9237	0.0021	0.19734
NIST610 - 23.d	3.935458	0.054207	0.9252	0.00235	0.39473
NIST610 - 24.d	3.935458	0.051884	0.9217	0.0023	0.040508
NIST610 - 25.d	3.932363	0.051803	0.9222	0.00255	0.17612
NIST610 - 26.d	3.94633	0.052171	0.9223	0.0025	0.094672
NIST610 - 27.d	3.947888	0.052213	0.9193	0.00255	-0.01577
NIST610 - 28.d	3.952569	0.052336	0.9227	0.0026	0.45544
NIST610 - 29.d	3.920031	0.051478	0.9198	0.00255	0.15218
NIST610 - 30.d	3.924647	0.05237	0.9215	0.00205	0.086904
NIST610 - 31.d	3.929273	0.053265	0.9156	0.00225	0.091632
NIST610 - 32.d	3.920031	0.053015	0.9176	0.0024	0.19624
NIST610 - 33.d	3.915427	0.05289	0.9202	0.0025	0.223
NIST610 - 34.d	3.91696	0.051398	0.9196	0.0019	0.085047
NIST610 - 35.d	3.929273	0.051721	0.9219	0.00245	0.03381
NIST610 - 36.d	3.947888	0.052992	0.921	0.0026	0.3952
NIST610 - 37.d	3.955696	0.053984	0.9241	0.00265	0.15711
NIST610 - 38.d	3.93391	0.05107	0.9205	0.0027	-0.00067
NIST610 - 39.d	3.903201	0.051799	0.9167	0.00215	-0.31999
NIST610 - 40.d	3.979308	0.053839	0.9183	0.0026	0.25171
NIST610 - 41.d	3.883495	0.051277	0.9198	0.0018	0.2679

NIST610 - 42.d	3.886514	0.051357	0.9181	0.00225	-0.09023
NIST610 - 43.d	3.963535	0.051842	0.9194	0.0017	0.18259
NIST610 - 44.d	4.001601	0.051241	0.9228	0.00205	0.060928
NIST610 - 45.d	3.971406	0.051259	0.921	0.00175	0.11863
NIST610 - 46.d	3.943218	0.051312	0.92	0.00195	0.091356
NIST610 - 47.d	3.96668	0.051924	0.9199	0.002	0.077437
NIST610 - 48.d	3.947888	0.050654	0.9202	0.0016	0.11565
NIST610 - 49.d	3.941663	0.050494	0.9187	0.00155	-0.19211
NIST610 - 50.d	3.943218	0.050534	0.9197	0.00155	0.029304
NIST610 - 51.d	3.94633	0.051393	0.9191	0.0018	0.16359
NIST610 - 52.d	3.971406	0.051259	0.9176	0.00185	0.007032
NIST610 - 53.d	3.957262	0.051678	0.9179	0.0015	0.064636
NIST610 - 54.d	3.93391	0.05107	0.9174	0.0019	0.11237
NIST610 - 55.d	3.94011	0.052783	0.9164	0.00155	0.20749
NIST610 - 56.d	3.947888	0.050654	0.9184	0.00175	-0.11885
NIST610 - 57.d	3.943218	0.050534	0.9168	0.0018	-0.06888
NIST610 - 58.d	3.938558	0.051966	0.9161	0.00215	0.038984
MY72 - 1.d	6.662225	0.15091	0.792	0.0155	0.52343
MY72 - 2.d	7.012623	0.181954	0.824	0.015	0.20842
MY72 - 3.d					
MY72 - 4.d	9.65251	0.237586	0.79	0.0175	0.57527
MY72 - 5.d	18.11594	0.361006	0.717	0.0165	0.44305
MY72 - 6.d	4.385965	0.11542	0.823	0.021	0.53177
MY72 - 7.d	16.52893	0.532751	0.726	0.0125	-0.09695

MY72 - 8.d	15.67398	0.393078	0.743	0.0145	0.2229
MY72 - 9.d	2.020202	0.063259	0.851	0.015	0.24357
MY72 - 10.d	3.389831	0.183855	0.809	0.014	0.19911
MY72 - 11.d	11.84834	0.238651	0.753	0.0125	0.46391
MY72 - 12.d	11.66861	0.326776	0.776	0.01	0.13066
MY72 - 13.d	21.78649	1.139163	0.672	0.016	-0.66159
MY72 - 14.d	7.936508	0.818846	0.8	0.065	0.34434
MY72 - 15.d	3.236246	0.099496	0.842	0.014	0.30148
MY72 - 16.d	1.953125	0.110626	0.906	0.0445	0.036547
MY72 - 17.d	3.225806	1.873049	0.9	0.33	-0.01747
MY72 - 18.d	13.1406	0.70797	0.74	0.011	-0.40153
MY72 - 19.d	0.825764	0.026934	0.868	0.015	-0.18036
MY72 - 20.d					
MY72 - 21.d					
MY72 - 22.d					
MY72 - 23.d	9.066183	0.168501	0.791	0.014	0.54504
MY72 - 24.d	0.37037	0.185185	0.83	0.415	NaN
MY72 - 25.d					
MY72 - 26.d	2.525253	0.086088	0.855	0.0135	-0.07453
MY72 - 27.d					
MY72 - 28.d	6.090134	0.133523	0.812	0.0135	0.31655
MY72 - 29.d					
MY72 - 30.d					
MY72 - 31.d					
MY72 - 32.d	1.908397	0.069198	0.857	0.014	0.10319

MY72 - 33.d	38.92565	0.674267	0.576	0.009	0.35949
MY72 - 34.d					
MY72 - 35.d	8.163265	0.246564	0.791	0.0135	0.30895
MY72 - 36.d	12.72265	0.258985	0.746	0.011	0.40882
MY72 - 37.d	3.205128	0.113001	0.811	0.014	0.346
MY72 - 38.d	3.846154	0.133136	0.821	0.0155	0.13722
MY72 - 39.d	5.524862	1.022558	0.714	0.0475	0.39417
MY72 - 40.d	8.333333	0.381944	0.791	0.012	-0.09153
MY72 - 41.d	5.56483	0.153288	0.798	0.011	0.15481
MY72 - 42.d	9.11577	0.357318	0.772	0.0235	0.09425
MY74 - 1.d	5.128205	0.157791	0.823	0.013	0.18957
MY74 - 2.d					
MY74 - 3.d	22.32143	0.697545	0.728	0.023	0.52388
MY74 - 4.d	54.05405	1.753105	0.475	0.013	-0.47004
MY74 - 5.d	50	1.75	0.491	0.009	-0.36862
MY74 - 6.d	64.35006	1.20087	0.395	0.0095	0.56306
MY74 - 7.d	33.44482	1.565978	0.609	0.011	-0.26859
MY74 - 8.d	7.633588	0.582717	0.8	0.0215	-0.06293
MY74 - 9.d	8.4246	0.19163	0.774	0.0175	0.52814
MY74 - 10.d	7.29927	0.426235	0.803	0.0195	-0.00683
	12.22494	0.478237	0.77	0.0235	-0.05475
MY74 - 12.d					
MY74 - 13.d	12.42236	0.277767	0.775	0.0175	0.41507
MY74 - 14.d					
MY74 - 15.d					

MY74 - 16.d	5.402485	0.1328	0.805	0.0155	0.39974
MY74 - 17.d					
MY74 - 18.d	9.532888	0.177208	0.796	0.017	0.35525
MY74 - 19.d					
MY74 - 20.d					
MY74 - 21.d	0.055556	0.016975	0.797	0.0105	-0.09626
MY74 - 22.d	9.99001	0.244511	0.811	0.0175	0.50025
MY74 - 23.d					
MY74 - 24.d	4.539265	0.103025	0.868	0.0185	0.52868
MY74 - 25.d	0.208333	0.054253	0.84	0.07	0.45356
MY74 - 26.d	38.31418	0.880786	0.606	0.017	0.38267
MY74 - 27.d	8.896797	0.391807	0.767	0.013	0.16541
MY74 - 28.d	20.57613	0.423377	0.709	0.0145	0.47374
MY74 - 29.d	27.85515	1.086274	0.629	0.0095	-0.43641
MY74 - 30.d	43.55401	1.043324	0.516	0.0135	0.29026
MY74 - 31.d	10.71811	0.281451	0.763	0.0215	0.51038
MY74 - 32.d					
MY74 - 33.d					
MY74 - 34.d	29.7619	0.708617	0.658	0.018	0.65345
MY74 - 35.d	7.479432	0.223768	0.814	0.0145	0.2858
MY74 - 36.d	23.14815	0.589421	0.697	0.0165	0.65917

AFT analytical details:

MY72	MY72.xml	Fri Sep 14 14:17:08 ACST 2018			
FastTracks: v3.0.19					
Pixel Calibration X:	0.087302				

Pixel Calibration Y:	0.087302				
Grain/Mica	Tracks	Area(cm2)	Density(tracks/cm2)	Average DPar(µmm)	DPar Std Deviation
Grain01	3	1.87E-05	1.61E+05	1	0.123187
Grain02	4	2.13E-05	1.88E+05	0.83	0
Grain03	31	2.29E-05	1.35E+06	1	0.192759
Grain04	1	1.42E-05	7.05E+04	0.94	0
Grain05	6	1.35E-05	4.44E+05		0
Grain06	2	1.09E-05	1.83E+05	0.64	0
Grain07	4	1.90E-05	2.11E+05	0.52	0
Grain08	10	4.12E-05	2.43E+05	0.99	0.191536
Grain09	1	2.30E-05	4.36E+04		0
Grain10	2	2.67E-05	7.51E+04		0
Grain11	6	1.56E-05	3.85E+05	1.06	0.228782
Grain12	9	1.68E-05	5.37E+05	0.97	0.171216
Grain13	18	1.94E-05	9.26E+05	1.19	0.2932
Grain14	4	2.11E-05	1.90E+05		0
Grain15	0	1.37E-05	0.00E+00		0
Grain16	1	2.39E-05	4.18E+04		0
Grain17	9	2.72E-05	3.31E+05	0.9	0.108114
Grain18	11	1.92E-05	5.73E+05	0.82	0.193721
Grain19	0	1.36E-05	0.00E+00		0
Grain20	5	1.97E-05	2.54E+05	0.88	0.113076
Grain21	1	7.08E-06	1.41E+05		0
Grain22	1	6.49E-06	1.54E+05		0
Grain23	0	1.04E-05	0.00E+00		0
Grain24	0	9.56E-06	0.00E+00		0
Grain25	1	1.30E-05	7.67E+04		0
Grain26	0	1.60E-05	0.00E+00		0
Grain27	7	1.13E-05	6.18E+05	1.17	0.221633
Grain28	3	2.01E-05	1.49E+05	0.74	0.144233
Grain29	1	1.26E-05	7.94E+04		0
Grain30	4	1.25E-05	3.21E+05	1.12	0.329984
Grain31	1	6.82E-06	1.47E+05		0
Grain32	2	2.25E-05	8.89E+04	1.23	0
Grain33	8	8.62E-06	9.28E+05	0.7	0.086612
Grain34	0	1.15E-05	0.00E+00		0
Grain35	1	1.04E-05	9.60E+04	0.59	0
Grain36	2	1.35E-05	1.48E+05		0
Grain37	0	5.73E-06	0.00E+00		0
Grain38	0	1.01E-05	0.00E+00		0
Grain39	3	1.39E-05	2.16E+05		0
Grain40	0	6.16E-06	0.00E+00		0
Grain41	3	9.59E-06	3.13E+05	0.74	0

Grain42	1	5.33E-06	1.88E+05	0.8	0

MY74	MY74.xml	Tue Sep 11 15:03:54 ACST 2018			
FastTracks: v3.0.19					
Pixel Calibration X:	0.087302	Alex Simpson			
Pixel Calibration Y:	0.087302				
Grain/Mica	Tracks	Area(cm2)	Density(tracks/cm2)	Average DPar(µmm)	DPar Std Deviation
Grain01	11	9.31E-05	1.18E+05	1.52	0.231186
Grain02	8	2.77E-05	2.89E+05	1	0.260488
Grain03	24	4.54E-05	5.29E+05	1.06	0.145538
Grain04	46	6.56E-05	7.02E+05	1.24	0.246143
Grain05	61	4.62E-05	1.32E+06	1.37	0.417593
Grain06	75	7.20E-05	1.04E+06	1.34	0.371736
Grain07	95	1.28E-04	7.43E+05	1.33	0.296095
Grain08	9	3.61E-05	2.50E+05	1.07	0.350893
Grain09	15	5.05E-05	2.97E+05	1.2	0.326838
Grain10	13	3.77E-05	3.45E+05	1.54	0.212893
Grain11	26	5.67E-05	4.58E+05	1.09	0.342794
Grain12	3	1.41E-05	2.12E+05	1.1	0.117252
Grain13	16	4.39E-05	3.65E+05	1.13	0.180306
Grain14	3	2.67E-05	1.13E+05		0
Grain15	0	7.79E-05	0.00E+00		0
Grain16	16	3.28E-05	4.88E+05	1.08	0.222967
Grain17	0	4.26E-05	0.00E+00		0
Grain18	14	2.81E-05	4.99E+05	1.05	0.263156
Grain19	0	3.16E-05	0.00E+00		0
Grain20	19	2.18E-05	8.72E+05	1.09	0.245389
Grain21	0	4.63E-05	0.00E+00		0
Grain22	3	1.85E-05	1.62E+05	0.79	0.122699
Grain23	6	2.14E-05	2.81E+05	0.96	0.121471
Grain24	26	5.98E-05	4.35E+05	1.1	0.26795
Grain25	0	5.13E-05	0.00E+00		0
Grain26	21	2.16E-05	9.73E+05	1.06	0.139653
Grain27	7	2.62E-05	2.67E+05	1.03	0.581595
Grain28	32	3.30E-05	9.70E+05	0.92	0.247987
Grain29	13	2.66E-05	4.89E+05	1.42	0.181628
Grain30	36	3.16E-05	1.14E+06	1.2	0.300183
Grain31	19	3.81E-05	4.99E+05	0.91	0.16577
Grain32	29	3.06E-05	9.46E+05	1.19	0.286877
Grain33	4	1.50E-05	2.67E+05	1.22	0.036328

Grain34	31	4.06E-05	7.63E+05	1.04	0.226181
Grain35	12	3.24E-05	3.70E+05	0.93	0.069785
Grain36	88	3.44E-05	2.56E+06	1.03	0.265687

MY74	MY74.xml	Thu Oct 04 12:31:26 ACST 2018								
FastTracks: v3.0.19										
Pixel Calibration X:	0.087302	Alex Simpson								
Pixel Calibration Y:	0.087302									
Length Name	Length Number	Type	Apparent Length	Corrected Z Depth	True Length	Azimuth	Dip	Angle to CAxis	Average DPar(µmm)	DPar Std Deviation
Length02	1	C	9.88	0	9.88	57.93	0	57.93	1	0.26
Length03	1	C	10.81	0.82	10.84	73.09	4.33	73.14	1.06	0.15
Length05	1	T	8.19	0.82	8.23	88.19	5.7	88.2	1.37	0.42
Length05	2	T	10.03	3.27	10.55	86.67	18.06	86.83	1.37	0.42
Length05	3	C	11.79	0	11.79	55.1	0	55.1	1.37	0.42
Length06	1	T	12.3	0	12.3	23.11	0	23.11	1.34	0.37
Length06	2	T	10.66	2.45	10.94	48.24	12.96	49.53	1.34	0.37
Length06	3	T	11.39	4.09	12.1	61.64	19.76	63.44	1.34	0.37
Length11	1	C	12.07	3.27	12.5	36.29	15.17	38.92	1.09	0.34
Length16	1	C	12.29	0	12.29	36.62	0	36.62	1.08	0.22
Length23	1	C	11.09	1.64	11.21	75.75	8.39	75.9	0.96	0.12
Length23	2	C	13.73	2.45	13.95	22.47	10.13	24.54	0.96	0.12
Length31	1	C	10.6	3.27	11.1	25.88	17.15	30.72	0.91	0.17
Length31	2	C	12.99	0	12.99	62.39	0	62.39	0.91	0.17
Length31	3	C	11.8	2.45	12.06	69.42	11.74	69.87	0.91	0.17
Length32	1	C	11.09	0	11.09	70.26	0	70.26	1.19	0.29

Length32	2	C	14.08	1.64	14.17	66.2	6.63	66.37	1.19	0.29
Length36	1	C	11.19	0.82	11.22	65.09	4.18	65.16	1.03	0.27

[10] APPENDIX B EXTENDED METHOD

[3] METHODS

[3.1] Calcite U-Pb

[3.1.1] Laboratory Processing

Calcite samples were selected and cut (in ~1cm^3 blocks) to reveal internal sections that cross-cut the veins. Slickenfibres were broken off using a small flathead screwdriver. Subsequently, the calcite pieces were mounted in 1-inch (2.5cm) round epoxy mounts using epoxy cure resin (5g epoxy resin and 1.15g epoxy hardener) and ground (using 2000 grit sandpaper) and polished (using 3µm polishing cloth) to reveal a smooth surface.

[3.1.2] LA-ICP-MS spot-analysis

For each calcite sample, elemental concentrations (table 3) were measured *in-situ* using laser ablation inductively coupled plasma mass spectrometry (LA-ICP-MS) with an ASI RESOlution-LR 193nm Excimer Laser System coupled to an Agilent 7900x mass spectrometer. Spot analyses were carried out in two analytical sessions (table 3), with standards interspaced throughout each session. For each sample, approximately 30 to 90 spots were ablated (at 110µm spot size). The data was reduced using Iolite software (Paton et al., 2011). Glass standard NIST614 was used as the primary standard for drift corrections and normalisation of the $^{207}Pb/^{206}Pb$ ratios (Woodhead & Hergt, 2007). Subsequently, an in-house matrix-matched carbonate reference material (WC-1) of known age (254 ± 7 Ma; isotope dilution U-Pb data; Roberts and Walker, 2017) was used for normalisation of the $^{206}Pb/^{238}U$ ratios. In more detail, normalisation was based on the measured versus accepted ratio derived

from the session-based drift-corrected mean of the WC-1 reference material (see Roberts and Walker, 2017 for further details). No downhole corrections were performed, instead the mean of each 30s ablation (excluding the first 2 s of data) was used (Roberts and Walker, 2017). In addition, an in-house calcite sample from the Prague Basin with known biostratigraphic age of ~424 Ma (Farkas et al., 2016), labelled 'Prague' was used as secondary standard for accuracy checks. Calcite tends to contain significant quantities of common Pb and thus requires a significant number of spots ablated for each sample to calculate an accurate U-Pb age. This age is calculated using a linear regression through the ^{238}U-^{206}Pb versus ^{207}Pb-^{206}Pb ratios for each sample on a Tera-Wasserburg Concorida plot (e.g. Chew et al., 2014). The lower intercept of this regression represents the U-Pb age of the sample, which – in the case of the calcite U-Pb method – reflects the timing of calcite growth. Tera-Wasserburg Concordia plots were made using IsoplotR (Vermeersch 2018).

[3.1.3] Calcite Elemental Mapping

Elemental mapping was conducted on selected Calcite U-Pb samples for which the spot analyses returned significantly dispersed age data, aiming to reveal a link between possible age populations and elemental zonation patterns. Following U-Pb analysis, the pieces were gently re-polished using the equipment detailed in section 3.1.1. Appropriate areas surrounding previously spot-analysed calcite sections were re-ablated and mapped, in raster mode, using the ASI RESOlution-LR 193nm Excimer Laser System coupled with the Agilent 7900x mass spectrometer. Spot sizes of 91 or 134µm (depending on the size of the area to be mapped) were used in the ablation rasters. Data reduction and plotting was conducted using Iolite (Paton et al., 2011). Analytical details are given in Table 3.

[3.2] Apatite Fission Track and Apatite U-Pb Analysis

[3.2.1] Laboratory Processing

Samples were received as mineral separates from Nick Gardiner (Curtin University, Perth). Optical examination was conducted to locate apatite grains under a binocular microscope. Apatite grains were individually picked onto double sided tape in rasters of between150-200 grains (depending on amount of apatitie grains). Grains were placed so that their c-axis was parallel to the tape surface. Grains were mounted in an EpoxyCure resin prepared with 5g epoxy resin and 1.15g epoxy hardener. The resin was used to cover the grain raster, and a glass slide was placed over the top so that the resin would stick to it. Resin set for ~24 hours. Tape was then removed, such that the grains were embedded in the resin (now attached to the glass slide). This mount was ground using 2000grit sandpaper and then polished using an autopolisher (3µm an 1µm diamond suspension fluid was used. This made the surface smooth enough to allow track counting. Samples were then etched (using a solution of 5M nitric acid (HNO_3) at 20±0.5^{o}C for 20±0.5 seconds) and then washed in distilled water

[3.2.2] Fission Track counting

Samples were coated in a 3nm layer of gold to enhance the imaging process. Apatite grains were identified (based on etched features (fission tracks) using a Zeiss AXIO Imager M2m Autoscan Syste. Mounts that did not contain these features were excluded. Iamges were then taken using the Zeiss AXIO Imager M2m Autoscan System, which allowed for surface track densities and confined track lengthes to be counted. The density of fission tracks in an apatite sample is known to be correlated with 238U concentration (Wagner & Van den haute, 1992). The age represented by the fission tracks correlates with passage of the grain through the apatite partial annealing zone (~60-120^{o}C) (Wagner & Van den haute, 1992).

[3.2.3] LA-ICP-MS Analysis

The concentration of Pb, U and Cl isotopes and other elements including REEs (table 5) were measured using laser ablation inductively coupled plasma mass spectrometry (LA-ICP-MS)

using an ASI RESOlution-LR coupled with an Agilent 7900x mass spectrometer. A single 30μm spot was ablated for each grain. Standards were interspaced throughout the analytical session. The data was reduced using Iolite software (Paton, Hellstrom, Paul, Woodhead, & Hergt, 2011) using NIST610 as the primary standard to calculate the U (and other elemental) concentrations, used in the AFT analysis. MAD standard (Madagascar) (Chew et al., 2014) was used as the primary standard for U-Pb analysis. The secondary standards used to check the accuracy of the results were McClure and Durango apatite (Chew et al., 2014).

[3.2.4] Apatite U-Pb analysis

Apatite tends to contain significant quantities of common rendering robust single grain AUPb age determinations (usually) impossible. Refer to calcite U-Pb section for details on age calculation. The lower intercept of the calculated regression represents the AUPb age for the sample, which represents the cessation of Pb diffusion (and thus the timing of cooling) below temperatures of 350-550^{o}C (Chew, Petrus, & Kamber, 2014).